Title	NEW COMPOSITE CATALYSTS FOR RING OPENING POLYMERIZATION OF EPOXIDES AND PROPIOLACTONES
Author(s)	Hayase, Shuji
Citation	大阪大学, 1983, 博士論文
Version Type	VoR
URL	https://hdl.handle.net/11094/27754
rights	
Note	

NEW COMPOSITE CATALYSTS FOR RING OPENING POLYMERIZATION

OF EPOXIDES AND PROPIOLACTONES

BY

SHUZI HAYASE

NOVEMBER 1982

CONTENTS

Chapter 1   General Introduction

Part I   A new catalyst for polymerization of epoxides

-- aluminum complex/silanol catalyst --

1) Background

Epoxy resins have been utilized as insulating mate-
rials, coating materials, adhesives and laminating mate-
rials in many fields. They are preferred for their elec-
trical and mechanical properties in consideration of the
coat.[1] In electrical industries, a number of different
epoxy resins have been used as the materials for insula-
tion of coils in generators and motors, molding compounds
for semiconductor encapsulation, and the laminates for
circuit plates. Excellent insulating properties, high
reliability and low cost have been required for these
materials.

There is a recent trend for many electrical appli-
ances to be of midget type, because of the savings in
energy and the ease in processing. The motor and the
generator is the example. The heat generated by elec-
tric current causes the rise of temperature of the insu-
lating materials. The midget type enhances the tempera-
ture rise. Insulating properties for epoxy resin cured
with commonly used catalyst are not sufficient for motor-
use at temperature above 160°C. Therefore the insulation

properties and heat resistant properties must be improved, especially in the temperature range from 150°C to 220°C.

For semiconductor encapsulation use, ionic impurities in the molding compound, namely, H^+, Na^+, K^+, Cl^-, F^-, $R-NH_3^+$, BF_4^-, AsF_6^- and so on, must be minimized to prevent corrosion of fine wiring from moisture and the impurities. Since the impurities deteriorate insulation of the molding compound, absence of impurities is preferred.

Epoxy resin monomers have more than two epoxy groups for curing. The monomer forms three dimensional networks in the presence of catalyst. The catalyst used is then buried in the matrix of the network. Therefore, the following properties will be influenced by the catalyst residue.

1) Insulation properties

2) Collosion properties on metal

3) Color change by aging at higher temperature

4) Heat resistant properties

The heat resistant properties mean weight loss of the cured resin when it was aged at high temperature. The catalyst for ring opening polymerization also degrades the polymer chain at that temperature. As shown above, the properties of cured epoxy resins can be improved by use of an appropriate catalyst or by modification of the catalyst.

The followings are curing catalysts which have been

commonly used for homopolymerization of epoxy resin monomers.[2]

1) tertiary amines (including heterocyclic bases
   such as imidazole and guanidine)

2) $BF_3 \cdot$amine complexes (e.g. $BF_3 \cdot$monoethylamine and
   $BF_3 \cdot$piperidine)

3) ammonium salts ($C_6H_5NH_3^+ \cdot AsF_6^-$ and $C_6H_5NH_3^+ \cdot PF_6^-$)

The dissipation factor of the epoxy resin cured with these
catalysts increases rapidly at the temperature above
150°C.[2]

2) Requirements for new catalysts

The following points are important for the develop-
ment of new catalysts.

1) Stability in air and toward moisture

2) Free from ionic species, e.g. halide anion,
   metal cation, H^+.

3) High catalytic activity for epoxide polymeriza-
   tion

Ethylene oxide is the simplest of epoxy resin mono-
mers. Ethylene oxide has been polymerized by use of the
following cationic and anionic catalyst.

1) Cationic catalyst[3]: $AlCl_3$, $SbCl_5$, BF_3, BCl_3,

$BeCl_2$, $FeCl_3$, $FeBr_3$, $SnCl_4$,

$TiCl_4$, $ZrCl_4$, $ZnCl_2$, PF_5.

2) Anionic catalyst : CH_3ONa[4], CaO, SrO[5], alkali

earth metal compounds[6],

organometallic catalysts[7].

These catalysts are not stable in air and are buried in the cured resin matrix as ionic impurities.

Water, alcohols and phenols have been examined as co-catalyst of cationic polymerization in the presence of BF_3 or $SnCl_4$.[8] As alcohols and phenols are non- or weakly ionic materials, they are suitable for the present catalyst. However when they were used in the presence of halogen-free-metal compound, namely, acetylacetonato complex and so on, their activities were insufficient.

3) Finding a new catalyst

Silanol is a hydroxy compound whose acidity is larger than alcohol and smaller than phenol.[9] It is known that silanols react with epoxides, forming Si-O-C bonds, in the presence of a catalytic amount of an aluminum complex.[10]

$$\equiv SiOH + CH_2\text{-}CH_2 \xrightarrow{\quad Al(acac)_3 \quad} \equiv Si\text{-}O\text{-}CH_2\text{-}\underset{\underset{OH}{|}}{CH_2}$$
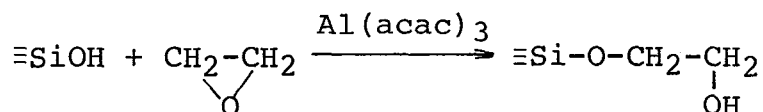
These compounds are used as epoxy-silicone resin. It was considered that if silanol reacted with epoxide and produced ring-opened compounds, ring-opening polymerization might be caused in the presence of a catalytic amount of

a composite catalyst-aluminum complex and silanol.

The addition of silanol to epoxide is also considered to be a termination step of polymerization. In order to prevent the silanol from the addition of silanol to epoxide, silanols with phenyl groups which would make the vicinity of the SiOH moiety bulky, were considered. The introduction of phenyl group would also strengthen the acidity of silanol and increase the degree of polymerization and retard the termination. When silanols with phenyl groups were used, the composite catalyst system (aluminum complex/silanol) showed the catalyst activity. The silanol at the active site, namely, ionic species, would disappear gradually at the curing temperature as shown in the following transformation to give a siloxane and water.

$$2SiOH \longrightarrow H_2O + Si-O-Si$$
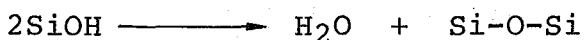
Therefore the cured epoxy resin will have excellent electrical properties. The epoxy resins cured with this catalyst had excellent insulating properties, especially in the temperature region from 150°C to 220°C, as mentioned later.

4) Activation of the catalyst

To improve the catalyst, reaction mechanism of the catalytic polymerization was investigated. The catalyst

activity was examined by use of cyclohexene oxide as a model compound of epoxy resin.

Substituent groups on SiOH would affect the polymerization largely, as mentioned in 3). Therefore, dependence of the catalytic activity on the structure of the silanol was investigated. The results are shown in chapter 3.

Phenol or thiol, whose acidity is stronger than that of silanol, did not have the catalytic activity. The results implied that the interaction between silanol and an aluminum complex was important in order to activate the catalyst. Therefore the dependence of the catalytic activity on the structure of aluminum complex and relation between the interaction strength and the catalytic activity were investigated (see Chapter 4).

From consideration of the substitution effects, two interaction mechanisms are possible. The active site was considered to be similar to Brönsted acid site of a silica-alumina catalyst.[11] The polymerization will be initiated by proton released by the interaction between the aluminum complex and silanol. The formation of an atactic polymer was also a consequence of a cationic mechanism.

Active site of the aluminum complex/silanol catalyst is SiO-H. If the properties of SiOH, for example, acidity or stability against self-condensation, were varied, the catalytic activity might be affected. Porous silica and

zeolite were known to interact with hydroxy compounds.
Therefore the activity of the aluminum complex/silanol
catalyst supported on the porous silica or zeolite was
investigated. The porous silica and zeolite resisted
deactivation more than the $Al(acac)_3$ only, and had higher
activity. The mechanism of the activation was examined
by use of ^{1}H-NMR spectroscopy (see Chapter 5).

The results from kinetics of the polymerization
showed reaction order on concentration of silanol to be
about 1.9. The results implied that aggregation of
silanols was important. Therefore effects of intramolecu-
lar hydrogen bond of silanol on catalyst activity were ex-
amined. In the preexperiment using diphenylsilanediol
oligomer $(HO(Ph_2SiO)_nH$; n: 2,3,4) as model of silanol
polymers, the trimer and the tetramer gave active catalyst
than the dimer in presence of the tris(acetylacetonato)-
aluminum, because they form an intramolecular hydrogen
bond.

n; 3,4
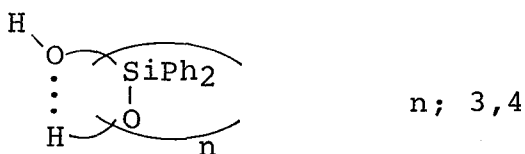
Catalyst activation caused by use of a silanol poly-
mer was also observed in case of tris(acetylacetonato)-
aluminum/silanol polymer. The experimental results using
silanol oligomer explained well the behavior of the poly-
merization with aluminum complex/silanol polymer. Bulky

groups neighboring the SiOH part and rigidity of silanol polymer chain are important for catalyst activation.

It was found that the interaction between aluminum complex and silanol was important for catalyst activation. The interaction was considered to be induced by UV-radiation, because it is known that acid dissociation was promoted and the hydrogen bonding, for example, one between cytosine and guanine, strengthens under UV-radiation.[12] The catalyst activity of the tris(acetylacetonato)aluminum/triphenylsilanol system increased about 3 - 4 times under UV-radiation (see Chapter 8).

5) Electrical properties of epoxy resin cured with aluminum complex/silanol catalyst

The electrical properties of epoxy resins (bisphenol A type, epikote 828, shell) cured with the present catalyst were compared with that cured with ordinary catalysts, namely, imidazole and $BF_3 \cdot$complex.[2] The value of electrical dissipation factor, volume resistivity and breakdown-voltage of the epoxy resin cured were excellent, compared with that cured by $BF_3 \cdot$complex.[2] The reason of such excellent electrical properties was examined by use of thermal depolarization charge (see Chapter 9). The results showed that the absence of any appreciable ionic species was important for the excellent electrical properties. As the polymerization was considered to be caused

cationically, disappearance mechanism of the cation was examined (see Chapter 9). Dependence of the electrical properties on the structure of the catalyst was also examined.

6) Latent catalyst

6-1) Activation by heat

A "clean" and active catalyst for epoxide polymerization was obtained as described above. For practical use, epoxy resins are provided as a composition containing catalyst. The epoxy resin composition must be stable before use and must be cured rapidly. Therefore, molecular design is necessary for the active catalyst which is generated by a trigger. Heat or UV-radiation is usually used as the trigger. This type of catalyst is called a latent catalyst. Compounds containing Si-OR groups were used as latent catalysts components. The SiOR group will be hydrolyzed by a small amount of water in epoxy resin at higher temperature, and silanol produced by hydrolysis will start the polymerization. The catalyst activity of aluminum complex/SiOR and the curing process were examined.

In the aluminum complex/alkoxysilane catalyst, the alkoxysilane was gradually hydrolyzed even at room temperature and the epoxy resin was gradually crosslinked. In order to prevent the reaction at room temperature, water in the epoxy resin was eliminated with zeolite 4A.

However the adsorbed water will be released at the temperature above 100°C. The composition was more stable in the presence of zeolite and the gelation of the composition was faster above 100°C.

The silicone compound which thermally liberates silanol in the absence of H_2O was found (see Chapter 10). The epoxide composition containing the catalyst was more stable at room temperature and active at higher temperature. The insulation properties for the epoxy resin cured with these catalysts were also excellent.

6-2) Activation by UV-radiation

The catalyst-curing epoxy resin with irradiation have recently attracted interest due to the processability and to the energy saving. The photo-generated catalyst will be most important as latent catalyst, because reaction starts at low temperature. Long pot life is necessary in the absence of UV-radiation.

Diazonium salts and some onium salts are known to be effective for the UV curing of the epoxy resins.[13] However diazonium salts had disadvantages; evolution of N_2 gas, and presence of ionic species which disturb insulation.

The UV-curable epoxy resins with good electrical properties may be obtained by the present photocatalyst. Such photoactive catalyst is composed by silylketones.

For example, $Ph_3SiCOPh$ ($n-\pi^*$ absorption at 424 nm ($\varepsilon = 292$) and $\pi-\pi^*$ absorption (257 nm (16200))) photodecomposes to Ph_3SiOH in the presence of H_2O or alcohols.[14] A new catalyst system (aluminum complex/$Ph_3SiCOPh$/alcohol) was thus investigated.

Other silicone compounds which isomerize to silanol directly under UV radiation were also investigated. However high activity has not been obtained. A compound with hemiacetal structure, $SiOCH(OH)$, formed by photolysis was considered to be suitable for the present purpose. If the hemiacetal is formed under UV-radiation, the silicon compound will decompose rapidly even at room temperature, forming silanol, as follows.

$$\boxed{} \xrightarrow{h\nu} \left(\begin{array}{c} Si-O-CH-R \\ | \\ OH \end{array} \right) \xrightarrow[\text{room temperature}]{\Delta} SiOH + \begin{array}{c} CH-R \\ \| \\ O \end{array}$$
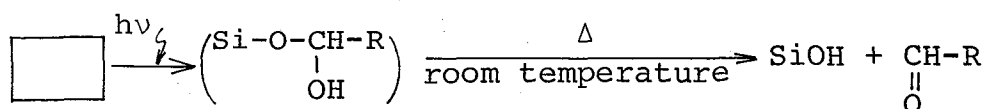
The hemiacetal may be produced by photooxidation of $Si-O-CH_2-Ph$ with aromatic nitro compound since it is known that p-methoxytoluene is photooxidized to p-methoxybenzylalcohol.[15]

$$CH_3-C_6H_4-OCH_3 \xrightarrow[\substack{\text{aromatic nitro} \\ \text{compound}}]{h\nu} HOCH_2-C_6H_4-OCH_3$$
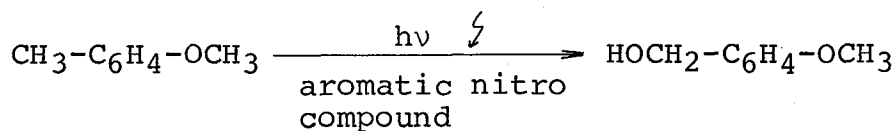
The photopolymerization catalyst, aluminum complex/triphenylsilylbenzyl ether/aromatic nitro compound system, polymerized cyclohexene oxide under UV radiation.

Expecting neighboring effects, ortho-nitrobenzylsilyl
ether was examined. The decomposition rate of the silyl
ether was fast and high catalyst activity was obtained.
The dependence of the catalyst activity on the wavelength
of UV and quantum yield were examined.
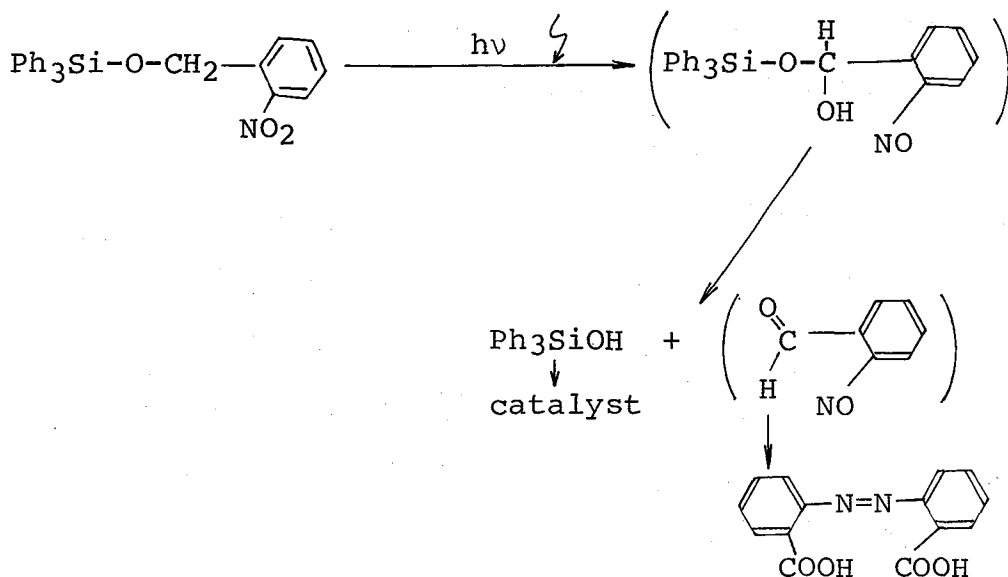
Epoxy resins with above photopolymerization catalyst
could be cured within 20 sec. and the cured epoxy resin
had excellent electrical and high heat resistance prop-
erties.

Part II   Selective synthesis of structually isomeric

           poly-β-ester and poly-δ-ester from

           β-(2-acyloxy-ethyl)-β-propiolactone with

           AlEt$_3$-H$_2$O and ZnEt$_2$-H$_2$O catalyst

The polymerization of β-substituted-β-propiolactones

have been studied in view of stereoregular polymerization in a systematic manner.[16] It has been found that an organoaluminum catalyst $(EtAlO)_n$, which is a modification of $AlEt_3-H_2O$ catalyst, tends to give stereoregular polymers while a related organozinc catalyst $(Et(ZnO)_2ZnEt)$, which is $ZnEt_2-H_2O$ catalyst, has little capability for stereoregulation. It is of interest to examine stereoregulation when ester group was introduced to the side chain of the lactone, because ester group of lactone ring might compete with that of side chain in coordination.

Thus, it was found that structurally isomeric polymers were formed by the ring opening polymerization of β-(2-acetoxyethyl)-β-propiolactone with $(EtAlO)n$ and $Et(ZnO)_2ZnEt$ catalyst. That is, the Al-catalyst catalyzed normal polymerization leading to the poly-β-ester, and the Zn catalyst formed isomerized poly-δ-ester as main product. The polymer structure was determined by NMR, T_1-value, thermal decomposition product and T_g. The dependence of the isomerization ratio on the structure of terminal substituent groups in the side-chain, and the reaction mechanism were examined.

References

1. H. Kakiuchi, "Epokishi Jushi" p.3, (1977), Shoko-do, printed in Japan; K. Hashimoto, "Epokishi Jushi" p.37 (1969), Nikkan Kogyo Shinbunsha, printed in Japan; P. B. Kekky, J. Appl. Polymer Sci., 6, 425 (1962); W. Erich, M. Bodnar, ibid., 3, 296 (1960); Shell Chemical Corp., Technical Literature; H. Lee, K. Neville, "Handbook of Epoxy Resins", McGraw-Hill, (1967); R. L. De Hoff, Corrosion, 17, 83 (1961); M. B. Neiman, J. Polymer Sci., 56, 383 (1962); H. Hirsch, F. Koved, Mod. Plastics, 42, 133 (1964); W. Colletti, L. Rebori, Insulation, 11, 27 (1965); E. Klopfenstein, H. Lee, Insulation, 4, 13 (1958).

2. P. Noak, M. Saure, Kunststoffe, 54, 557 (1964); F. X. Ventrice, Mod. Plastics, 45, 201 (1967); H. L. Vincent, P. E. Oppliger and C. L. Frye, ACS Preprints "Organic coating and plastics chemistry", 28, 504 (1968); J. Clark, D. D. Perrin, Quart. Rev. 18, 295 (1964); H. K. Hall, J. Am. Chem. Soc., 79, 5441 (1957); W. A. Henderson, C. A. Streuli, J. Am. Chem. Soc., 82, 5791 (1960); E. S. Narracott, Brit. Plastics, 26, 120 (1966); J. J. Harris, S. C. Temin, J. Appl. Polymer Sci., 10, 523 (1966); A. S. Sherr, A. A. Krupnik, J. Appl. Polymer Sci., 9, 2707 (1965).

3. A. S. Eastham, Fortschr. Hochpolymer-Forsch., 2, 18 (1960)

4. S. Perry, H. Hibbert, Can. J. Res., $\underline{8}$, 102 (1933)

5. H. Staudinger, H. Lehmann, Ann., $\underline{505}$, 41 (1933)

6. A. E. Gurgiolo, U. S. Pat., 2,934,505;

    W. L. Bresslar, A. E. Gurgiolo, U. S. Pat.,

    2,917,470

7. R. O. Colclough, G. Gee, W. C. E. Higginson,

    J. B. Jackson, M. Litt, J. Polymer Sci., $\underline{34}$, 171

    (1959); N. Nakaniwa, K. Ozaki, J. Furukawa, Macromol.

    Chem., $\underline{138}$, 197 (1970)

8. K. E. Russell and L. G. M. C. Vail, Can. J. Chem.,

    $\underline{57}$, 2355 (1979); R. F. Bauer, R. T. LaFlair and

    K. E. Russell, Can. J. Chem., $\underline{48}$, 1251 (1970)

9. R. M. Salinger and R. West, J. Organometal. Chem.

    $\underline{11}$, 631 (1968)

10. H. M. Bank, U. S. Pat. 3971747

11. H. A. Benesi, J. Phys. Chem., $\underline{61}$, 970 (1957);

    R. H. Hansford, Ind. Eng. Chem., $\underline{39}$, 849 (1947);

    C. L. Thomas, Ind. Eng. Chem., $\underline{41}$, 2564 (1949);

    M. W. Tamele, Discussions Faraday Soc., $\underline{8}$, 270 (1960);

    P. B. Venuto, L. A. Hamilton and P. S. Landis, J.

    Catalysis, $\underline{5}$, 484 (1966); G. T. Kerr, ibid., $\underline{15}$,

    200 (1969); W. K. Hall, Chem. Eng. Progr. Symp.

    Ser., $\underline{63}$, 68 (1967)

12. P. Suppan, Principles of Photochemistry, The Chemical

    Society Monographs, No.22, The Chemistry Society

    Publications (1972), T. Matuura, "Yuki Hikari Kagaku",

Chemistry Monograph No.20, p.179, Kagaku Dojin, Kyoto (1976)

13. J. V. Crivello, J. H. W. Lam, J. E. Moore and S. H. Schroster, J. Radiat. Curing, 5, 2 (1978); J. V. Crivello, J. H. W. Lam, Macromolecules, 10, 1307 (1977); J. V. Crivello, J. H. W. Lam, J. Polymer Sci., Polym. Chem. Ed., 17, 2877 (1979); ibid., 17, 1047 (1979); ibid., 1021 (1980); ibid., 17, 977 (1979); ibid., 16, 2441 (1978)

14. A. G. Brook, J. Am. Chem. Soc., 82, 5102 (1960); ibid., 91, 355 (1969)

15. J. Libman, J. Chem. Soc., Chem. Comm., 868 (1977); R. Hurley, A. C. Test, J. Am. Chem. Soc., 88, 4330 (1966); J. A. Barltop, N. J. Bunce, J. Chem. Soc., (C), 1467 (1968)

16. K. Teranishi, T. Araki and H. Tani, Macromolecules, 5, 660 (1972); H. Tani, S. Yamashita and K. Teranishi, Polym. J., 3, 417 (1972); K. Teranishi, M. Iida, T. Araki, S. Yamashita and H. Tani, Macromolecules, 7, 421 (1974); M. Iida, T. Araki, K. Teranishi and H. Tani, Macromolecules, 10, 275 (1977); M. Iida, S. Hayase and T. Araki, Macromolecules, 11, 490 (1978)

Chapter 2   New Polymerization Catalyst

2-1   Introduction

From the concept of new catalyst described in Chapter 1, a new composite polymerization catalysts were found. In this Chapter, profiles of the catalyst are described.
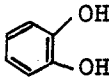
2-2   Profiles of the composite catalysts

The new catalytic systems are composed of an aluminum complex and a silanol compound. As shown in Table 1. conversion in polymerization of cyclohexene oxide with $Al(acac)_3/Ph_2Si(OH)_2$ catalyst is compared with that with other catalyst systems: metal complex/$Ph_2Si(OH)_2$ or $Al(acac)_3$/hydroxy compound.

The metal complex or $Ph_2Si(OH)_2$ alone was not active in the polymerization. However, the addition of $Ph_2Si(OH)_2$ to the metal complex catalytically polymerized cyclohexene oxide. $Al(acac)_3$ and $Al(O-iPr)_3$ had high activity when they were combined with $Ph_2Si(OH)_2$. The resulting poly(cyclohexene oxide)(soft temp. (50°C)) had about 4400 molecular weight by ger permeation chromato-graphy. A polymer prepared with conventional cationic catalysts (OEt_3BF_4 and $BF_3 \cdot OEt_2$) was tacky and the mo-lecular weight was only 900.

Composite systems of $Al(acac)_3$ with mono- and difunc-tional alcohols, phenols and monofunctional thiol were

Table 1 Polymerization of Cyclohexene Oxide by Various Catalyst Systems[a]

Metal compound	-OH compound	Polymerization time (h)	Polymer yield(%)	MW
—	$Ph_2Si(OH)_2$	40	0	—
$Al(acac)_3$	—	46	0	—
$Al(OiPr)_3$	—	46	0	—
BF_3OEt_2[b]	—	46	70	900
$TiO(acac)_2$	$Ph_2Si(OH)_2$	46	12	3200
$Cr(acac)_3$	$Ph_2Si(OH)_2$	46	7	4000
$Zr(acac)_4$	$Ph_2Si(OH)_2$	46	4	1700
$Zn(acac)_2$	$Ph_2Si(OH)_2$	46	3	—
$Co(acac)_3$	$Ph_2Si(OH)_2$	50	3	3300
$Cu(acac)_2$	$Ph_2Si(OH)_2$	46	2	3300
$Fe(acac)_3$	$Ph_2Si(OH)_2$	50	2	2800
$Mn(acac)_2$	$Ph_2Si(OH)_2$	46	1	3000
$VO(acac)_2$	$Ph_2Si(OH)_2$	46	1	3000
$Ni(acac)_2$	$Ph_2Si(OH)_2$	46	0.5	4000
$Al(OiPr)_3$	$Ph_2Si(OH)_2$[c]	47	16	4400
$Al(acac)_3$	$Ph_2Si(OH)_2$	40	30	4400
OEt_3BF_4[d]	—	40	9	—
$Al(acac)_3$	PhSH	40	0	—
$Al(acac)_3$	Ph_3CSH	40	0	—
$Al(acac)_3$	PhOH	40	0	—
$Al(acac)_3$	Ph_3COH	40	0	—
$Al(acac)_3$	EtOH	40	0	—
$Al(acac)_3$	$HOCH_2CH_2OH$	40	0	—
$Al(acac)_3$	Ph_3SiOH[e]	20	52	—
$Al(acac)_3$	(catechol, benzene ring with OH and OH)	20	0	—
$Al(acac)_3$	Ph_3GeOH	5	0	—
$Al(acac)_3$	Ph_3SnOH	5	0	—

[a]Polymerization temperature, 40°C; catalyst concentration, metal compound, 0.05 mol%; OH compound, 0.15 OH equivalent %.

[b]0.01 mol%.

[c]0.05 OH equivalent %.

[d]0.2 mol%.

[e]0.05 OH equivalent %.

inactive for the polymerization of cyclohexene oxide.
Salinger and West[1] reported the acidity of various silanols,
alcohols, phenols, and thiols by potentiometry and gave
the following sequence:

$$PhSH > Ph_3CSH > PhOH > Ph_3SiOH > Ph_3COH$$
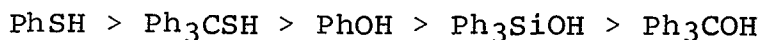
The acidity of $Ph_2Si(OH)_2$ appears to be between the values
for Ph_3SiOH and Ph_3COH. Among $Al(acac)_3$/hydroxy compound
systems only the $Al(acac)_3$/silanol system, such as
$Al(acac)_3/Ph_2Si(OH)_2$ and $Al(acac)_3/Ph_3SiOH$, was active in
the polymerization of cyclohexene oxide (Table 1) and the
catalyst activity of the $Al(acac)_3$/OH-containing systems
did not relate directly to the acidity of hydroxy com-
pounds.

West et al.[2] related the acidity of silanol to $p\pi$-
$d\pi$-orbital interaction between the vacant p-orbital of Si
and the p-orbital of oxygen. Therefore, the hydroxides
of Ge and Sn, which have electron configurations similar
to those of Si(IV group), could also be cocatalysts.
Among the systems, $Ph_3SiOH/Al(acac)_3$, $Ph_3GeOH/Al(acac)_3$,
and $Ph_3SnOH/Al(acac)_3$, however, only $Ph_3SiOH/Al(acac)_3$
catalyst showed catalytic activity. West et al.[2] also
reported that the $p\pi$-$d\pi$ interaction between metal and
oxygen decreased in the sequence Si-O > Ge-O > Sn-O.
The difference in catalytic activity is to be attributed
to the strength of the interaction.

Figure 1 shows the time-conversion curves when $Al(acac)_3/Ph_2Si(OH)_2$ and $Al(acac)_3/SH6018$ were used as catalysts. Polymerization with $Al(acac)_3/Ph_2Si(OH)_2$ catalyst was initially fast but stopped at low conversion. On the other hand, polymerization with $Al(acac)_3/SH6018$ catalyst continued for a longer time. The difference in catalytic activity between $Ph_2Si(OH)_2$ and SH6018 may be due to the polymer effects described in Chapter 7. Figure 1 also shows a time-conversion curve in which additional SH6018 was added to the polymerization system at the point at which the polymerization rate became slow. In this case polymer conversion increased at the point of SH6018 addition. Addition of $Al(acac)_3$, however, did not increase polymer conversion. From the above the decrease in polymer conversion probably occurs because the silanol is consumed. Thus silanol probably plays an important role in the polymerization of cyclohexene oxide.

Table 2 shows the influence of $Ph_2Si(OH)_2/Al(acac)_3$ ratio on polymer conversion, where the $Al(acac)_3$ is constant at 0.05 mol%. Polymer conversion increased in proportion to the $Ph_2Si(OH)_2/Al(acac)_3$ ratio. The molecular weight of polymers was constant at 4400. On the other hand, the influence of $Al(acac)_3/Ph_2Si(OH)_2$ ratio on polymer conversion, where $Ph_2Si(OH)_2$ is constant at 0.15 OH equivalent %, is also shown in Table 2. Polymer yield was decreased with an increase in the $Al(acac)_3/Ph_2Si(OH)_2$
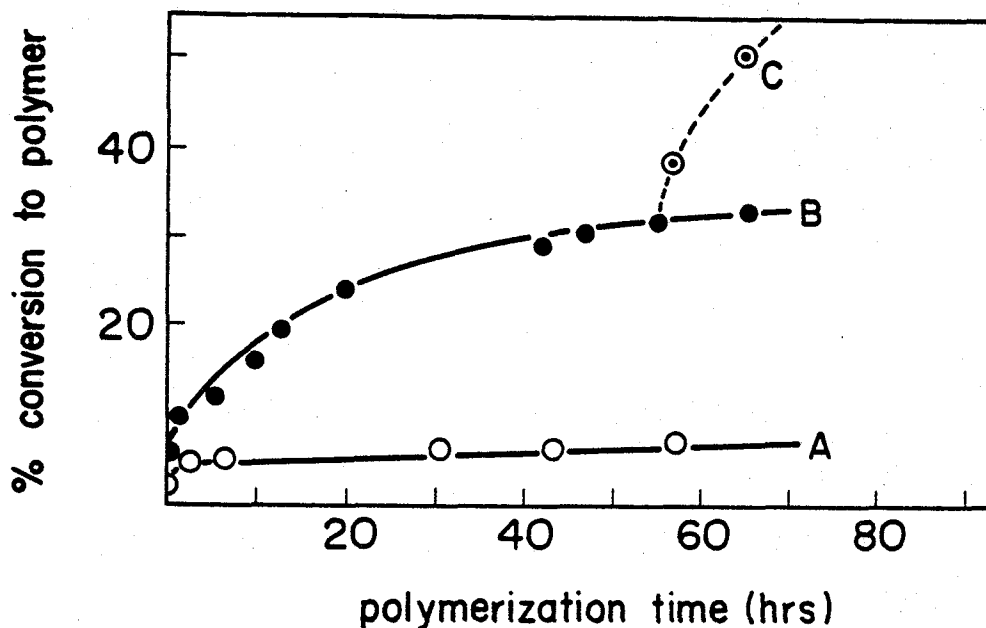
Figure 1   Polymerization of cyclohexene oxide: poly-
merization temperature, 40°C; Al(acac)$_3$, 0.05 mol%;
Ph$_2$Si(OH)$_2$, 0.05 OH equivalent %; SH6018, 0.05 OH
equivalent %.   (A) Al(acac)$_3$/Ph$_2$Si(OH)$_2$;
(B) Al(acac)$_3$/SH6018;   (C) addition of more SH6018
to (B) at 55 h (0.05 OH equivalent %).

Table 2   Polymerization of Cyclohexene Oxide[a]

Al(acac)$_3$ mol %	Ph$_2$Si(OH)$_2$ mol %	Polymerization time (h)	conversion (%)	M.W.
0.05	0.05	1	5	4400
0.05	0.10	1	9	4400
0.05	0.15	1	12	4400
0.05	0.20	1	17	4400
1.5	0.075	86	27	-
3.0	0.075	86	24	-
8.7	0.075	86	20	-

a) polymerization temperature 40°C.

ratio. This polymerization behavior is explained by a
decrease in SiOH in the polymerization system which is
consumed by the side reactions discussed in Chapter 3.

References

1. R. M. Salinger and R. West, J. Organometal. Chem. 11,
   631 (1968)

2. R. West and R. H. Baney, J. Am. Chem. Soc., 81, 6145
   (1959)

Chapter 3   Dependence of Catalytic Activity on Silanol

Structure

3-1   Introduction

Profile of polymerization of cyclohexene oxide with Al(acac)$_3$/Silanol catalyst showed that silanol plays an important role for the polymerization. In this Chapter, the structure of silanol was varied, and the dependence of the catalyst activity on the structure of silanol was described.

3-2   Stability of silanol compounds in self-condensation

Silanols are unstable and in some cases condense to oligo or polysiloxanes. The stability of the silanols used as cocatalysts was examined in THF in the presence of Al(acac)$_3$, shown in Figure 1. Disubstituted Si compounds like Ph$_2$Si(OH)$_2$ and MePhSi(OH)$_2$ were thermally unstable, but trisubstituted compounds like Et$_3$SiOH, Ph$_3$SiOH, MePh$_2$SiOH, and Me$_2$PhSiOH were relatively stable. These compounds did not condense under polymerization conditions. Therefore polymerization behavior was examined by using trisubstituted compounds as cocatalysts to eliminate any effect due to self-condensation.
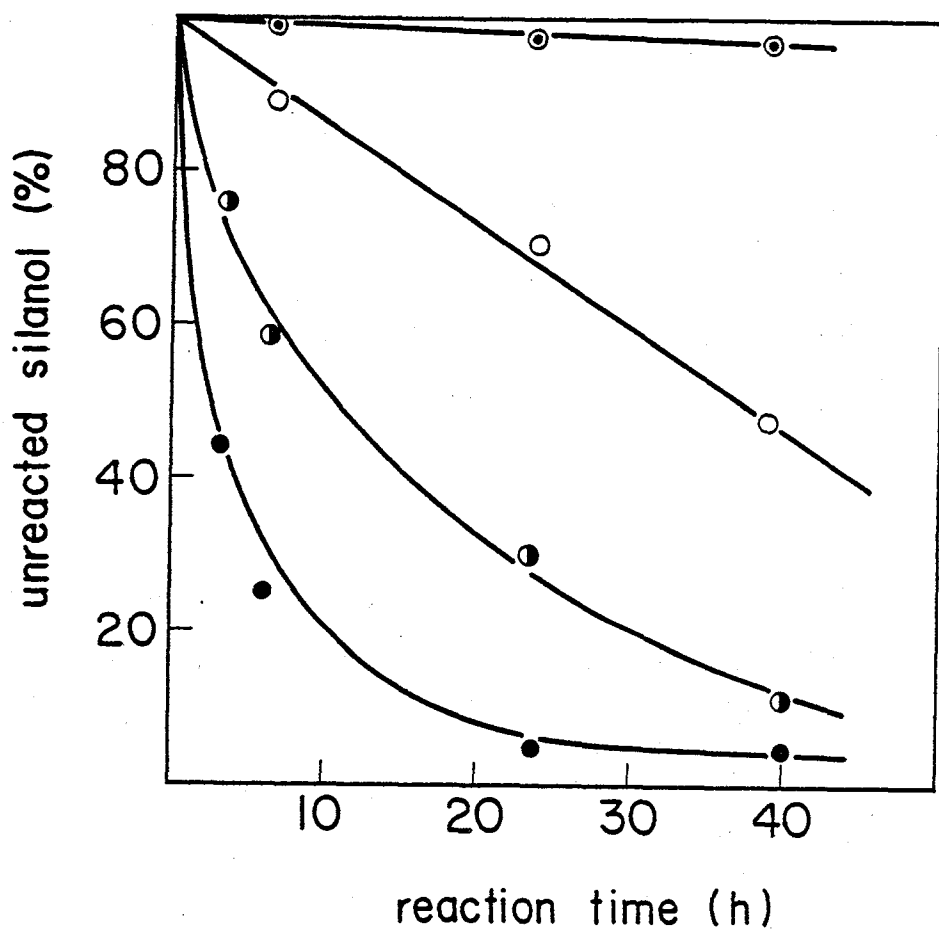
Figure 1   Stability of various silanols: (—●—)
MePhSi(OH)$_2$-Al(acac)$_3$; (—◐—) EtPhSi(OH)$_2$-
Al(acac)$_3$; (—○—) Ph$_2$Si(OH)$_2$-Al(acac)$_3$; (—◉—)
R$_3$SiOH-Al(acac)$_3$; R$_3$SiOH; Ph$_3$SiOH, Ph$_2$(CH$_2$=CH)SiOH,
MePh$_2$SiOH, Me$_2$PhSiOH, Et$_3$SiOH.

3-3 Polymerization behavior with Al(acac)₃-R₃SiOH

catalyst

Figure 2 shows the conversion-time curve of polymer with Al(acac)$_3$-R$_3$SiOH catalysts. The catalytic activity for silanols with electron-with-drawing substituents like Ph$_3$SiOH or Ph$_2$(CH$_2$=CH)SiOH was higher than that for silanols with electron-donating substituents like MePh$_2$SiOH or Me$_2$PhSiOH. The relationship between the relative acidity of these cocatalysts and the relative catalytic activity is described in Figure 3. The abscissa shows the difference in ^{1}H-NMR chemical shift between the SiOH signal measured in d$_6$-DMSO and that measured in CDCl$_3$ as the relative acidity. The ordinate shows the initial rate of polymerization, when the rate with Al(acac)$_3$-Ph$_3$SiOH catalyst is 1, as the catalytic activity. Apparently, the larger the relative acidity of silanol, the higher the relative catalytic activity.

In Figure 2 polymerization behavior with Al(acac)$_3$/Ph$_3$SiOH catalyst is different from the behavior with Al(acac)$_3$/Ph$_2$(CH$_2$=CH)SiOH catalyst; that is, the former polymerization continued with time but the latter stopped at low conversion. Cyclohexene oxide was polymerized by 10 mol% of Al(acac)$_3$ and 10 mol% of silanol in d$_8$-THF, and the polymerization behavior was examined by ^{1}H-NMR to determine the difference. The intensity of signal due to SiOH decreased with polymerization time, but the rate of
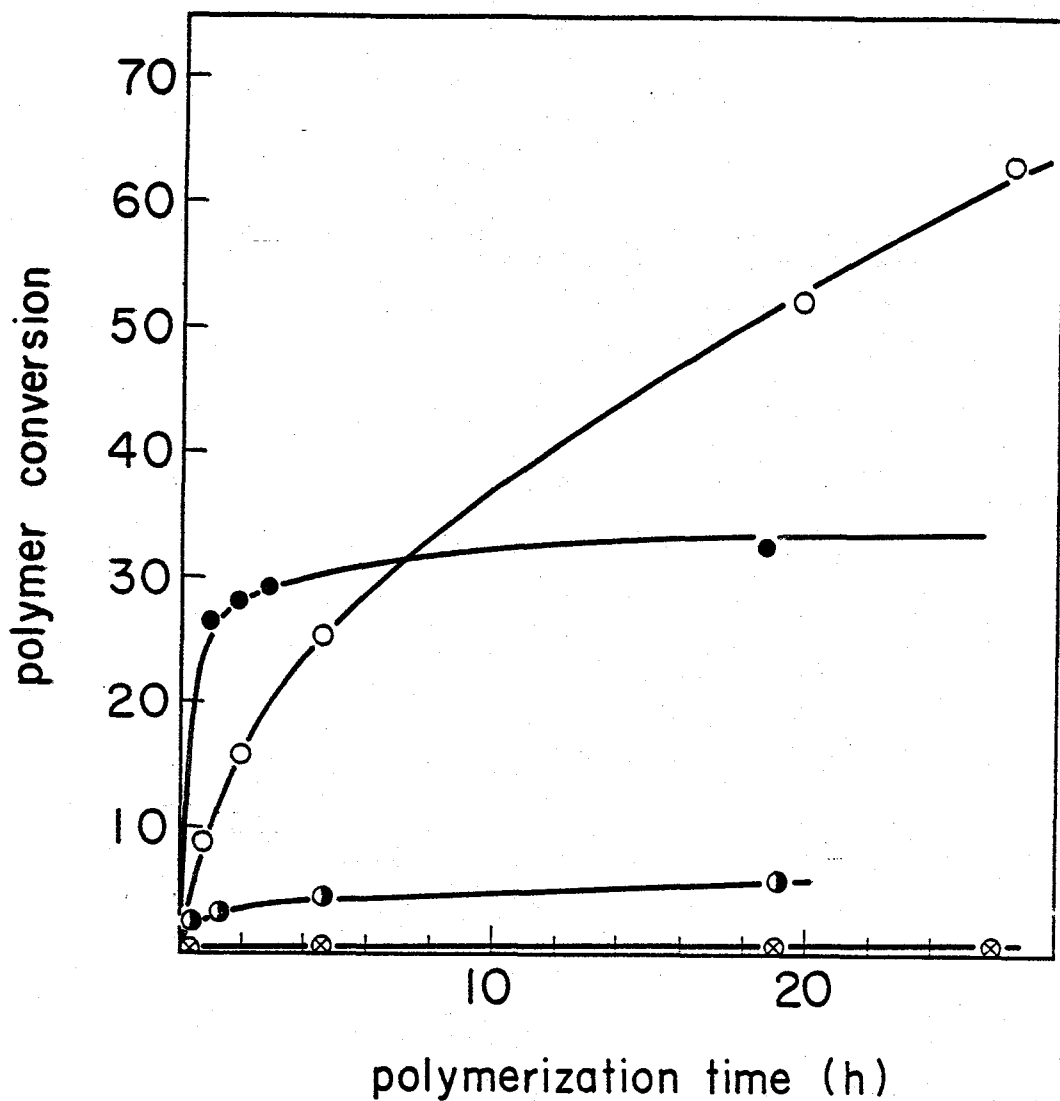
Figure 2   Polymerization of cyclohexene oxide: (—O—)
Ph$_3$SiOH-Al(acac)$_3$;   (—●—) Ph$_2$(CH$_2$=CH)SiOH-Al(acac)$_3$;
(—◐—) MePh$_2$SiOH-Al(acac)$_3$;   (—⊗—) Me$_2$PhSiOH-
Al(acac)$_3$.   Al(acac)$_3$ 0.05 mol%, silanol 0.05 mol%,
40°C,
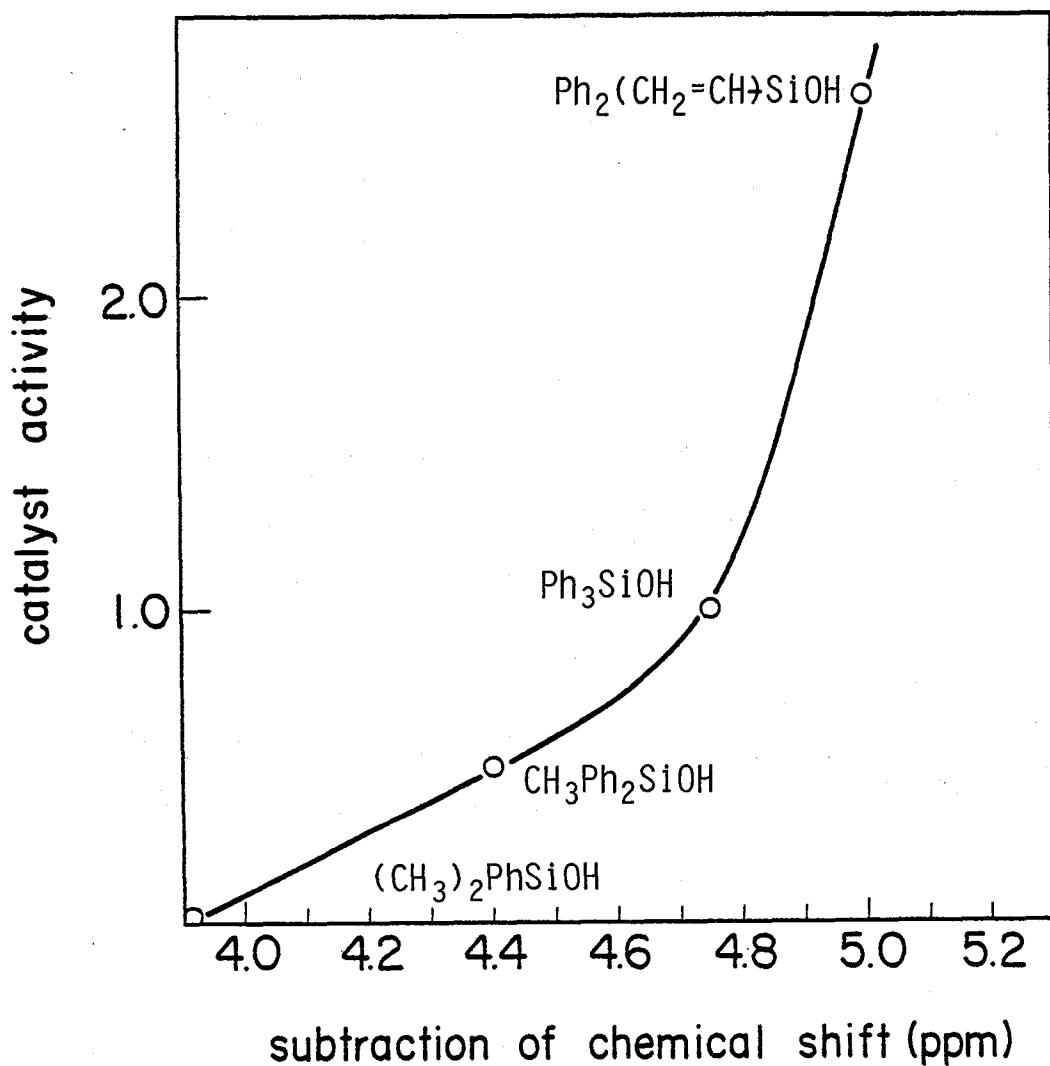
Figure 3   Relation between the relative catalytic ac-
   tivity and the relative acidity.   Relative catalytic
   activity: the rate with Al(acac)$_3$-Ph$_3$SiOH catalyst
   = 1.   Polymerization conditions, see Figure 2.

decrease with Ph_3SiOH was smaller than the corresponding rate with $MePh_2SiOH$ and $Ph_2(CH_2=CH)SiOH$, as shown in Figure 4. It was believed that these decreases were not caused by self-condensation of silanols (Fig. 1) but by the addition of the silanol to the epoxide. In case of $Al(acac)_3/Ph_3SiOH$ catalyst the polymerization continues with time because steric hindrance makes it difficult to add Ph_3SiOH to epoxide. In case of $Al(acac)_3/MePh_2SiOH$ and $Al(acac)_3/Ph_2(CH_2=CH)SiOH$ catalysts, however, $Ph_2(CH_2=CH)SiOH$ and $MePh_2SiOH$ add to the epoxide more easily than Ph_3SiOH because of the reduced steric hindrance.

Figure 5 shows that the molecular weight of the polymer obtained by $Al(acac)_3-Ph_3SiOH$ catalyst is larger than that obtained by $Al(acac)_3-MePh_2SiOH$ catalyst. The termination step may be slower with the bulky silanol.

3-4 Kinetics of polymerization with $Al(acac)_3-Ph_3SiOH$ catalyst

The polymer conversion was plotted against the polymerization time to find a first order of concentration of cyclohexene oxide (Fig. 6).

The k (rate constant) was determined by the slope in Figure 6 and log k was plotted against log (silanol) (concentration of silanol), as shown in Figure 7. The reaction order n of the concentration of silanol was about
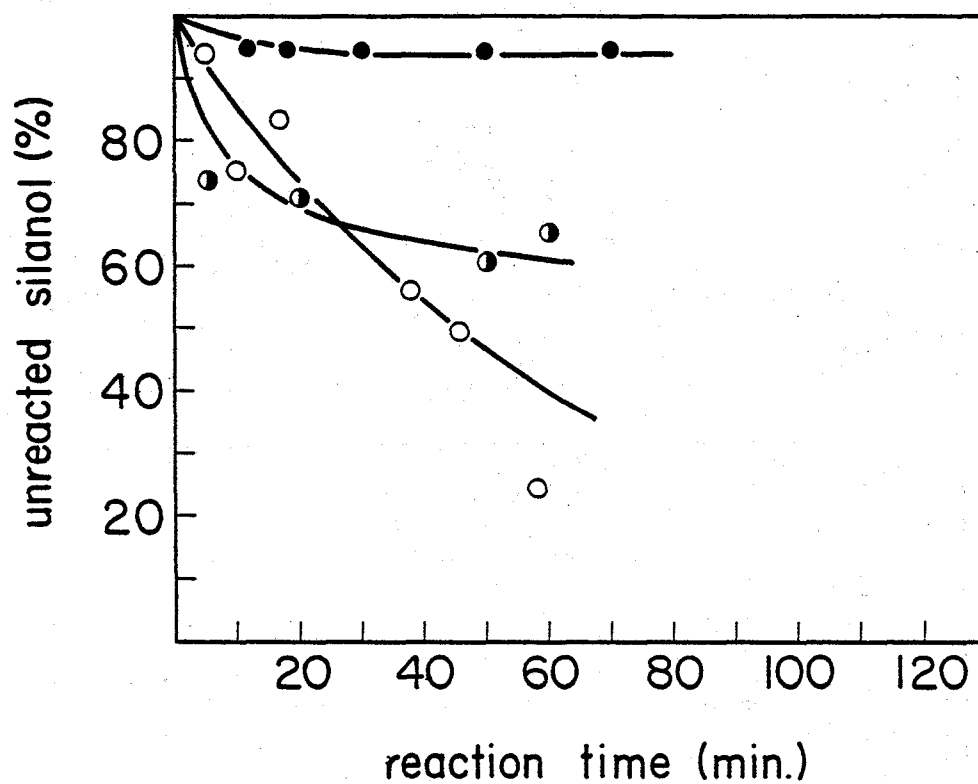
Figure 4   Decrease in silanol compounds in the polymeri-
    zation system: ($—\bullet—$) $Ph_3SiOH/Al(acac)_3$; ($—\mathbb{O}—$)
    $MePh_2SiOH/Al(acac)_3$; ($—\circ—$) $Ph_2(CH_2=CH)SiOH/$
    $Al(acac)_3$
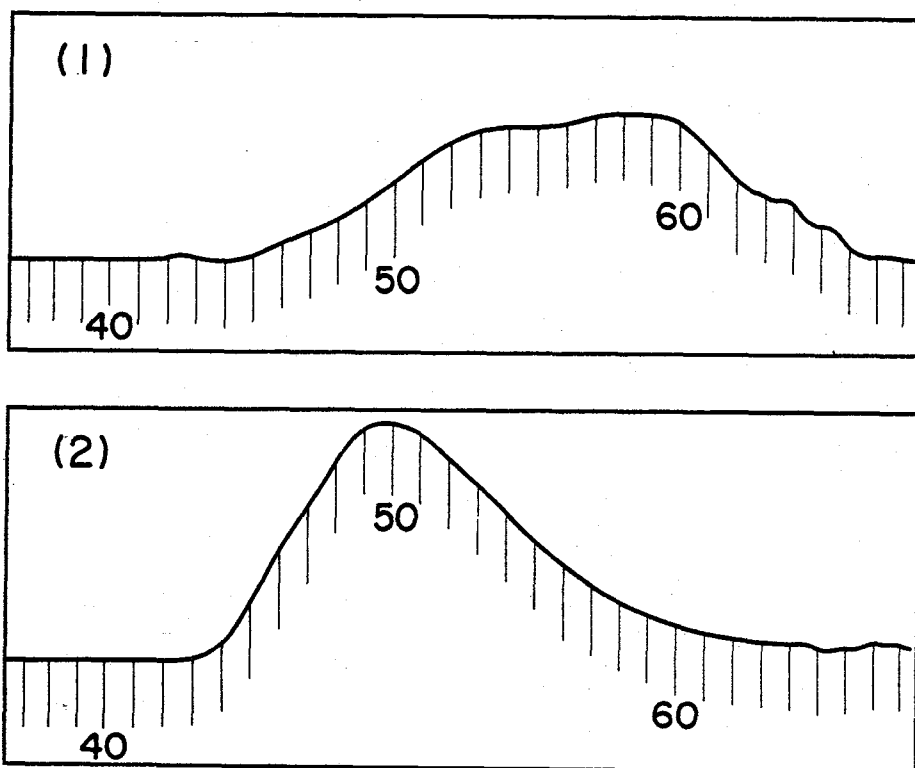
Figure 5   GPC curves of polycyclohexene oxide:

(1) $Ph_2MeSiOH/Al(acac)_3$; (2) $Ph_3SiOH/Al(acac)_3$
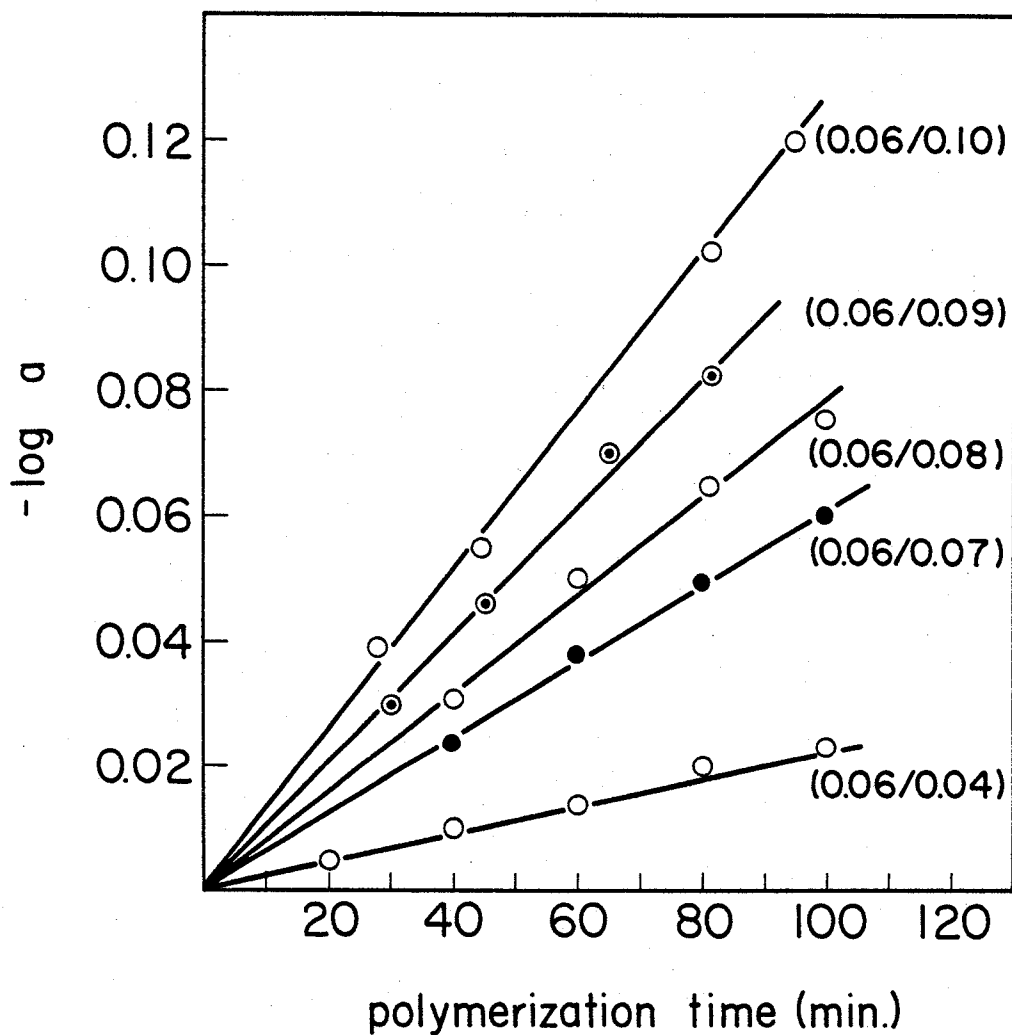
Figure 6   First-order plot of cyclohexene oxide
    polymerization.   The values in parentheses show
    catalytic concentration $(Al(acac)_3/Ph_3SiOH)$
    (mol%/mol%): (a) polymer conversion.
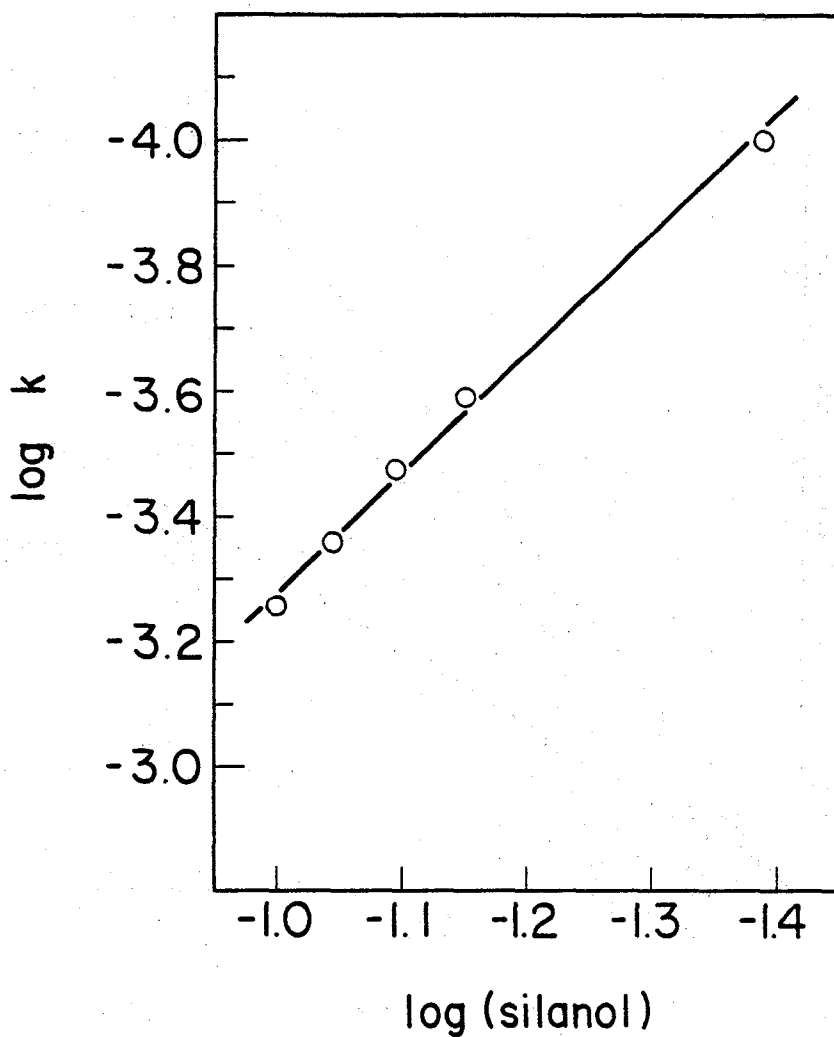
Figure 7   Relation between log k and log (silanol):
  k; rate constant, (silanol); concentration of
  silanol.

1.9 from the slope. Therefore it is believed that two silanol groups participate in the polymerization reaction.

3-5   Interaction of silanol with $Al(acac)_3$

$Al(acac)_3$ could not react with silanol and could not form another compound before polymerization, a condition supported by the fact that the signal of $Al(acac)_3$ did not change when the polymerization catalyzed by 10 mol% of $Al(acac)_3$ and Ph_3SiOH was followed by ^1H-NMR. Therefore it is believed that the interaction between $Al(acac)_3$ and silanol is important for polymerization. When the ^1H-NMR spectrum of the Ph_3SiOH alone was measured in $CDCl_3$ the sharp signal of SiOH was observed. This signal shifted to a lower field and broadened when $Al(acac)_3$ was added. The shift was larger as the $Al(acac)_3/Ph_3SiOH$ ratio was increased, as shown in Table 1. Measured at the same concentration, the value of the shift decreased in the following sequence: $Al(acac)_3$-Ph_3SiOH > $Al(acac)_3$-$Ph_2MeSiOH$ > $Al(acac)_3$-Ph_3GeOH, which related to the catalytic activity.

3-6   Conclusion

The results showed that in order to obtain active catalyst, it was necessary to strengthen the acidity of the silanol, to prevent the silanol from self-condensa-

Table 1   Chemical Shift of OH Signal[a]

| OH compound | Presence of Al(acac)$_3$ | | Absence of Al(acac)$_3$ | | (A)−(B) or (C)−(B) (ppm) |
	Al(acac)$_3$ / OH compound (mol/mol)	in CDCl$_3$ (C) (ppm)	in CDCl$_3$ (B) (ppm)	in DMSO (A) (ppm)	
Ph$_3$SiOH	1/3[b]	2.49	2.36	—	0.13
Ph$_3$SiOH	2/3[b]	2.55	2.36	—	0.19
Ph$_3$SiOH	1[b]	2.60	2.36	—	0.24
Ph$_3$SiOH	4/3[b]	2.63	2.36	—	0.27
MePh$_2$SiOH	1/3[b]	2.11	2.03	—	0.08
MePh$_2$SiOH	2/3[b]	2.16	2.03	—	0.13
MePh$_2$SiOH	1[b]	2.21	2.03	—	0.18
MePh$_2$SiOH	4/3[b]	2.24	2.03	—	0.21
Ph$_3$GeOH	1[b]	1.72	1.60	—	0.12
Ph$_3$SiOH	—	—	2.36	7.12	4.73
Ph$_3$GeOH	—	—	1.60	5.36	3.76
Ph$_3$SnOH	—	—	1.71	3.00	1.29

a) Measuring condition, 35°C.

b) Concentration of silanols was constant at 0.17 mol/L in CDCl$_3$.

tion and to prevent the silanol from the addition to epoxide, which terminated the polymerization. To realize such properties, it seems necessary to introduce an electron-withdrawing group and a bulky group in the neighbour of silanol moiety. Silanols such as diphenylsilanediol, triphenylsilanol and diphenylvinylsilanol were effective as an active catalyst component.

Chapter 4   Dependence of Catalytic Activity in the
Structure of Chelating Ligand on Aluminum

4-1 Introduction

The polymerization of cyclohexene oxide with various metal compound/diphenylsilanediol catalyst systems has been examined. Since the catalysts were deactivated after a certain period, the catalyst deactivation caused by self-condensation of diphenylsilanediol and the addition to epoxides had to be considered. Therefore, the catalyst activity was examined with a triphenylsilanol which does not self-condense and add to epoxides easily, as shown in Table 1. The catalyst activity varied with identity of metal chelates, as follows: $Al(acac)_3$ > $SnCl_2(acac)_2$ > $MoO_2(acac)_2$ > $Zr(acac)_4$ > $Cr(acac)_3$ > $Fe(acac)_3$ > $Rh(acac)_3$. In order to examine the interaction between these compounds and the triphenylsilanol, the half-value width of the SiOH in the triphenylsilanol was measured with ^{1}H-NMR in an equimolar solution of metal compound/triphenylsilanol in $CDCl_3$, as shown in Table 1. The polymer conversion correlated with the interaction strength. Table 1 also shows the relation between the polymer conversion and the interaction of $Al(acac)_3$-phenol, $Al(acac)_3$-thiphenol. The extent of the interaction between them was much smaller than that between the $Al(acac)_3$ and the triphenyl-silanol with lower acidity than that of the thiophenol or

Table 1　Polymerization of CHO with a Metal
Compound/Ph_3SiOH Catalyst[a]

Metal compound	Polymer conversion (%)	Half value width of silanol (Hz)
$Al(acac)_3$	100	24
$SnCl_2(acac)_2$	25.0	14
$MoO_2(acac)_2$	12.0	—
$Zr(acac)_4$	8.5	10
$Rh(acac)_3$	1.9	10
$Fe(acac)_3$	2.4	—
$Cr(acac)_3$	2.6	—
*$Al(acac)_3$-PhOH	0	8
*$Al(acac)_3$-PhSH	0	9

a) Polymerization conditions:　48 h at 40°C, metal
compound 0.05 mol%, Ph_3SiOH 0.05 mol%.

*PhOH or PhSH was added instead of the Ph_3SiOH.

the phenol.[1] The polymer conversion was also low. There-
fore, the interaction strength between them was not caused
by the acidity of OH compounds only. The interaction was
appreciable especially in the case of the combination be-
tween aluminum complex and silanol, and a high catalyst
activity was found.

4-2   Polymerization with a tris(β-diketonato)aluminum/
      triphenylsilanol system

      The results of the previous section implied that the
interaction between silanol and aluminum complex was im-
portant in order to activate the catalyst. Therefore,
the dependence of the structure of aluminum complex on
the catalytic activity and relation between the interac-
tion strength and the catalytic activity were investi-
gated. The catalyst activity was first examined with
tris(β-diketonato)aluminum/triphenylsilanol catalyst sys-
tem. The resultant initial polymerization rate, a half-
value width of SiOH and a weight-average molecular weight
are shown in Table 2. The catalyst activity for tris(β-
diketonato)aluminum with electron withdrawing groups
(trifluoromethyl, phenyl, p-fluorophenyl group) was low.
Especially, the catalyst activity was negligible for the
aluminum complexes with two electron withdrawing groups,
such as DFPhPD and PhFBD. The aluminum catalyst had
higher activity when electron donating groups were sub-

Table 2   Polymerization of CHO with a Tris(β-diketonato)aluminum/Ph$_3$SiOH Catalyst[a]

Abbreviation	Ligand	Polymn. rate (mol/min./mol cat.)	Half value width of SiOH (Hz)	$\overline{M_w}$ x 10^{-3}
DFPhPD	p-FC$_6$H$_4$COCH$_2$COp-FC$_6$H$_4$	0	—	—
PhFBD	CF$_3$COCH$_2$COPh	0	13	—
FPD	CF$_3$COCH$_2$COCH$_3$	0.6	19	17
PhPD	CH$_3$COCH(Ph)COCH$_3$	2.0	—	15
DMFHD	(CH$_3$)$_3$CCOCH$_2$COCF$_3$	1.4	10	16
acac	CH$_3$COCH$_2$COCH$_3$	3.7	24	16
BzBD	PhCH$_2$COCH$_2$COCH$_3$	0.8	—	15
TMPD	(CH$_3$)$_2$CHCOCH$_2$COCH(CH$_3$)$_2$	4.2	30	17
DPM	(CH$_3$)$_3$CCOCH$_2$COC(CH$_3$)$_3$	18.4	—	16
ACH	CH$_3$COCHCO(CH$_2$)$_4$	6.4	23	15

a) Polymerization conditions; 40°C, Al compound 0.05 mol%, Ph$_3$SiOH 0.05 mol%

stituted. Moreover, higher catalyst activity was observed
when the half value width of the SiOH signals increased
(see Table 2). The interaction between aluminum complex
and silanol was correlated with the catalytic activity.

4-3 Polymerization with tris(β-ketoesterato)aluminum/
triphenylsilanol system

pk$_a$ of ethylacetoacetate is 11.2 and larger than
that of acethylacetone (9.76).[2] Therefore electron den-
sity of carbonyl oxygen of tris(ethylacetoacetato)aluminum
was considered to be larger than that of tris(acethyl-
acetonato)aluminum and high activity was expected. As
shown in Table 3, improvement in the catalytic activity
was found when tris(β-ketoesterato)aluminum was used.
The catalyst activity was also enhanced by introducing an
electron donating group. It decreased when a phenyl
group was introduced to the ligand and increased when a
methyl group was substituted. The introduction of an
alkyl group to ester moiety of the ligand was also effec-
tive for the catalytic activation.

The molecular weight for the polymer obtained with
catalysis of tris(β-ketoesterato)aluminum/triphenylsilanol
was higher than that obtained with tris(β-diketonato)-
aluminum/triphenylsilanol. The variation in ligand prop-
erties did not appreciably change the molecular weight.
The ^{1}H-NMR spectrum of a mixture of tris(β-ketoesterato)-

Table 3　Polymerization of CHO with a Tris(β-ketoesterato)aluminum/Ph$_3$SiOH Catalyst[a]

abbreviation	Ligand	Polymn. rate (mol/min./mol cat.)	$\overline{M_w}$ x 10^{-3}
EtPhPD	PhCOCH$_2$COOC$_2$H$_5$	4.2	29
Etaa	CH$_3$COCH$_2$COOC$_2$H$_5$	7.0	31
nPraa	CH$_3$COCH$_2$COOC$_3$H$_7$	9.8	30
iBuaa	CH$_3$COCH$_2$COOC$_4$H$_9$	12.6	31
EtMtaa	CH$_3$COCH(CH$_3$)COOC$_2$H$_5$	8.8	31
tBuaa	CH$_3$COCH$_2$COOC(CH$_3$)$_3$	13.0	30

a) Polymerization conditions;　40°C, Al compound 0.05 mol%, Ph$_3$SiOH 0.05 mol%

aluminum and triphenylsilanol showed that a part of the
ligand was free, as shown in Figure 1. This was not ob-
served in case of the tris(β-diketonato)aluminum/triphenyl-
silanol system. The amount of free ligand reached equili-
brium values at 15 - 20 mol%, (Al(Etaa)$_3$: 18 mol%, Al
Al(nPraa)$_3$: 18 mol%, Al(iBuaa)$_3$: 20 mol%, Al(tBuaa) :
15 mol%) within ten minutes after mixing equimoles of
tris(β-ketoesterato)aluminum with triphenylsilanol at
25°C. The free ligand ratio did not change appreciably
by the ligand variation.

4-4   Polymerization with a tris(*ortho*-carbonylphenolato)

    aluminum/triphenylsilanol catalyst systems

    The above results implied that a species of an alu-
minum compound, obtained after the aluminum complex
reacted with triphenylsilanol, was more active in the
presence of triphenylsilanol. Therefore, the catalytic
activity of a tris(*ortho*-carbonylphenolato)aluminum/
triphenylsilanol catalyst system was investigated to
determine the relation between the catalytic activity
and the molar ratio of the liberated ligand.

    Resultant polymerization results are shown in Table
4. The extent of the ligand liberation was measured only
in case of tris(salicylaldehydato)aluminum as 25 mol%.
The catalytic activity of tris(*ortho*-carbonylphenolato)-
aluminum/triphenylsilanol was generally higher than that
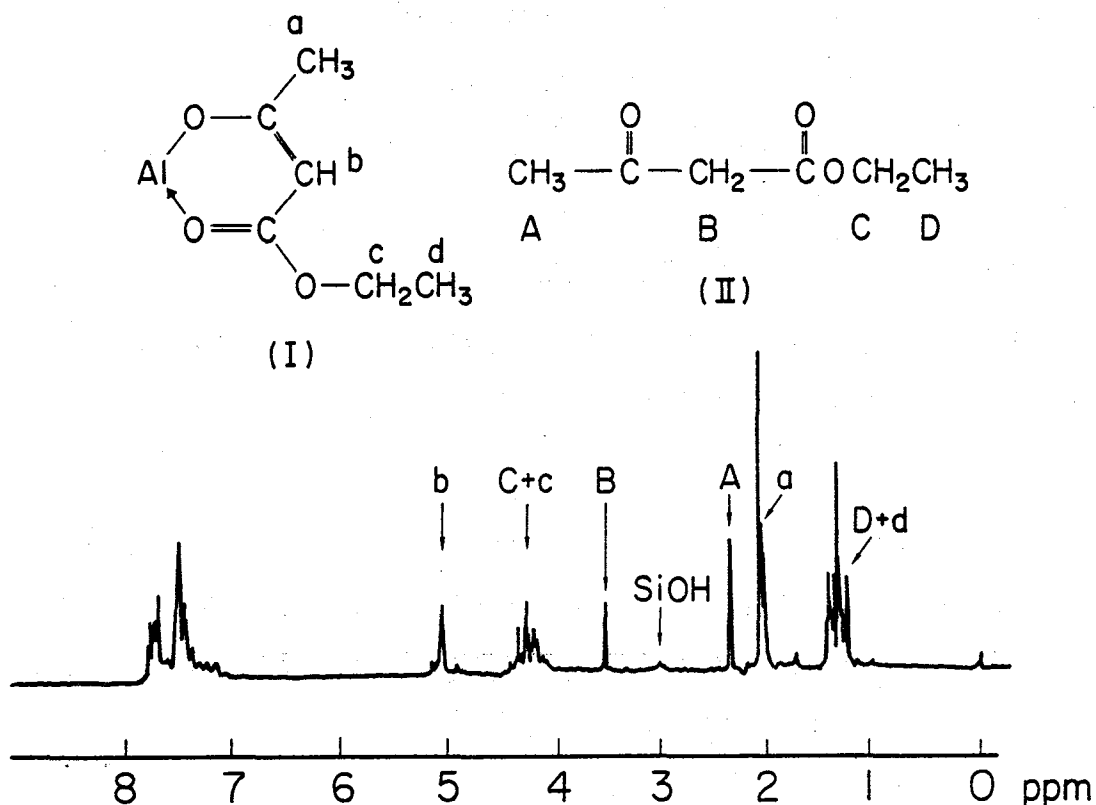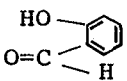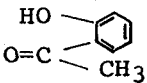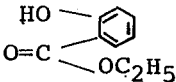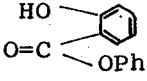
Figure 1 ^{1}H-NMR spectrum for Al(Etaa)$_3$/Ph$_3$SiOH catalyst system:

Capital letter: signal of liberated ligand.

Small letter: signal of Al(Etaa)$_3$. Refer to the experimental section for the measurement of interaction strength between aluminum complex and silanol.

Table 4   Polymerization of CHO with a Tris(*ortho*-carbonylphenolato) aluminum/Ph$_3$SiOH Catalyst[a)]

Abbreviation	Ligand	Polymerization rate (mol/min./mol cat.)	$\overline{M_w}$ x 10^{-3}
SA	HO—⬡ O=C—H	59	37
AP	HO—⬡ O=C—CH$_3$	74	35
EtSA	HO—⬡ O=C—OC$_2$H$_5$	112	37
φSA	HO—⬡ O=C—OPh	109	36
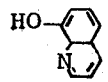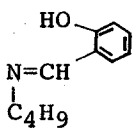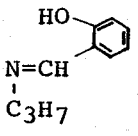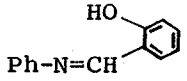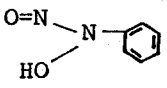
a) Polymerization conditions;   40°C, Al complex 0.05 mol%, Ph$_3$SiOH 0.05 mol%

of tris(β-ketoesterato)aluminum/triphenylsilanol or tris-(β-diketonato)aluminum/triphenylsilanol. The same substitution effect was also seen, namely, introduction of an electron donating group activated the catalyst. The weight-average molecular weight for the polymer, obtained with the tris(*ortho*-carbonylphenolato)aluminum/triphenylsilanol, was higher than that obtained with a tris(β-ketoesterato)aluminum/triphenylsilanol.

4-5 Polymerization with N, O-chelates of aluminum compound/triphenylsilanol catalyst system

The catalytic activity of N, O-chelates of aluminum compound was considered to be higher than that of O, O-chelating aluminum complex because a SiOH moiety would probably interact with the nitrogen stronger than the oxygen. However, a tris(oxinato)aluminum and a Schiff base-type aluminum complex with an alkyl group bonding to nitrogen did not have catalytic activity. Aluminum complex with a phenyl group, bonding to the coordinating nitrogen, had catalyst activity, as shown in Table 5. The substitution effect on the catalyst activity reversed as compared to the case of the O, O-chelated aluminum complex. This fact implied that the catalyst activity was retarded by strong interaction. A moderate interaction between an aluminum complex and a triphenylsilanol is required for the catalyst activity.

Table 5   Polymerization of CHO with a N,O-chelated Aluminum Complex/Ph3SiOH Catalyst[a]

Abbreviation	Ligand	Polymerization rate (mol/min./mol cat.)
OX	HO—[quinolin-8-ol structure]	0
SA·nBu	HO—[salicylaldehyde N=CH, C4H9 structure]	0
SA·nPr	HO—[salicylaldehyde N=CH, C3H7 structure]	0
SA·A	HO—[salicylaldehyde Ph-N=CH structure]	1.0
NPHA	O=N, HO—N—[phenyl structure]	3.4

a) Polymerization conditions;   40°C, Al complex 0.05 mol%, Ph3SiOH 0.05 mol%

4-6 Spin lattice relaxation time (T_1) for the ^{1}H-NMR

signal assigned to SiOH Group
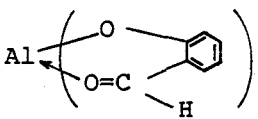
The interaction of a triphenylsilanol with an aluminum complex was considered to occur at the SiOH moiety. The T_1 value for ^{1}H-NMR signal assigned to SiOH was found to be influenced by the interaction strength.

The results are shown in Table 6. T_1 value for a triphenylsilanol in $CDCl_3$ was 2.5 seconds. On an equimolar addition of a tris(β-diketonato)aluminum to the triphenylsilanol in $CDCl_3$, the T_1 value of the SiOH peak decreased to 1.4 - 2.2 seconds. On the other hand, on addition of an equimolar quantity of a tris(β-ketoesterato)-aluminum or a tris(salicylaldehydato)aluminum, the T_1 value for the signal due to the SiOH decreased to 0.5 - 0.8 second. Namely, the interaction between a triphenylsilanol and the aluminum complex, which did not liberate the ligand, was smaller than that between a triphenylsilanol and the aluminum complex, which liberated the ligand.

4-7 Reaction scheme

In case of the tris(β-diketonato)aluminum, the ligand was not liberated by the reaction with a diphenylsilanediol. In an equimolar mixture of cyclohexene oxide, diphenylsilanediol and Al(acac)$_3$, the copolymer of the cyclohexene oxide and the diphenylsilanediol was obtained. An acetyl-

Table 6   Variation on T_1 Values for an NMR Signal Assigned
to the SiOH of the Ph$_3$SiOH in the Presence of an
Aluminum Complex[a]

Aluminum compound	T_1 (sec.)
——	2.5
Al(CH$_3$COCHCOCH$_3$)$_3$	1.9 ∿ 2.2
Al((CH$_3$)$_2$CHCOCHCOCH(CH$_3$)$_2$)$_3$	1.4 ∿ 2.2
Al(CH$_3$COCHCOOC$_2$H$_5$)$_3$	0.5
Al(CH$_3$COC(CH$_3$)COOC$_2$H$_5$)$_3$	0.7

0.8

a) T_1 values were determined with ten different times:
0.05, 0.10, 1.00, 1.50, 1.60, 1.70, 1.80, 1.90, 2.00, 10
second for Al(CH$_3$COCHCOOC$_2$H$_5$)$_3$/Ph$_3$SiOH, Al(CH$_3$COC(CH$_3$)COOC$_2$H$_5$)$_3$/

Ph$_3$SiOH, Al /Ph$_3$SiOH system. 0.05, 0.10, 0.50,

0.70, 1.00, 1.30, 1.50, 1.70, 2.00, 10 second for Ph$_3$SiOH,
Al(CH$_3$COCHCOCH$_3$)$_3$/Ph$_3$SiOH, Al((CH$_3$)$_2$CHCOCHCOCH(CH$_3$)$_2$)$_3$/
Ph$_3$SiOH system. T_1 values of Al(CH$_3$COCHCOCH$_3$)$_3$/Ph$_3$SiOH
and Al((CH$_3$)$_2$CHCOCHCOCH(CH$_3$)$_2$)$_3$/Ph$_3$SiOH system were
calculated from null point.

acetone residue was not involved in the copolymer. The signal of the Al(acac)$_3$ in the ^{1}H-NMR spectrum did not change during the polymerization with 10 mol% of the Al(acac)$_3$/triphenylsilanol catalyst system in d$_8$-THF. The catalytic activity correlated with the acidity of a trisubstituted silanol and the electronegativity of the C=O moiety for the aluminum complex. The catalyst activity also correlated with the interaction strength between a silanol and an aluminum complex. Interaction mechanism as shown in Figure 2 is proposed.

The SiOH proton is detached from the oxygen when the triphenylsilanol interacts with the tris(β-diketonato)-aluminum. The separated proton will cationically polymerize the cyclohexene oxide.

In an another initiation mechanism, a silanol interacts with an aluminum with a coordinative unsaturation, as shown in Figure 3.

According to this mechanism, an aluminum complex with electron withdrawing groups should be active because the chelate ring of the aluminum complex will easily be lost. However no such trend was observed.

When using a tris(β-ketoesterato)aluminum/triphenyl-silanol and a tris(*ortho*-carbonylphenolato)aluminum/triphenylsilanol catalyst, a part of the ligand was found to be liberated from the aluminum complex. The following compound was considered to be formed by the reaction be-

tween the catalyst components.

$$AlL_3 + nHOSiPh_3 \longrightarrow L_{3-n}Al(OSiPh_3)_n + nLH$$

$L_{3-n}Al(OSiPh_3)_n$ formation was confirmed with the IR absorbance of a Si-O-Al linkage (1070 cm^{-1}) in the product after an ethyl acetoacetate was removed from the reaction mixture of the tris(ethylacetoacetato)aluminum and the triphenylsilanol. However, a compound containing Al-O-SiR$_3$ linkages, such as $((CH_3)_3SiO)_3Al$, was not catalytically active at the low catalyst concentration, such as 0.05 mol%. Therefore, a SiOH moiety was considered to be necessary for the catalyst activity. Considering the interaction strength between an aluminum complex and a triphenylsilanol, as inferred with the T_1 measurement, interaction mechanism as shown in Figure 3 was proposed.

Thus, the silanol is activated at two points. The silanol is activated by the interaction of the aluminum with the oxygen of the SiOH and by the interaction of a oxygen in Al-O-Si linkage with the proton of the SiOH. Therefore, the interaction between the silanol and the aluminum complex would be stronger than that in the tris-(β-diketonato)aluminum/triphenylsilanol system. The reaction was similar to a silica-aluminum catalyst. The catalyst is considered to be a soluble model system of the silica-alumina catalyst.[3] The following facts suggest the new consideration. SiO_2-ZrO_2 and SiO_2-TiO_2
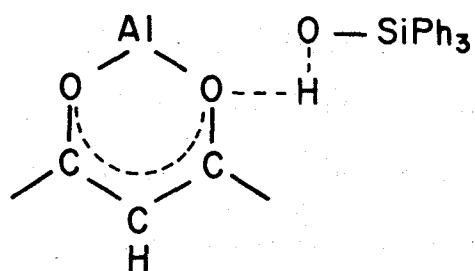
Figure 2

Interaction mechanism I

Figure 3
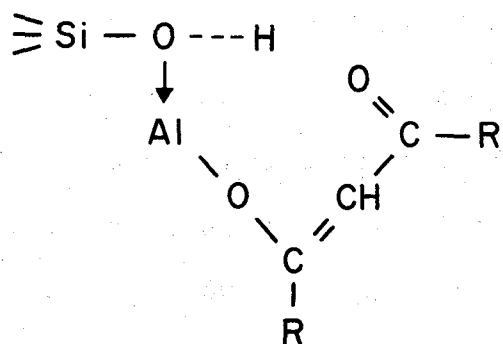
Interaction mechanism II

Figure 4
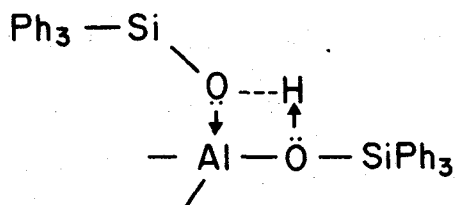
Interaction mechanism III

besides SiO_2-Al_2O_3 are as two component metal oxide cata-
lysts containing a strong acidity point.[4] The $Zr(acac)_3$/
silanol and $TiO(acac)_2$/silanol also polymerized a cyclo-
hexene oxide, however their activity was lower than the
$Al(acac)_3$/silanol system. As an unreacted aluminum com-
pound was also present in the polymerization system, the
interaction was considered to be caused by the interac-
tion mechanisms I and III.

Eastham et al. have reported a polymerization of
ethylene oxide with a BF_3-H_2O catalyst system. The poly-
merization was catalyzed by $H^+ \cdot [BF_4OH]^-$ species.[5]
Russell and Vail reported a $SnCl_4$-phenols catalyst system
for a cationic polymerization of a isobutene.[6] Here, the
polymerization was catalyzed by the activated proton of
phenols and a phenolate anion was present as a counter
anion. Termination was considered to be caused by the
attack of the phenolate ion or a proton transfer.[6] In the
present catalyst, a silanol is considered to play a simi-
lar role to that for the phenol. The mechanism of poly-
merization with the aluminum complex/silanol catalyst
could estimate from that with silica-alumina catalyst.

Initiation mechanism as shown in Figure 5 was con-
sidered. The initiation caused by H^+ similar to Brönsted
acid was supported by the fact that the polymer structure
obtained with the aluminum complex/silanol was atactic as
mentioned the following section. The silanolate anion
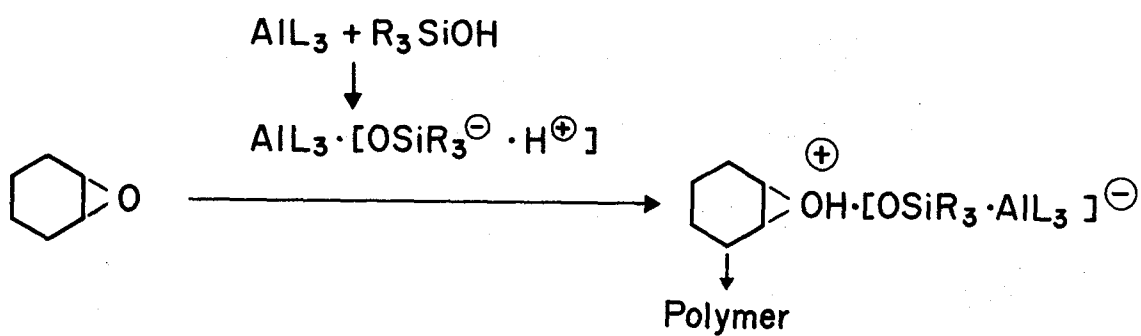
Figure 5   Polymerization mechanism

will be present as a counter anion.

The termination was considered to be caused by the silanolate anion addition to a polymer end. The presumption on the termination was supported by the following factors.

a) When a cyclohexene oxide was polymerized by 100 mol% of the Al(acac)$_3$/Ph$_2$Si(OH)$_2$ catalyst, a copolymer of cyclohexene oxide and Ph$_2$Si(OH)$_2$ was obtained. When a polymeric silanol, such as SH6018 (Toray silicone, molecular weight, about 1600), was used, a GPC curve of the polymer had two peaks. The higher molecular weight peak disappeared after NaOH treatment. This fact shows that the polymer had a C-O-Si≡ linkage due to the termination.

b) When the cyclohexene oxide was polymerized with the Al(acac)$_3$/trisubstituted silanol catalyst, the amount of silanol with less bulky substituents decreased with polymerization time in the polymerization system. However no such trend was observed when a silanol with bulky substituents was used. The molecular weight of the polymer was lower than that obtained with the silanol with bulky substituents.

c) When the silanol with bulky substituents was used, the polymerization activity was higher than that observed with the less bulky substituent. Silanols have been known to react with epoxide to form the C-O-Si linkage.[7]

The polymerization proceeded with a considerable

chain transfer, which was indicated by the fact that the molecular weight of the polymer obtained by Al(acac)$_3$/ Ph$_2$Si(OH)$_2$ catalyst system did not depend on polymerization time. To obtain the information about the chain transfer step, the ^{1}H-nmr spectrum of the oligomer, obtained with an equimolar quantity of the Al(acac)$_3$/ Ph$_2$Si(OH)$_2$ catalyst, was examined. Olefinic proton signals at 4.5 ~ 4.8 ppm[6] indicated the reaction as shown in Figure 6. The chain transfer reaction was considered to contain a proton transfer from the polymer end to the catalyst anion.[6]

4-8 Conclusion

The followings are found to be important for the present catalytic polymerization.

1) α-position of carbonyl group in ligand is substituted with electron donating groups.

2) The ratio of reaction between aluminum complex and silanol is about 20 ~ 25 mol%, where an equimolar aluminum complex is used with silanol.
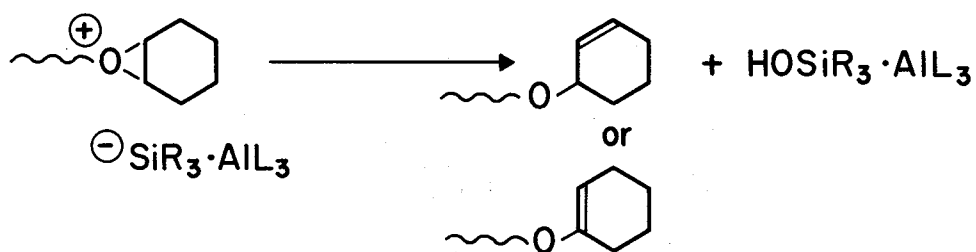
Figure 6   Termination mechanism

References

1. R. M. Salinger and R. West, J. Organometal. Chem. $\underline{11}$, 631 (1968)

2. M. Calvin, K. W. Wilson, J. Am. Chem. Soc., $\underline{67}$, 2003 (1945)

3. M. W. Tamele, Dis. Faraday Soc., $\underline{8}$, 270 (1960)

4. K. Shibata, T. Kiyoura, J. Kitagawa, T. Sumiyoshi and K. Tanabe, Bull. Chem. Soc. Japan, $\underline{47}$, 1064 (1974)

5. D. J. Worsford and A. M. Eastham, J. Am. Chem. Soc. $\underline{79}$, 900 (1957); A. E. Bastham, "The Chemistry of Cationic Polymerization", P. H. Plesch, ed., Pergamon Press, New York, 1963, Chapter 10; G. A. Latremouille, G. T. Merrall, and A. M. Eastam, J. Am. Chem. Soc., $\underline{82}$, 120 (1960), ibid., Can. J. Chem., $\underline{38}$, 1967 (1960)

6. K. E. Russel and L. G. M. C. Vail, Can. J. Chem., $\underline{57}$, 2355 (1979); R. F. Bauer, R. T. LaFair and K. E. Russell, Can. J. Chem., $\underline{48}$, 1251 (1970)

7. H. M. Banc, U. S. Pat. 3971747

Chapter 5   Catalyst Supported on Zeolite and Porous Silica

5-1   Introduction

SiOH and Al-O-Si moieties are also found on the sur-
faces of zeolite and SiO_2.   Therefore it is expected that
a combination of zeolite/silanol and silica gel/aluminum
compound will polymerize cyclohexene oxide.   Porous silica
interacts with silanol compounds to result in a change of
silanol properties, which in turn will influence catalytic
activity.

5-2   Aluminum compound/silicagel catalyst

Figure 1 shows the polymer conversion-time curve for
the cyclohexene oxide polymerization with $Al(acac)_3$/silica
gel catalyst.   The behavior of the catalyst was similar to
that of $Al(acac)_3$/diphenylsilanediol catalyst; that is,
after fast polymerization, the rate subsided.   It was
found that 0.36 wt% of hydrogen was contained in this
silica gel by hydrogen analysis in dry N_2.   If water is
eliminated by heat, SiOH is considered present.   The
amount of SiOH in silica gel calculated using this value
was 2 mol % to the cyclohexene oxide.   When the polymer
yield was compared under the same catalyst concentration,
the catalytic activity of $Al(acac)_3$-silica gel was about
1/100 that of the $Al(acac)_3$-diphenylsilanediol catalyst
system.
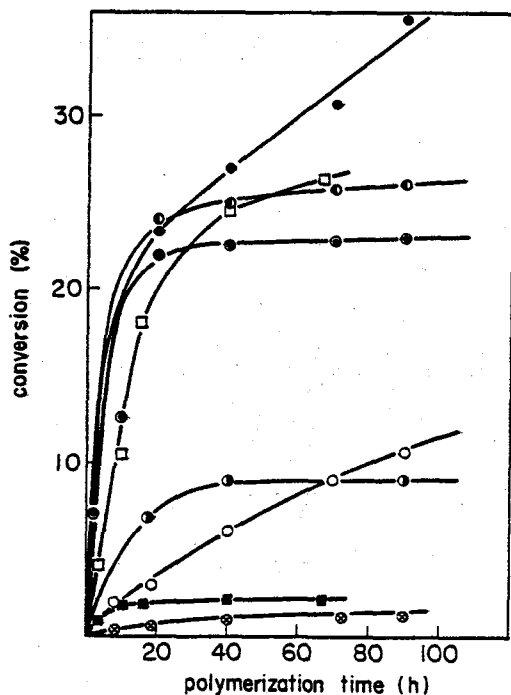
Figure 1   Polymerization of cyclohexene oxide by various
catalysts*:   polymerization temperature 40°C; catalyst
(—□—) Al(acac)$_3$-MePhSi(OH)$_2$-silica C, (—■—)
Al(acac)$_3$-MePhSi(OH)$_2$, (—◐—) Al(acac)$_3$-Ph$_2$Si(OH)$_2$-
silica C, (—●—) Al(acac)$_3$-Ph$_2$Si(OH)$_2$-9F, (—◉—)
Al(acac)$_3$-Ph$_2$Si(OH)$_2$, (—◑—) Al(acac)$_3$-silica gel,
(—⊗—) 9F, (—○—) 9F-Ph$_2$Si(OH)$_2$;   concentration
Al(acac)$_3$, 0.05 mol%; inorganic compound, 5 wt%,
Ph$_2$Si(OH)$_2$, 0.15 OH equivalent %.[†]

* Al(acac)$_3$ and silica C have low catalyst activity in
  cyclohexene oxide polymerization. The time-polymer
  conversion curves shown in Figure 1 were corrected
  by the amount of polymer obtained by catalysis of
  Al(acac)$_3$-silica C.

† OH equivalent, the molecular weight of silanol com-
  pound divided by the amount of SiOH in the silanol
  compound;(mol%), (mol of catalyst/mol of monomer) x
  100;OH equivalent %, (OH equivalent of catalyst/mol
  of monomer) x 100.

5-3 Zeolite/silanol catalyst system

The zeolites used were 4A, 5A, 6A, and 9F. These
zeolites by themselves gave only a low amount of polymer
at 40°C. However, the zeolite-silanol system polymerized
cyclohexene oxide. The polymer conversion-time curve is
presented in Figure 1, and shows that this catalyst re-
sisted deactivation more than the diphenylsilanediol-
Al(acac)$_3$ catalyst did. The effect of pore size on
polymer yield was examined, and the results are shown in
Figure 2. There is a large increase between 4A and 5A.
The molecular weight of polymer obtained with zeolite 5A-
diphenylsilanediol catalyst was three times as was obtained
with Al(acac)$_3$-diphenylsilanediol catalyst (Fig. 3).

We suggest that the activity of this catalyst is due
to the stability of silanol during the polymerization pro-
cess. In order to examine this possibility, the thermal
stability of diphenylsilanediol supported by zeolite was
studied in THF with GPC. Silanol compounds readily form
siloxane by self-condensation; consequently a substantial
amount of silanol in the polymerization system will be
lost and catalytic activity will decrease. Thus it is
expected that stabilization of silanol enhances catalytic
activity. As shown in Figure 4, the stability of
diphenylsilanediol supported by zeolites decreased in the
order 5A >> 3A > Al(acac)$_3$.
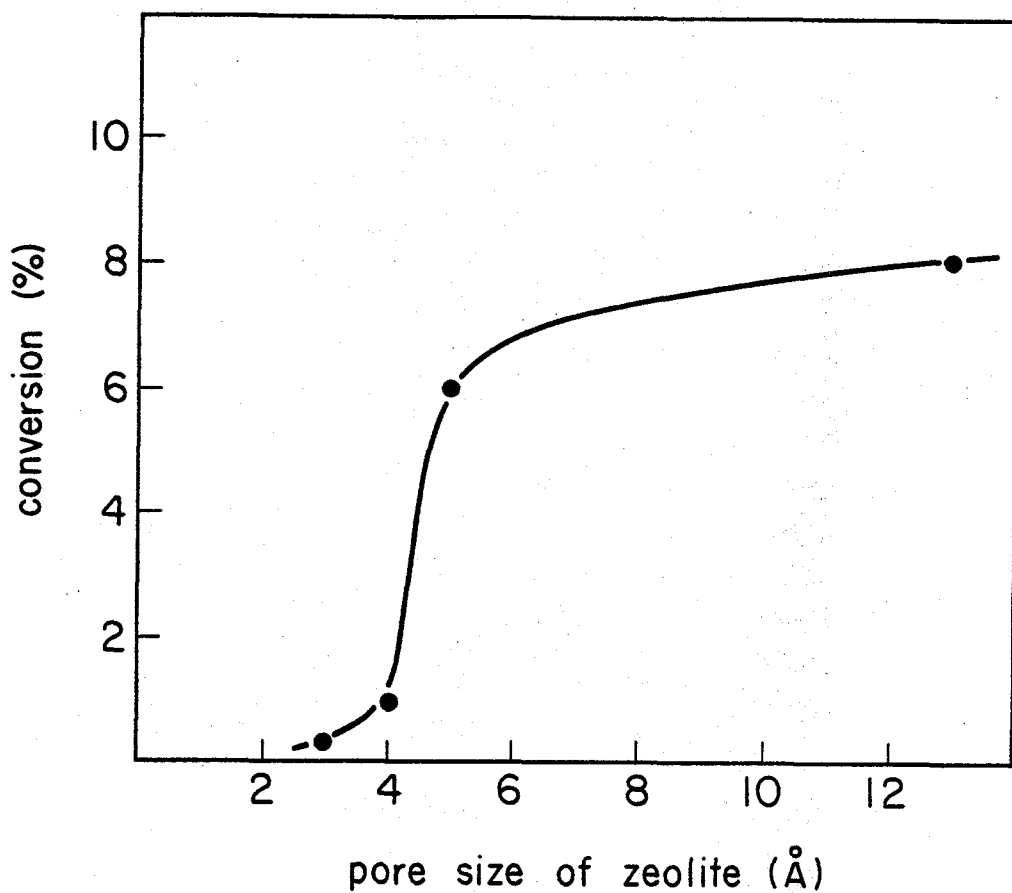
Figure 2   Polymerication of cyclohexene oxide with
   $Ph_2Si(OH)_2$ supported on zeolites: catalyst concen-
   tration, $Ph_2Si(OH)_2$, 0.15 OH equivalent %; zeolite,
   5 wt%; polymerization conditions, 40°C, 70 h.
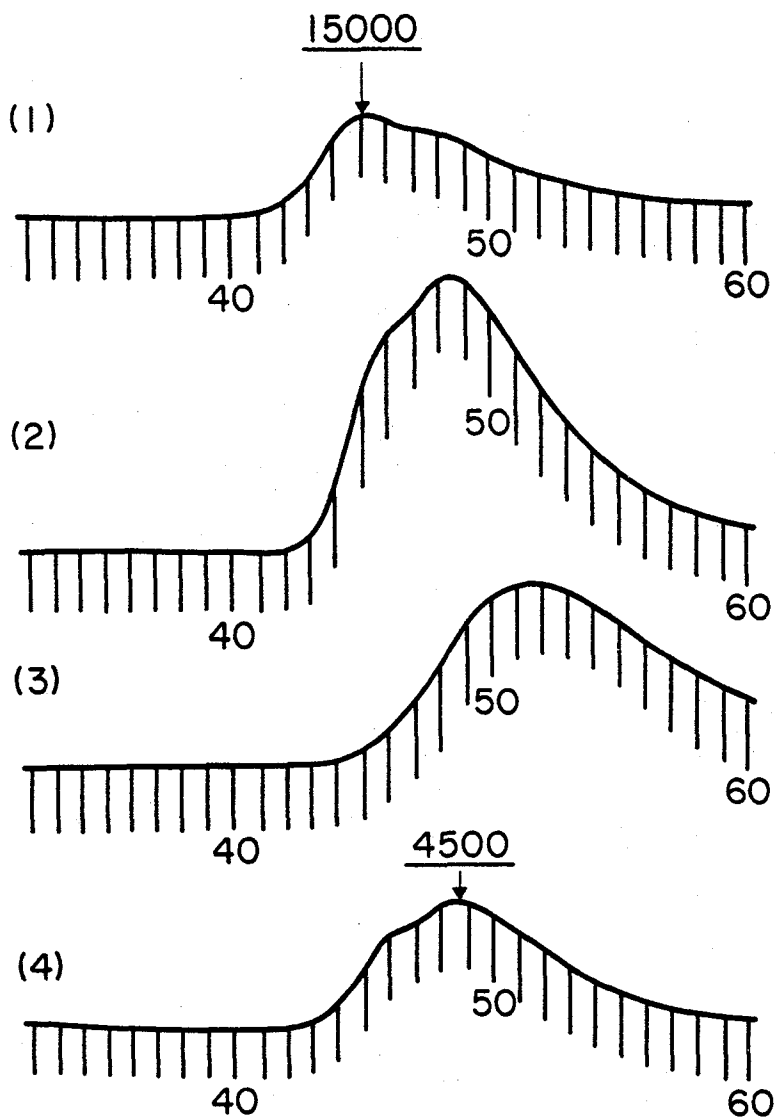
Figure 3   GPC curves for polymers obtained by various
   catalysts: (1) zeolite 5A-$Ph_2Si(OH)_2$, (2) $Al(acac)_3$-
   $Ph_2Si(OH)_2$-silica C, (3) $Al(acac)_3$-silica gel,
   (4) $Al(acac)_3$-$Ph_2Si(OH)_2$.
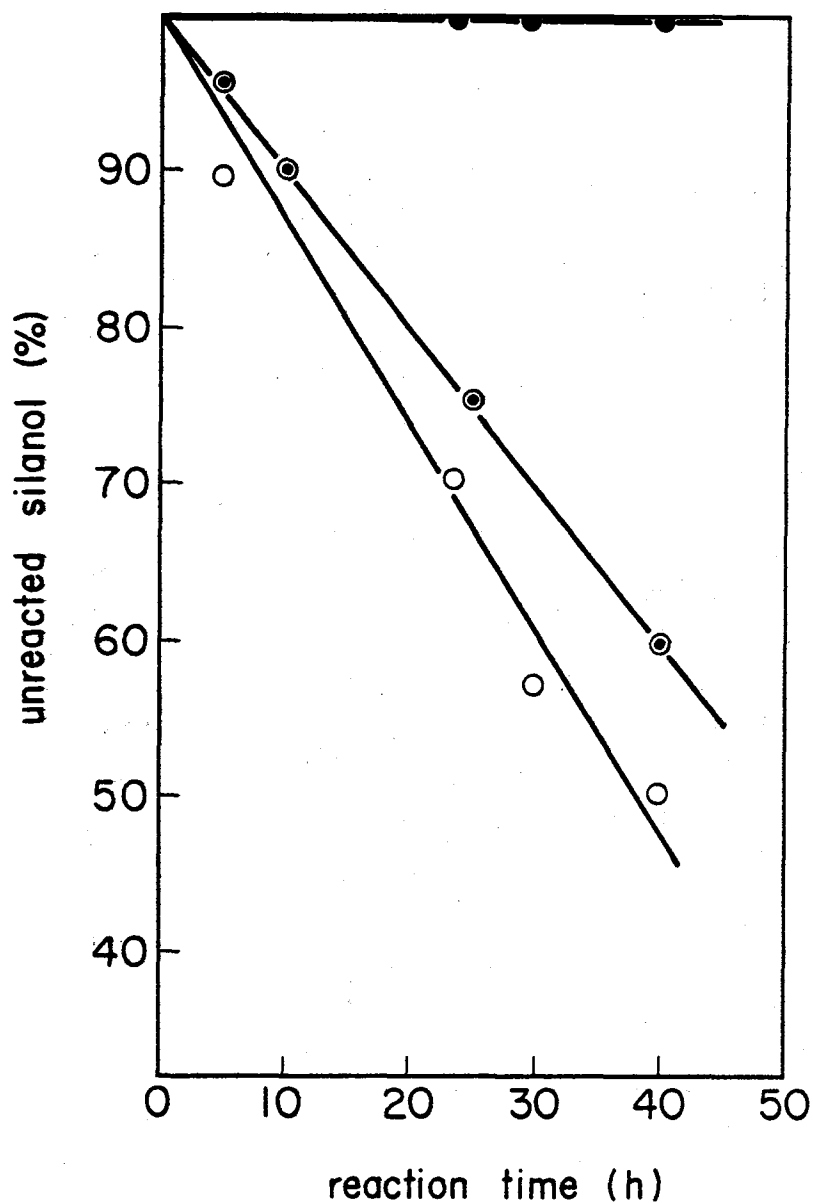
Figure 4   Stability of $Ph_2Si(OH)_2$ supported by zeolites
at 40°C: solvent, THF; $Al(acac)_3/Ph_2Si(OH)_2 = 1(mol/$
OH equivalent); $Ph_2Si(OH)_2$, 2.4 wt% to THF; zeolite,
5 wt% to THF; (—○—) $Ph_2Si(OH)_2-Al(acac)_3$ (—●—)
$Ph_2Si(OH)_2-5A$, (—◉—) $Ph_2Si(OH)_2-3A$.

To investigate the interaction between zeolite and diphenylsilanediol in detail, NMR spectra of diphenyl-silanediol were measured in the presence of zeolite in d_8-THF. The SiOH difference in chemical shift between diphenylsilanediol only and diphenylsilanediol in the presence of zeolite will be proportional to the magnitude of the interaction between the silanol and the zeolite. The interaction between zeolite and diphenylsilanediol decreased in the sequence, 9F > 5A > 4A > 3A, which relates to catalytic activity as shown in Figure 5. From these results it appears that, in the zeolite/diphenylsilanediol catalyst system, the silanol is activated by interaction with zeolite and catalytic activity is enhanced.

Figure 1 also shows the polymer conversion-time curve for the zeolite $9F/Al(acac)_3/Ph_2Si(OH)_2$ catalyst system. Polymerization conversion did not level off but continued to increase, and the polymer was obtained at high yield. Moreover, molecular weight of this polymer was higher than that polymerized by an $Al(acac)_3$-$Ph_2Si(OH)_2$ catalyst, as shown in Table 1.

5-4 $Al(acac)_3$/silanol compound catalyst system supported by porous silica

As mentioned before, polymer conversion is changed by using silanol compound as cocatalyst, as follows: (i) Silanols with a phenyl group, e.g., $Ph_2Si(OH)_2$, were more

Table 1   Polymerization of Cyclohexene Oxide[a]

Run	Al(acac)$_3$ (mol%)	Ph$_2$Si(OH)$_2$ (mol%)	Polymer- ization time (h)	Adsor- bent	(wt%)	Polymer conversion (%)	M_n	M_w
1	0.05	0.075	40	3A	5	20	2600	5400
2	0.05	0.075	40	4A	5	18	2900	5800
3	0.05	0.075	40	5A	5	26	5400	9700
4	0.05	0.075	40	9F	5	28	4400	8600
5	...	0.150	40	5A	5	8	7500	13,000
6	...	0.225	40	5A	5	10	7000	12,500
7	...	0.300	40	5A	5	18	6300	11,700
8	0.05	0.150	20	5A	5	35	4400	8700
9	0.05	0.225	20	5A	5	43	3900	7800
10	0.05	0.300	20	5A	5	60	3300	6900
11	0.05	0.075	40	...	...	22	2300	4500

a) Polymerization temperature 40°C.
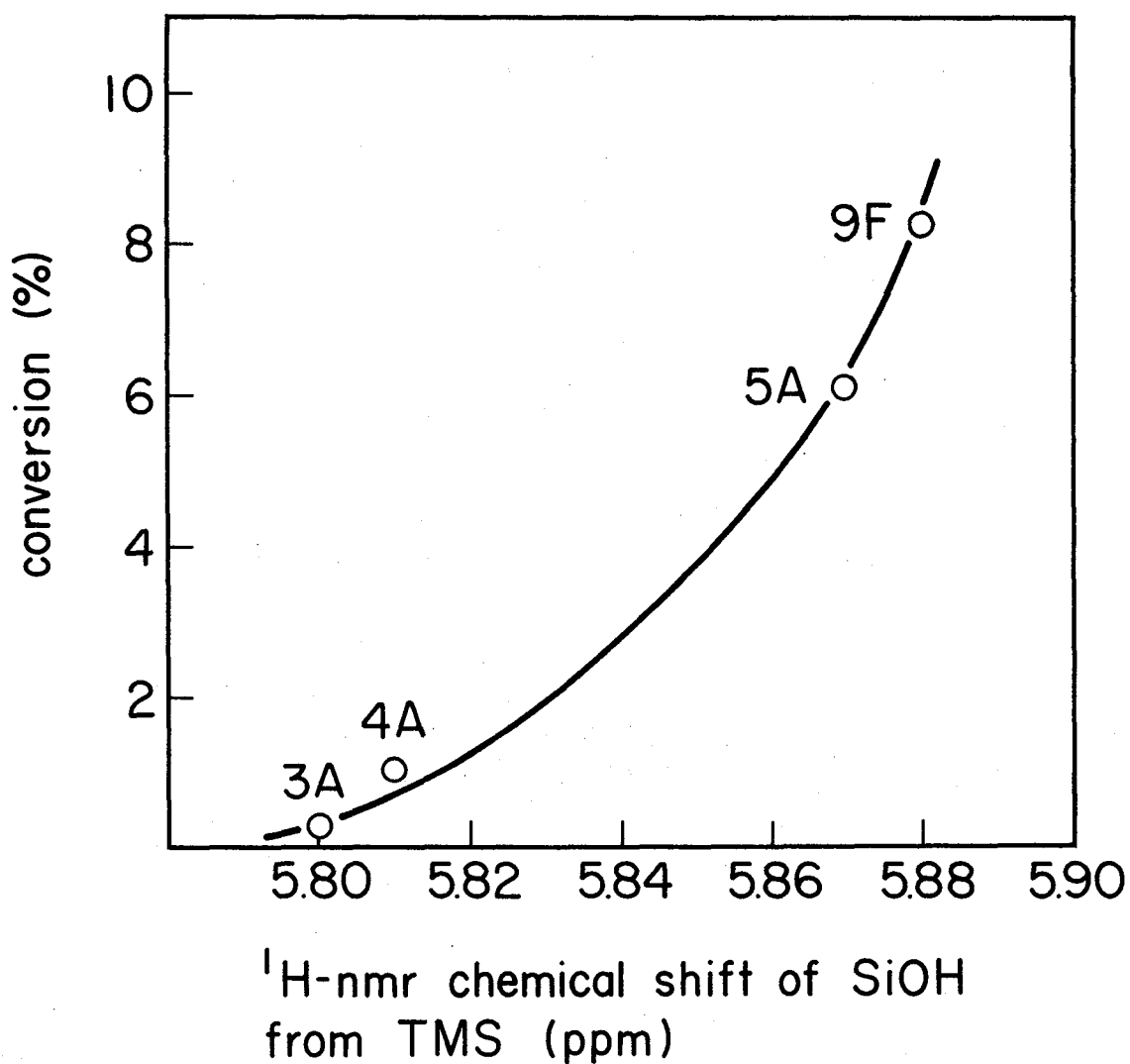
Figure 5   Relationship between polymer yield and
    chemical shift of SiOH. Polymerization conditions
    are the same as in Fig. 2. NMR spectra for
    $Ph_2Si(OH)_2$ were measured in d_8-THF in the presence
    of dispersed zeolite.

active than silanols with a methyl group. (ii) Monomeric silanol compound was less active than polymeric silanol compound.

These phenomena may be attributed to the stability and acidity of the silanol compound, which may be explained by substitution and aggregation of silanols. If these two effects could be achieved by another method, polymer conversion would increase. It is known that OH compounds are strongly adsorbed on the surface of porous silica by strong hydrogen bonding.[1] The chemical properties of silanol may be strongly influenced by the presence of porous silica. Therefore catalytic activity may be affected by using porous silica as a support.

The stability of silanol against self-condensation in the presence of Al(acac)$_3$ combined with porous silica was examined by GPC and compared with that observed in the presence of Al(acac)$_3$ only. The amount of unreacted silanol was plotted with time as shown in Figure 6 using diphenylsilanediol or methylphenylsilanediol as the silanol compound. The figure shows that these silanol compounds are stable on the porous silica.

Figure 1 also shows the polymer conversion-time curve in cyclohexene oxide polymerization with the catalyst systems Al(acac)$_3$-diphenylsilanediol and Al(acac)$_3$-methyl-phenylsilanediol, respectively, in the presence and absence of porous silica. The effect of porous silica was espe-
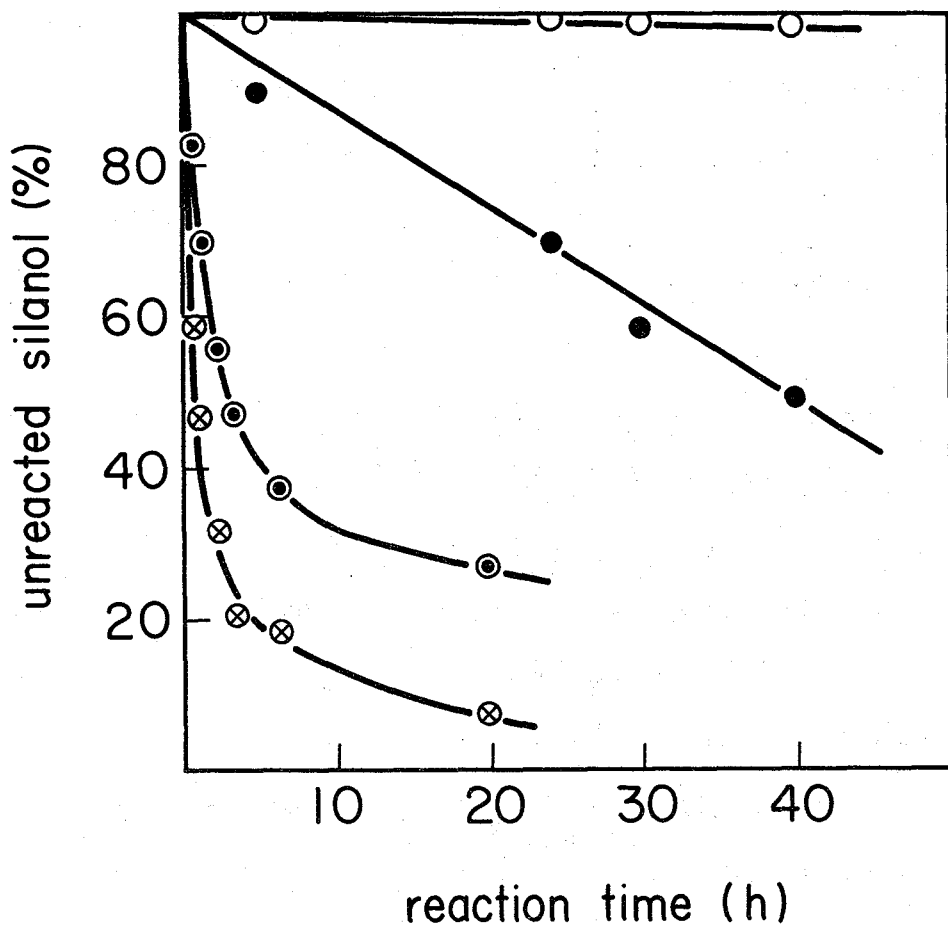
Figure 6   Stability of $Ph_2Si(OH)_2$ and $MePhSi(OH)_2$ supported by silica-C.   Reaction conditions are the same as in Fig. 4; silica C, 5 wt% to THF: (—○—) $Al(acac)_3$-$Ph_2Si(OH)_2$-silica C, (—●—) $Al(acac)_3$-$Ph_2Si(OH)_2$, (—◉—) $Al(acac)_3$-$MePhSi(OH)_2$-silica C, (—⊗—) $Al(acac)_3$-$MePhSi(OH)_2$.

cially pronounced for the Al(acac)$_3$-methylphenylsilanediol catalyst as compared with the Al(acac)$_3$-diphenylsilanediol catalyst. This phenomenon may be explained as follows: Catalyst activation on porous silica would be due to the stability and acidity of the silanol compound. The effect of porous silica on methylphenylsilanediol stabilization against self-condensation was not large enough to explain the effect of porous silica on polymer conversion, compared with the effect on diphenylsilanediol stabilization. Therefore the increase in acidity and stabilization against the addition to epoxide by aggregation would be important. Methylphenylsilanediol with its methyl group would have lower acidity and lower stabilization against addition to epoxide than diphenylsilanediol with its phenyl groups. Diphenylsilanediol would have strong acidity and stabilization against addition to epoxide to some degree in itself. When methylphenylsilanediol and diphenylsilanediol interact with porous silica, the increase in acidity and stability would be greater in methylphenylsilanediol than in diphenylsilanediol.

The interaction between silanol and porous silica was examined by NMR. Among many silicas, some activited the Al(acac)$_3$/silanol compound catalyst, some had no effect, and others deactivated. When the NMR spectrum of diphenylsilanediol was measured in d$_8$-THF in the presence of porous silica-C, which activated the catalyst, the SiOH signal was

broad and shifted high field. This fact shows that the diphenylsilanediol SiOH formed hydrogen bonds with the silica surface. On the other hand, the SiOH signal measured in presence of porous silica-F, which did not activate the catalyst, hardly changed compared with the absence of porous silica. In Figure 7, the abscissa shows the difference between the half-value width of the SiOH signal and the half-value width of CH_2 in THF, and gives the relative strength of interaction. The ordinate shows polymer conversion. Figure 7 shows that the greater the interaction with silica, the higher the polymer conversion.

The amount of SiOH on surface of porous silica was estimated from the elemental analysis of H after removal of the adsorbed water (in dry N_2). This amount of H was associated with the relative strength of the interaction between diphenylsilanediol and silica, as shown in Figure 8. It is believed that the interaction was between diphenylsilanediol and SiOH on the silica surface. As seen above, the increase in catalytic activity in the presence of porous silica was caused by the stabilization of organosilanol and the increase in organosilanol acidity, which were due to the hydrogen bond between organosilanol and the SiOH on the porous silica surface.
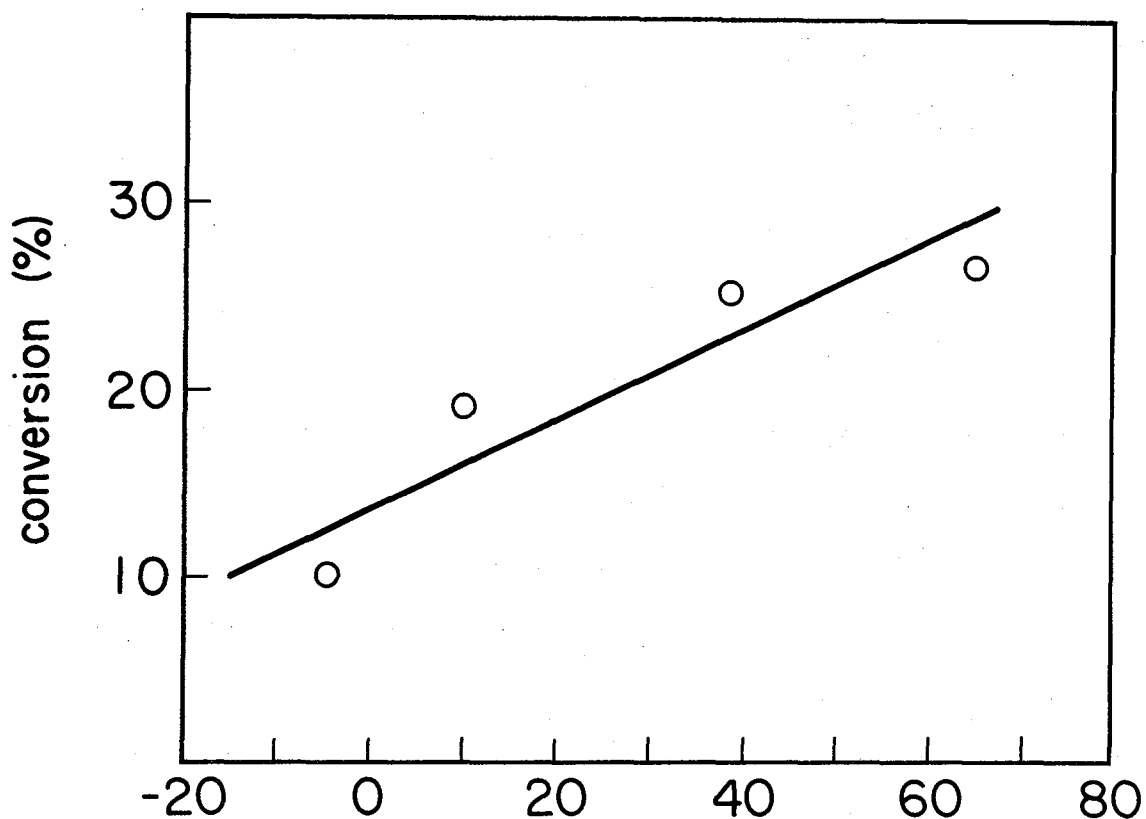
Figure 7   Relation between polymer yield and signal
   width of ^{1}H-NMR.   Polymerization conditions are the
   same as in Fig. 1.   Polymerization time, 15 h;   NMR
   spectra for $Ph_2Si(OH)_2$ were measured in d_8-THF in the
   presence of dispersed porous silica (90 MHz).
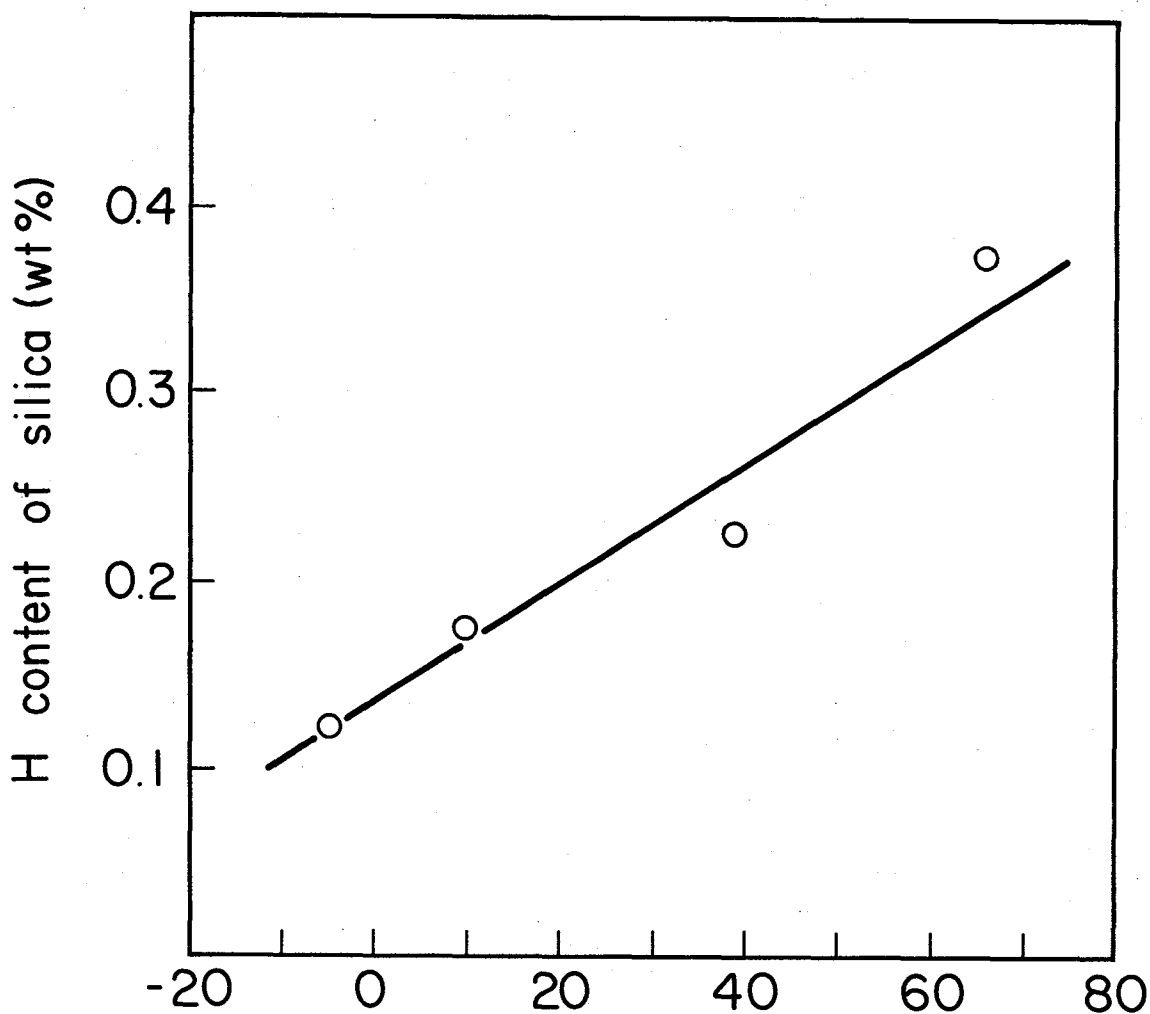
Figure 8   Relation between H content of porous silica
and signal width of ^{1}H-NMR.   Polymerization conditions
and NMR measurement conditions are the same as in
Fig. 7.

5-5　Molecular weight distribution of the polymer

The molecular weight distribution of the polymer obtained from $Al(acac)_3/Ph_2Si(OH)_2$/porous silica was the same as that obtained from $Al(acac)_3/Ph_2Si(OH)_2$ alone, as shown in Figure 3.　When cyclohexene oxide was polymerized in the presence of porous silica, polymer conversion increased, while the molecular weight distribution was the same.

Figure 3 also shows the molecular weight distribution of the polymer obtained from $Al(acac)_3$/silica gel.　In this case, the molecular weight of polymer was lower than that obtained from $Al(acac)_3/Ph_2Si(OH)_2$.

In the zeolite/$Ph_2Si(OH)_2$ catalyst system, the molecular weight of the polymer changed with the pore size of the zeolite used; the largest-molecular-weight polymer was obtained from zeolite5A/$Ph_2Si(OH)_2$ catalyst.　The polymer obtained with zeolite/$Al(acac)_3/Ph_2Si(OH)_2$ catalyst had a molecular weight intermediate between that of the polymer made with $Al(acac)_3/Ph_2Si(OH)_2$ and that made with zeolite/$Ph_2Si(OH)_2$ (Table 1).

Reference

1. A. W. Baker and A. T. Shulgin, J. Am. Chem. Soc., 81,
    1523 (1959); R. West and C. S. Kraihanzel, J. Am. Chem.
    Soc., 81, 765 (1961); R. West, ibid., 81, 1614 (1959),
    M. R. Basila, J. Chem. Phys., 35, 1151 (1961); ·
    S. Kohama, Nippon Kagaku Kaishi, 81, 69 (1960)

Chapter 6   Microstructure of Poly(Cyclohexene Oxide)

6-1   Introduction

Microstructure of poly(cyclohexene oxide) was investigated by Bacskai[1] and Malhotra[2] using ^{1}H-NMR spectroscopy.   Bacskai concluded that poly(cyclohexene oxide) polymerized by AlEt$_3$ had stereoregular all-trans structure and Malhotra concluded that a polymer polymerized by triphenylmethyl cation had cis-trans mixed structure.

Microstructure of poly(cyclohexene oxide) might be varied by the polymerization catalyst and will reflect the properties of the catalysts.   The microstructure might also be varied by use of a catalyst supported on porous silica or zeolite.   In this Chapter, structure of the polymers is described in detail.

6-2   Structure of poly(cyclohexene oxide) polymerized by catalysis of Al(acac)$_3$/silanol system

Figure 1 shows the ^{13}C-NMR spectrum of poly(cyclohexene oxide) obtained by catalysis of the Al(acac)$_3$/Ph$_2$Si(OH)$_2$.   Three peaks were found for each carbon and this may be interpreted by either of the following:

(1) Mixture of cis and trans structure.

(2) Equilibrium mixtures of diaxial and diequatorial structure of the main chain.
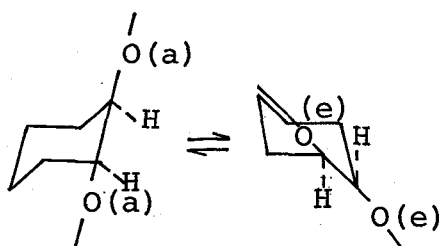
(3) Mixture of diisotactic and disyndiotactic
structures.
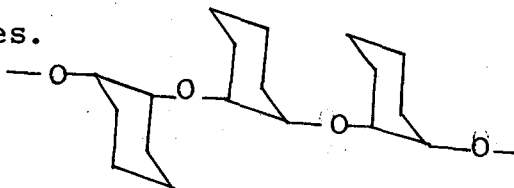
In regard to the first possibility Elderfield reported[3] that alicyclic epoxide gave the trans form by cationic catalyst. Bacskai concluded[1] that a polymer by $AlEt_3$ had an all-trans structure by comparing the ^{1}H-NMR spectra of the polymer with that of cis- and trans-1,2 cyclohexane diol. By comparing the ^{13}C-NMR spectra the C-1 signal of the polymer was shown to have chemical shift differences of only 0.61 and 1.80 ppm, but the difference in the C-1 chemical shift between cis- and trans-1,2-cyclohexane diol was 4.75 ppm (Table 1). From the above it is impossible to regard the structure of the polymer as cis and trans. In regard to the second possibility the ^{13}C-NMR spectra were measured at 30, 60, and 90°C (Fig. 1), but the spectral pattern was the same. Therefore these chemical shift changes are not caused by the equilibrium
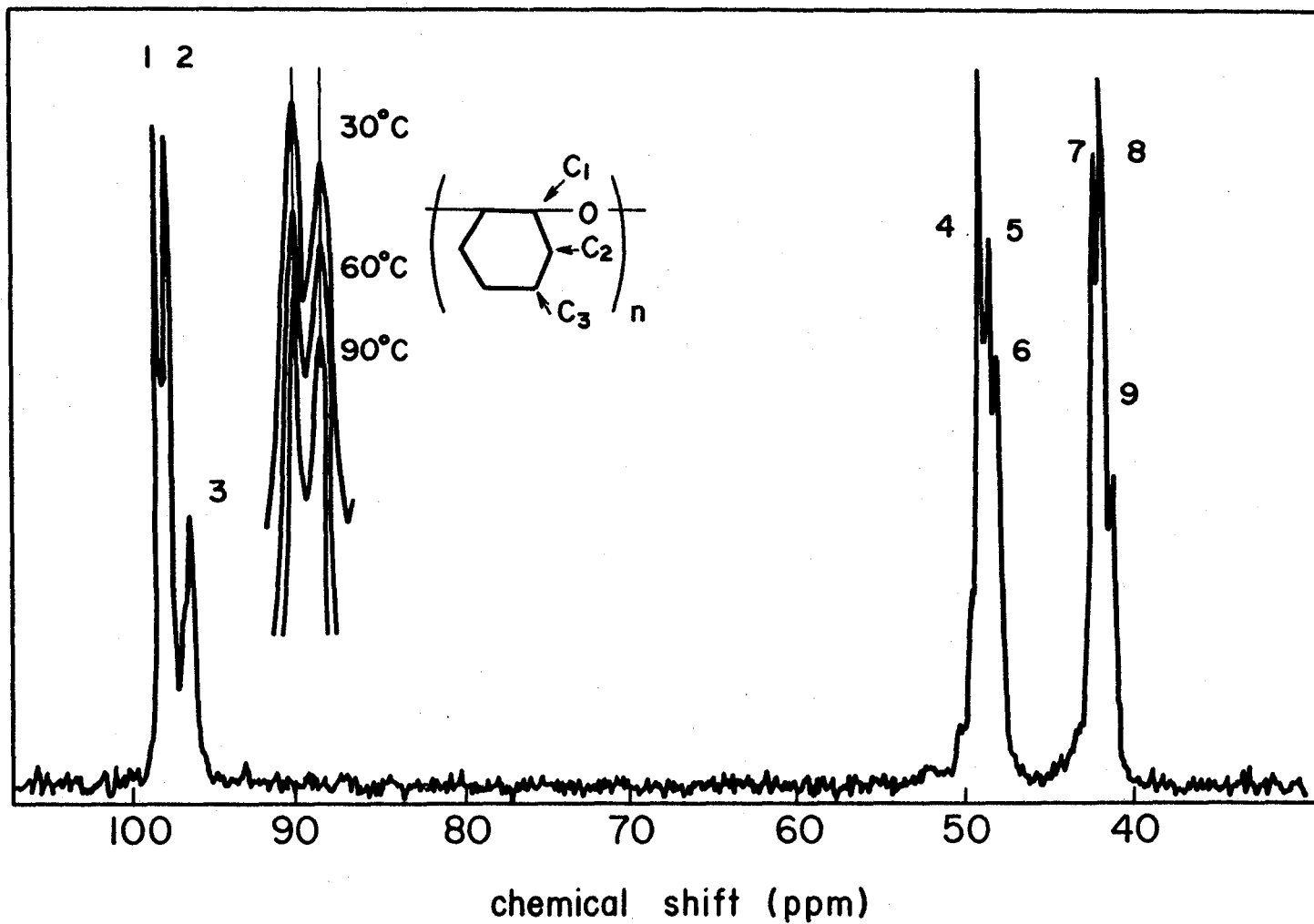
Figure 1 ^{13}C-NMR spectrum for poly(cyclohexene oxide):
measured at 30°C in C_6D_6.

Table 1   Assignment and Spin-Lattice Relaxation Time for Poly(cyclohexene oxide) and 1,2-Cyclohexane Diol(cis-trans Mixture) in ^{13}C-NMR spectrum[a]

Signal	Carbon	Polymer[a]		Cyclohexanediol[b]	
		Chemical Shift (ppm)	T_1 (s)	Chemical Shift (ppm)	T_1 (s)
1	C_1	98.68	0.3_0	95.98	3.4_5
2	C_1	98.07	0.3_0	91.23	3.7_1
3	C_1	96.89	0.3_0	—	—
4	C_2	50.25	0.1_4	53.56	1.8_8
5	C_2	49.65	0.1_5	50.59	2.0_0
6	C_2	49.34	0.1_4	—	—
7	C_3	43.53	0.1_6	44.89	1.7_8
8	C_3	43.15	0.1_6	42.23	1.9_3
9	C_3	42.42	0.1_5	—	—

[a] Measured at 60°C in C_6D_6.

[b]
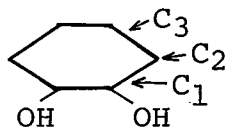
mixtures. Spin-lattice relaxation time (T_1) can be used for peak assignments. In this case the T_1s were measured to distinguish the properties of individual carbons (Table 1). Because the T_1s for C-1 signals were almost the same, these signals were assignable as carbons in the main chain of polymer, but the first possibility could not be studied by T_1 measurement because the T_1 difference was too small even for a monomeric compound like 1,2-cyclohexane diol.

According to the above, the chemical shift changes are due to the third possibility. Vandenberg reports[4] that the complexities in the ^{13}C-NMR of the 2,3-epoxybutenes are due to atactic structure. Oguni et al., also report[5] that the three signals of the methine carbon in amorphous poly (propylene oxide) are due to triad tacticity. Thus the three signals of C-1 are due to the same triad tacticity and the polymer will have an atactic structure. This conclusion is supported by the x-ray diffraction curve. No change in the x-ray diffraction curve and half-value width were observed between the polymer treated at 40°C for 1 week (crystallization process) and the polymer treated at 80°C and immediately cooled to -196°C (quenching process). These polymers are essentially amorphous because of its atactic structure.

^{13}C-NMR spectra of poly(cyclohexene oxide) polymerized with Al(acac)$_3$/silanol, zeolite/silanol compound, and

Al(acac)$_3$/silanol compound/porous silica were almost the same. Figure 2 shows the ^{13}C-NMR spectral pattern for polymers prepared with various catalysts. As polymerized on the surface of inorganic compounds, these polymers would have a random structure.
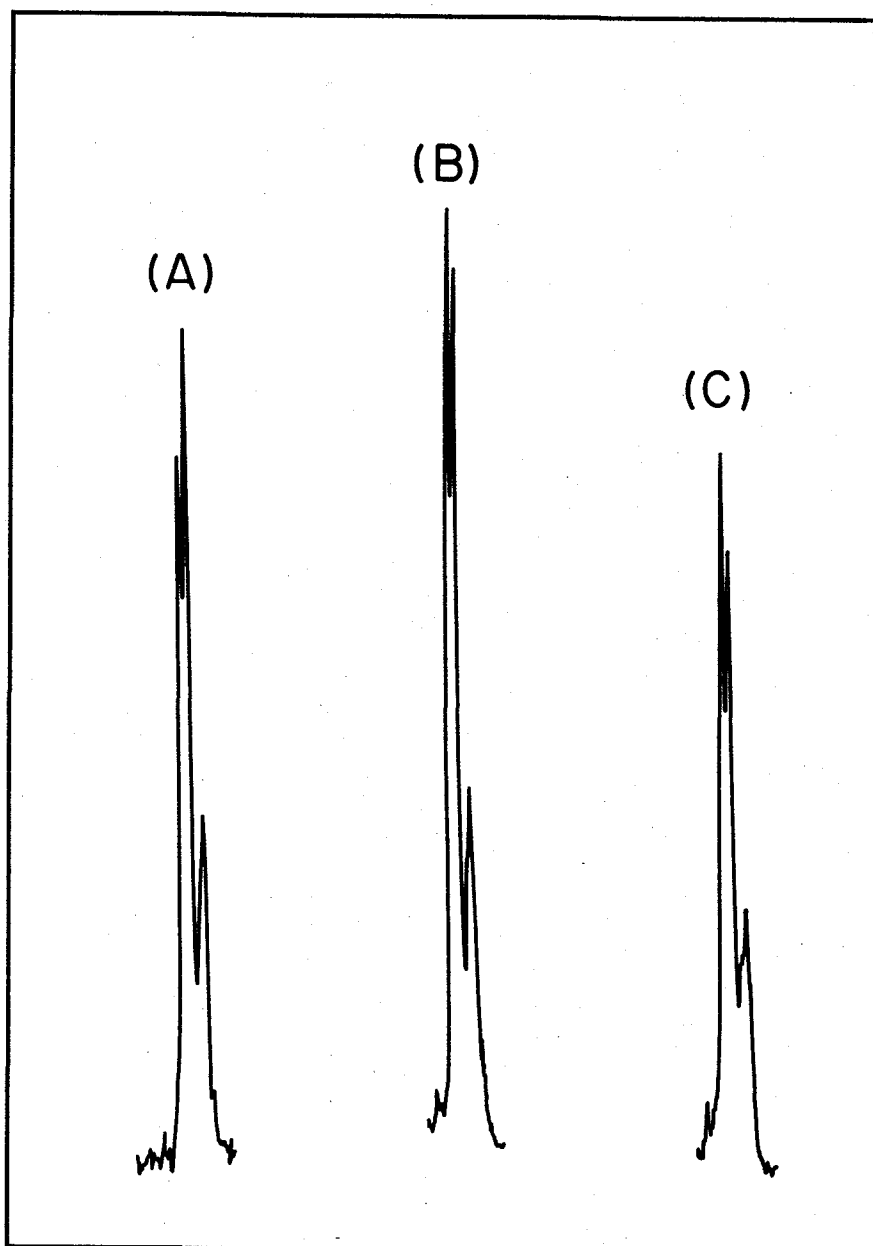
Figure 2 ^{13}C-NMR spectra assignable to C-1 of poly-
(cyclohexene oxide). Catalysts: (A) $Ph_2Si(OH)_2$
zeolite 5A, (B) $Al(acac)_3$-$Ph_2Si(OH)_2$-silica,
(C) $Al(acac)_3$-$Ph_2Si(OH)_2$; C-1, carbon bonding to
oxygen.

References

1. R. Bacskai, J. Polymer Sci., A-1, 2777 (1963)

2. S. L. Malhotra, J. Macromol. Sci. Chem., A-12, 1379 (1978)

3. R. C. Elderfield, Ed., Heterocyclic Compounds, Vol. 1, Wiley, New York, 1953, p30

4. C. E. Foll, Soc. Chem. Ind. Monogr. No. 26, 103-138; E. J. Vandenberg, J. Polymer Sci., A-1, 7, 525 (1969); ibid., J. Polymer Sci., 47, 489 (1960)

5. N. Oguni, K. Lee and H. Tani, Macromolecules, 5, 819 (1972); ibid., Polymer J., 11, 755 (1979)

Chapter 7 Effect of Intramolecular Hydrogen Bonds of

Silanol on the Catalyst Activity

7-1 Introduction

Aggregation of silanol was found to be important for the catalyst activation with porous silica. The effect of aggregation was also implied in the polymerization with $Al(acac)_3/SH6018$ described in Chapter 2.

In order to examine the effect of intramolecular hydrogen bond, first, an oligomer of diphenylsilanediol was used as silanol. Because the oligomer is more suitable for consideration of the reaction mechanism, as compared to the polymer of silanol. Then, the effects of silanol polymers were investigated.

7-2 Aluminum complex/$HO(Ph_2SiO)_nH$ catalyst system

(n; 1, 2, 3 and 4)

Catalytic activity of an aluminum complex/$HO(Ph_2SiO)_nH$ system was investigated as a function of n in order to examine the effect of intramolecular hydrogen bonding of silanols, because the hydrogen bonding varied with the number on n.

Table 1 gives the polymerization results. The catalytic activity for $Al(acac)_3/HO(Ph_2SiO)_nH$ (0.05 mol%/0.05 mol%) varied with the number of n as follows. 1 > 4 > 3 > 2. The diphenylsilanediol is distinct from the others in

Table 1   Polymerization of Cyclohexene Oxide with Aluminum Complex/HO(Ph$_2$SiO)$_n$OH Catalyst.[a]

Aluminum complex		n of silanol		Ligand liberation (mol%)	Solvent CHO/PhCH$_3$[1] (v/v)	Polymer conversion (%) ( ): polymerization time (min.)		
Al(acac)$_3$	0.05	1	0.05	—	1/0	12(2)	30(10)	37(20)
	0.05	2	0.05	—	1/0	3(2)	9(10)	12(21)
	0.05	3	0.05	—	1/0	8(2)	12(3)	23(10)
	0.05	4	0.05	—	1/0	9(2)	27(10)	34(20)
Al(Etaa)$_3$	0.025	2	0.025	30	1/0	19(3)	27(8)	32(15)
	0.025	3	0.025	43	1/0	14(3)	24(8)	30(15)
	0.025	4	0.025	33	1/0	24(3)	35(8)	39(15)
	0.05	1	0.05	30	7/3	19(2)	30(5)	34(10)
	0.05	2	0.05	30	1/0	5(2)	12(5)	14(10)
	0.05	3	0.05	43	7/3	3(2)	8(5)	8(10)
	0.05	4	0.05	33	7/3	25(2)	35(5)	39(10)
Al(SA)$_3$	0.025	1	0.025	42	1/0	90(3)	—	100(10)
	0.025	2	0.025	50	1/0	90(3)	—	100(10)
	0.025	3	0.025	65	1/0	16(3)	20(8)	22(14)
	0.025	4	0.025	41	1/0	90(3)	—	100(10)

a) Polymerization temperature, 40°C   1) CHO: cyclohexene oxide

view of its acidity and bulkiness. The catalytic activity
due to the intramolecular hydrogen bond should be compared
among the Dimer, the Trimer and the Tetramer. The SiOH
group of diphenylsilanediol oligomers can form the intra-
molecular hydrogen bond if they are longer than the Trimer.[1]
It is well-known that hydrogen bonding between OH groups
makes the acidity strong.[2] As mentioned in Chapter 3,
catalytic activity increased with an increase in the
silanol acidity. The catalytic activity variation de-
pending on the value of n is explained in term of the
acidity increment due to the intramolecular hydrogen
bonding.

Catalytic activity in the presence of other aluminum
complexes was also examined.

Followings are described in Chapter 4. Both Al(Etaa)$_3$
and Al(SA)$_3$ interacted with silanols to liberate a part of
the ligand from the aluminum chelate. The resultant
aluminum compound had Si-O-Al linkage. The ratio of reac-
tion was estimated from the ratio of ligand liberation.
The resultant aluminum compound which had no catalytic
activity by itself interacted with the residual silanol
and showed higher catalytic activity.

When the aluminum complex was mixed with an equimolar
amount of oligosilanols, the aluminum complex also reacted
with the oligosilanols as shown in Table 1 as the ratio of
ligand liberation. Ligand liberation from the aluminum

complex was greatest when the trimer was used. Fig. 1 and 2 shows the probable reaction products.

The structures of the products were confirmed as follows. Al(Etaa)$_3$ was mixed with an equimolar amount of the Dimer or the Trimer. The resultant ethyl acetoacetate from the Al(Etaa)$_3$ was removed under reduced pressure. The structure of the residual reaction mixture was estimated with ^{1}H-NMR and IR spectroscopy. The peak at 1070 cm^{-1} in the IR spectra showed the presence of Al-O-Si linkage. The ^{1}H-NMR spectra showed that the reaction product from the Trimer and Al(Etaa)$_3$ had one ethyl acetoacetate group, however that from the Dimer and the Al(Etaa)$_3$ had two ethyl acetoacetate groups. The probable structures of reaction products are shown in Fig. 1 and 2 (IA and IIA structure).

The catalytic activity of Al(Etaa)$_3$/HO(Ph$_2$SiO)$_n$H (0.025 mol% / 0.025 mol%) or (0.05 mol% / 0.05 mol%) varied with n as follows.

$$4 > 1 > 2 > 3$$

The catalytic activity of Al(SA)$_3$/HO(Ph$_2$SiO)$_n$H (0.025 mol%/ 0.025 mol%) was also lowest for n = 3. The results are explained by the fact that the Trimer reacts with the aluminum complex readily and the amount of SiOH group decreased in the polymerization system. Because catalyst activity is due to the amount of Al-O-Si linkage and the amount of Si-OH in polymerization system, catalyst activity
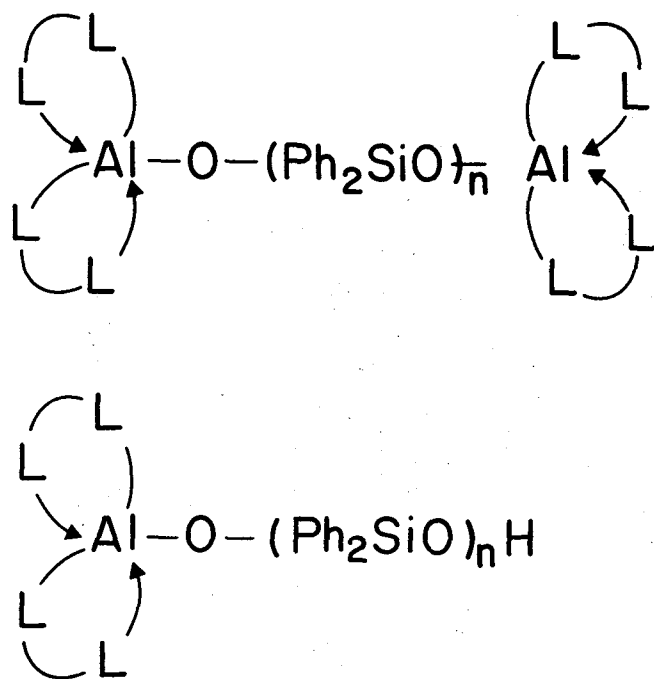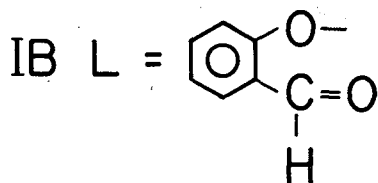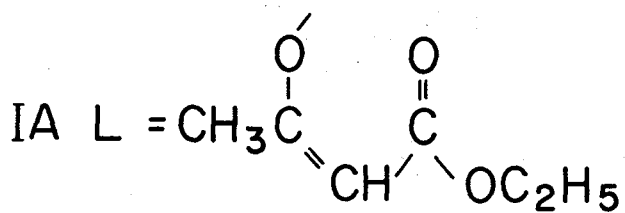
Figure 1   Structure of residual aluminum complex.

$n = 3$

II   L = Ligand

IIA L = CH_3C ... (structure)
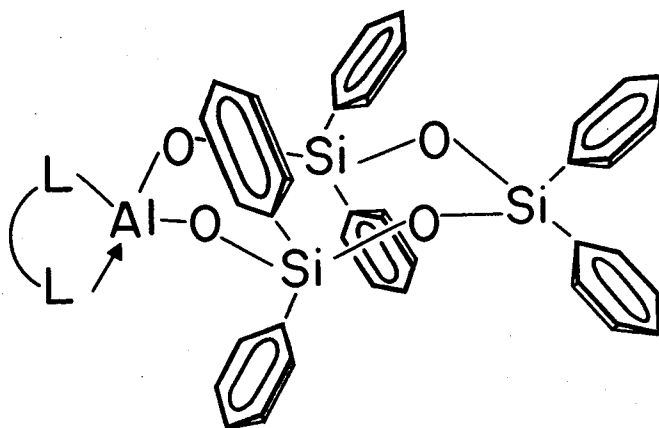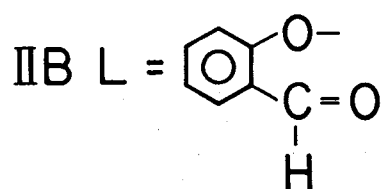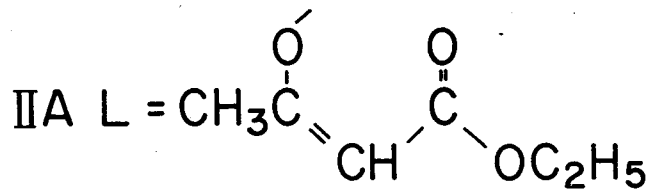
IIB L = (structure)

Figure 2   Structure of residual aluminum complex.

at n = 3 will be lowest. A suitable extent of reaction
between aluminum complex and silanol will be important for
the catalyst activation.

7-3   Al(SA)$_3$/Trimer + Dimer or Monomer catalyst system

If the ratio of Trimer to Dimer or Monomer + Trimer is
changed gradually from 0 to 1 under the same SiOH concen-
tration, the ratio of reaction between Al(SA)$_3$ and the
oligosilanols will change gradually, then the catalytic
activity may have a maximum at a ratio of Trimer to Dimer
or Monomer + Trimer. The catalytic activity of mixed
silanol systems, Trimer/Dimer, and Trimer/Monomer was
examined, where the silanol concentration in the poly-
merization system was constant at 0.05 mol% to cyclohexene
oxide, and Al(SA)$_3$ was used as the aluminum component.
Table 2 shows the results. Ligand liberation from the
aluminum complex did indeed gradually increase and the
maximum polymer conversion and the maximum molecular weight
were obtained at the ratio of 1 : 9 mol (Trimer:Dimer or
Trimer:Monomer).

Instead of the ratio of the ligand liberation, it was
also considered that the structure of IIB was more active
than that of IB in the presence of silanol. Because IIB
had two Si-O-Al linkage in a molecule. Where, II and I
mean aluminum complex only, not containing additional
silanol.

Table 2   Dependence of Conversion on the Ratio of Trimer/Dimer or Trimer/Monomer.[a]

the ratio of $HO(Ph_2SiO)_3OH/$ $HO(Ph_2SiO)_nOH+$ $HO(Ph_2SiO)_3OH$ (mol/mol)	n	Polymer conversion (%)	Ligand[b] liberation (%)	Molecular weight M_w	M_n
0	1	38	40		
0.1	1	64	41		
0.3	1	61	41		
0.5	1	54	44		
0.7	1	39	46		
0.9	1	20	48		
1.0	1	18	50		
0	2	35	43	41600	19100
0.1	2	39	43	69700	31900
0.3	2	33	45	63100	26300
0.5	2	30	45	64500	29400
0.7	2	22	47	57300	26300
0.9	2	21	48	55700	23700
1.0	2	20	50	64700	27200

a) Polymerization conditions: Al(SA)$_3$ 0.05 mol% to CHO, the trimer + the dimer or the monomer 0.05 mol% to CHO, at 40°C for 50 minutes, CHO/toluene 2/1(v/v)

b) Al(SA)$_3$(0.16M) and silanol (0.16M) in the mixture of d_8-THF and d_6-acetone(1/1(v/v)).

The catalytic activity of IA or IIA/triphenylsilanol (0.02 mol% / 0.05 mol%) system instead of IB or IIB/triphenylsilanol was examined. The results are shown in Table 3. IA or IIA had a slight catalytic activity by itself. However, when 0.05 mol% of triphenylsilanol was added, IIA/triphenylsilanol became a more active catalyst than IA/triphenylsilanol, as shown in Table 3.

The results of the catalyst activity on the ratio of Trimer/Monomer or Dimer + Trimer was explained from the three points. 1) ratio of Si-O-Al linkage 2) the amount of resultant silanol 3) difference in catalyst activity between I and II aluminum structures in presence of silanol. Namely, when the ratio of the Trimer increased under the constant silanol concentration, the ratio of II aluminum structure increased and the concentration of the SiOH group decreased, then the polymer yield also decreased. However, when an appropriate amount of II structure was present in the polymerization system, namely, a small amount of the active species formed, the polymer conversion was maximum.

7-4 Aluminum complex/1,4-bis(hydroxydimethylsilyl)benzene

system

1,4-bis(hydroxydimethylsilyl)benzene (HMSB) has a similar molecular length of the Trimer (molecular length between SiOH oxygen: HMSB, 9.96 Å; the trimer, 9.90 Å. However, HMSB can not hydrogen bond intramolecularly

Table 3　Polymerization of CHO with Aluminum
Complex/Ph$_3$SiOH Catalyst[a]

Catalyst	Polymeri-zation time (min.)	Polymer conversion (%)			Molecular weight	
		25	50	80	M_w	M_n
IA/Ph$_3$SiOH		39	42	45	56400	29800
IA only		0	1	1	53100	25900
IIA/Ph$_3$SiOH		53	57	61	69500	36700
IIA only		1	2	3	48500	25200

a) Polymerization conditions:　Aluminum complex 0.02 mol%
to CHO, Ph$_3$SiOH 0.05 mol% to CHO, CHO/toluene;
5/4.5 (v/v) 40°C

because it has a benzene ring. Therefore, the catalytic activity of the aluminum complex/HMSB system was compared with that of the aluminum complex/phenyldimethylsilanol (monomer unit of HMSB) system to explain the effect of the intramolecular hydrogen bond on the catalytic activity.

Table 4 shows the relative acidity of the silanols and ratio of the ligand liberation. The acidity of HMSB was slightly higher than that of dimethylphenylsilanol. Al(Etaa)$_3$ reacted with the two silanol compounds, liberating almost the same amount of the ligand. Al(SA)$_3$ reacted with dimethylphenylsilanol, liberating 27 mol% of salicylaldehyde, however, the reaction of Al(SA)$_3$ with HMSB gave a precipitate and 33 mol% of the salicylaldehyde was liberated in the system. The large value could be explained in terms of shift of equilibrium caused by precipitation. Therefore, the ratio of the ligand liberation of Al(SA)$_3$/dimethylphenylsilanol system probably will also be the same as that on the Al(SA)$_3$/HMSB system, if they are compared in solution.

The catalytic activity of Al(acac)$_3$/HMSB was higher than that of Al(acac)$_3$/dimethylphenylsilanol. The catalytic activity of the HMSB system was also higher when Al(SA)$_3$ was used instead of Al(acac)$_3$. The catalyst deactivation seen in Al(SA)$_3$/Trimer system was not observed. The results are reasonable when the intramolecular hydrogen bonding is considered. (Table 5).

Table 4   Relative acidity of 1,4-Bis(hydroxydimethylsilyl)benzene and
Phenyldimethylsilanol and Ligand Liberation

Silanol	(B) in CDCl$_3$ from TMS (Hz)	(A) in d$_6$-DMSO from TMS (Hz)	Relative acidity (A) − (B)	Al complex	Ratio of ligand liberation (%)
Phenyldimethyl silanol	190	528	338 (3.77 ppm)	Al(Etaa)$_3$ Al(SA)$_3$	15 27
1,4-bis(hydroxy dimethylsilyl) benzene	184	526	342 (3.82 ppm)	Al(Etaa)$_3$ Al(SA)$_3$	17 −

Table 5　Polymerization of CHO with Aluminum Complex/
Ph$(CH_3)_2$SiOH and Aluminum Complex/HMSB[1]
Catalyst

Catalyst	Polymer conversion (%)		
Al(acac)$_3$/Ph$(CH_3)_2$SiOH	20 min.[2]	63 min.	175 min.
	1.2	1.4	1.5
Al(acac)$_3$/HMSB	2.2	2.8	3.0
Al(Etaa)$_3$/Ph$(CH_3)_2$SiOH	25 min.	85 min.	145 min.
	1.6	1.8	1.9
Al(Etaa)$_3$/HMSB	3.6	3.9	4.0
Al(SA)$_3$/Ph$(CH_3)_2$SiOH	25 min.	34 min.	50 min.
	2.2	2.5	2.5
Al(SA)$_3$/HMSB	9.2	10.0	10.5

Polymerization conditions:　40°C, Al complex, 0.05 mol%

silanol compound, 0.05 mol% to CHO on Ph$(CH_3)_2$SiOH,

0.025 mol% to CHO on HMSB

1) HMSB:　1,4-bis(hydroxydimethylsilyl)benzene

2) Polymerization time.

7-5 Aluminum complex/diphenyl(4-vinylphenyl)silanol

(DVPS) catalyst system

From the experiment using silanol oligomers, a dependence on an effect of silanol chain length was anticipated in the Al(acac)$_3$/silanol catalyst system. However in the Al(Etaa)$_3$/silanol or the Al(SA)$_3$/silanol system, the following silanol was considered to give the polymer effects.

    a) the silanol with intramolecular hydrogen bond.

    b) the silanol which reacts with an appropriate

       amount of aluminum complex.

Table 6 shows the polymer conversion of cyclohexene oxide when Al(acac)$_3$/mono(DVPS) and Al(acac)$_3$/poly(DVPS) were used. The polymer conversion with Al(acac)$_3$/poly(DVPS) catalyst system increased about five times, compared with that with Al(acac)$_3$/mono(DVPS) catalyst system. The catalyst would be activated by the acidity increment due to the aggregation of the silanol (intramolecular hydrogen bonding). The consideration was supported by the following experiment. When the DVPS copolymerized with styrene was used under the same SiOH concentration for preventing the silanol from the aggregation, the polymer conversion decreased.

The catalytic activity of Al(SA)$_3$/poly(DVPS) was higher than that of Al(SA)$_3$/mono(DVPS). In the case of DVPS, the deactivation seen in the Al(SA)$_3$/Trimer catalyst system was not observed. The results are supported by the

Table 6　Polymerization of CHO with Aluminum Complex/polymeric Silanol and the Ligand Liberation.

catalyst	concentration[1] of silanol to CHO (mol%)	solvent CHO/PhCH$_3$ (v/v)	polymer conversion				the ratio of ligand liberation (%)	Mw	Mn
			[2] 5min.	10min.	15min.	20min.			
Al(acac)$_3$/monoDVPS	0.05	3/1	5	8	11	13	–	–	–
Al(acac)$_3$/polyDVPS(Mw8000)	0.05	3/1	35	50	60	65	–	–	–
Al(acac)$_3$/polyDVPS(Mw8000)	0.035	neat	58	64	66	67*	–	40000	13000
Al(acac)$_3$/poly(DVPS:styrene(1:1))(Mw12000)	0.035	neat	53	58	63	65*	–	46000	18000
Al(acac)$_3$/poly(DVPS:styrene(1:2))(Mw11000)	0.035	neat	49	54	57	62*	–	41000	20000
Al(acac)$_3$/poly(DVPS:styrene(1:4))(Mw10000)	0.035	neat	45	51	55	60*	–	46400	21000
Al(acac)$_3$/poly(DVPS:styrene(1:8))(Mw9000)	0.035	neat	40	46	50	53*	–	47000	21000
Al(acac)$_3$/poly(DVPS:styrene(1:16))(Mw9000)	0.035	neat	14	25	30	33*	–	22000	7000
			[2] 5min.	10min.	20min.				
Al(SA)$_3$/monoDVPS	0.02	3/1	21	25	28*		25	45000	15000
Al(SA)$_3$/poly(DVPS:styrene(1:2))	0.02	3/1	45	54	58*		25	75200	29000
Al(SA)$_3$/poly(DVPS:styrene(1:4))	0.02	3/1	43	49	54*		26	76000	35000
Al(SA)$_3$/poly(DVPS:styrene(1:8))	0.02	3/1	37	45	48*		26	63000	31000
Al(SA)$_3$/poly(DVPS:styrene(1:16))	0.02	3/1	10	12	13*		26	44000	19000
Al(SA)$_3$/polyDVPS	0.02	3/1	51	56	62*		26	75000	30000
Al(Etaa)$_3$/mono(DVPS)			———————				16		
Al(Etaa)$_3$/poly(DVPS)			———————				17		
			[2] 5min.	20min.	40min.	60min.			
Al(acac)$_3$/SH6018[4]	0.05[3]	neat	23	37	42	43*	0	62000	33000
Al(Etaa)$_3$/SH6018[4]	0.05[3]	neat	28	47	50	53*	23	81000	41000
Al(SA)$_3$/SH6018[4]	0.05[3]	neat	13	18	22	25*	35	44000	23000

polymerization conditions:　40°C　1) The concentration of aluminum complex was the same as that of silanol compound, 2) polymerization time, 3) equivalent %, OH equivalent of SH6018/mol of monomer, 4) polymerization temperature, 45°C.

* Molecular weight of this polymer was measured.

fact that the ligand liberation of Al(SA)$_3$ did not change with the DVPS used, mono(DVPS) and poly(DVPS), as shown in Table 6. Table 6 also shows the molecular weight of the polymer. Maximum value was obtained when $1:1 \sim 1:4$ DVPS : styrene polymers were used.

7-6 Aluminum complex/SH6018 catalyst system

When poly(DVPS) was used as a silanol component, the catalytic activity of Al(SA)$_3$/poly(DVPS) was higher than that of Al(acac)$_3$/poly(DVPS). However, when a silicone resin containing SiOH(SH6018, Toray silicone, Mw 1600, OH equivalent about 400) was used as a silanol component, the catalytic activity and molecular weight varied with the aluminum compound as follows. (Table 6)

$$Al(Etaa)_3 > Al(acac)_3 > Al(SA)_3$$
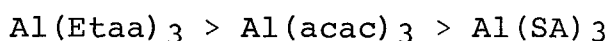
The ratio of the ligand liberation of Al(SA)$_3$ was especially high in case of Al(SA)$_3$/SH6018 catalyst system, as shown in Table 6. The phenomenum could be explained by the facts obtained in the experiment of aluminum complex/ oligosilanol catalyst system, namely, poly(DVPS) could make the intramolecular hydrogen bond with an appropriate ratio of the reaction between aluminum complex and silanol, however, SH6018 could do it with large ratio of the reaction. The difference would be due to the silanol structure, that is, the rigidity of polymer chain, and bulkiness around the SiOH group, and position of SiOH.

References

1. G. I. Harris, J. Chem. Soc. (B), _1970_, 492

2. A. W. Baker and A. T. Shulgin, J. Am. Chem. Soc.,
    _81_, 1523 (1959); R. West and C. S. Kraihanzel,
    J. Am. Chem. Soc., _81_, 765 (1961); R. West, ibid.,
    _81_, 1614 (1959), M. R. Basuka, J. Chem. Phys.,
    _35_, 1151 (1961); S. Kohama, Nippon Kagaku Kaishi,
    _81_, 69 (1960)

Chapter 8   Polymerization under UV Irradiation

8-1   Introduction

In Chapter 4 and 5 it was shown that interaction be-
tween aluminum complex and silanol was important for the
catalyst activation. The interaction was considered to
be induced by UV-radiation, because it is known that
under UV-radiation acid dissociation was promoted to
strengthen the hydrogen bonding, for example, between
cytosine and guanine.[1]

8-2   Polymerization profiles

The results on polymerization under UV-radiation are
shown in Figures 1, 2 and 3. The catalyst activity of
the Al(acac)$_3$/triphenylsilanol system increased about
3 - 4 times under UV-radiation, especially 254 nm radia-
tion. However the catalyst, Al(Etaa)$_3$ or Al(SA)$_3$/tri-
phenylsilanol system was not activated.

The difference in polymerization behavior under UV-
radiation implied the difference in the mechanism of
interaction as mentioned in Chapter 5. Namely, interac-
tion between Al(acac)$_3$ and triphenylsilanol will be one
between carbonyl oxygen and SiO-H. Chelation will weaken
the double bonding of carbonyl, however, the properties
as carbonyl will remain yet. The interaction between
cytosine and guanine occurs between the N-H and the
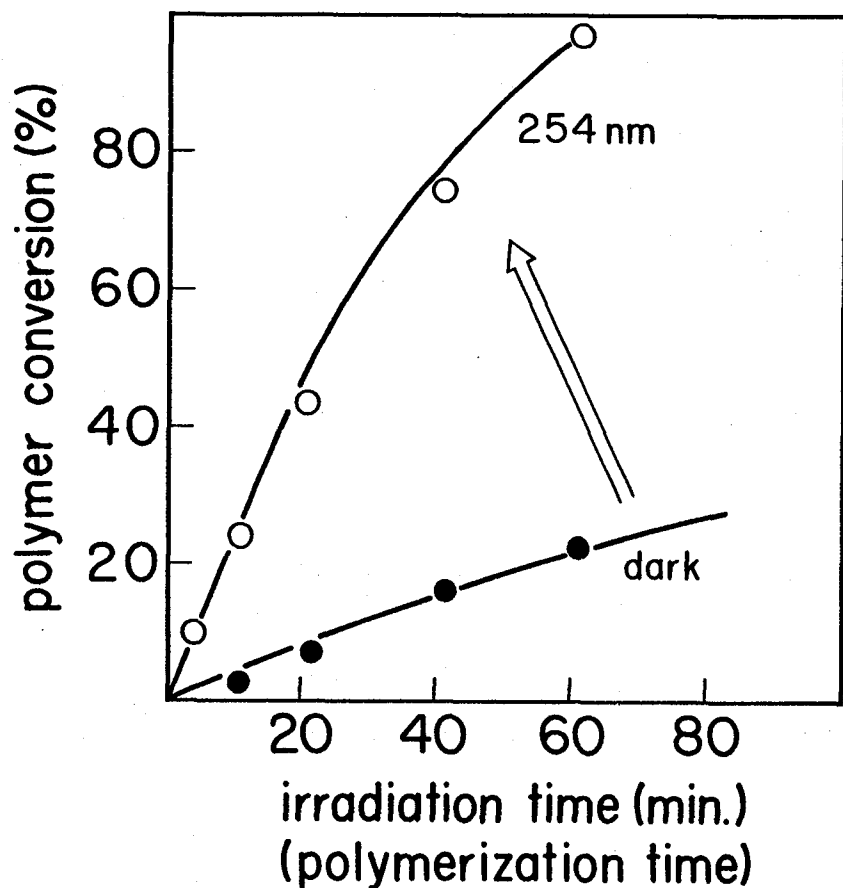
Figure 1   Polymerization of cyclohexene oxide under UV
   radiation: polymerization conditions: 40°C, 400W-
   high pressure mercury lamp, Al(acac)$_3$ 0.03 mol%,
   Ph$_3$SiOH 0.03 mol%.
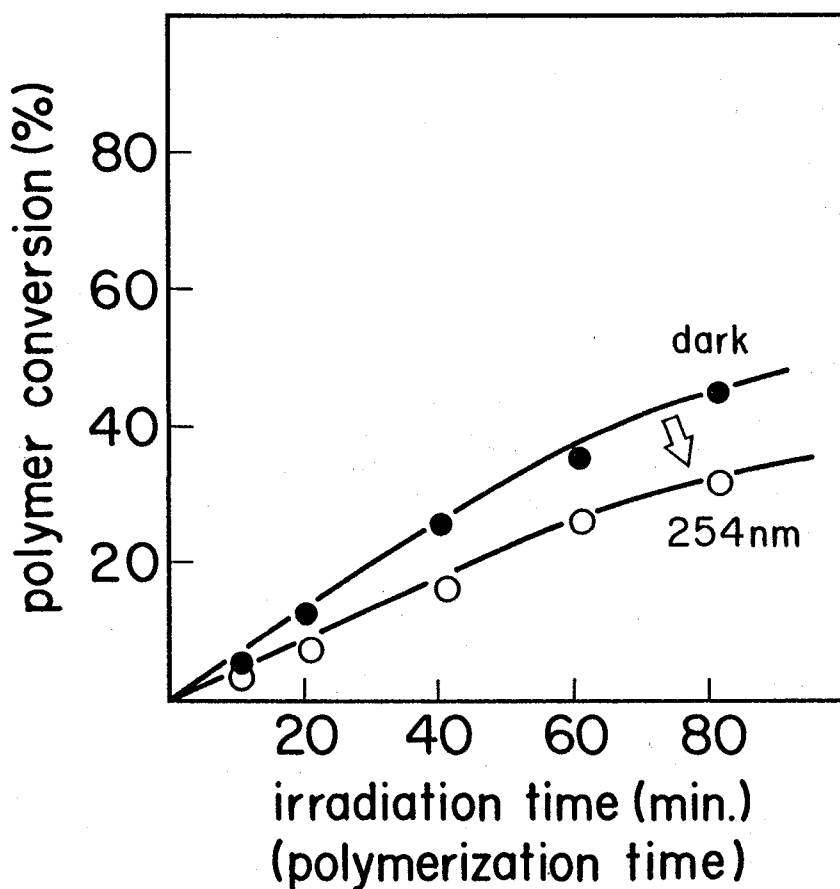
Figure 2   Polymerization of cyclohexene oxide under
    UV radiation.   Polymerization conditions are the same
    as in Figure 1.   Al(Etaa)$_3$ 0.015 mol%, Ph$_3$SiOH 0.015
    mol%.
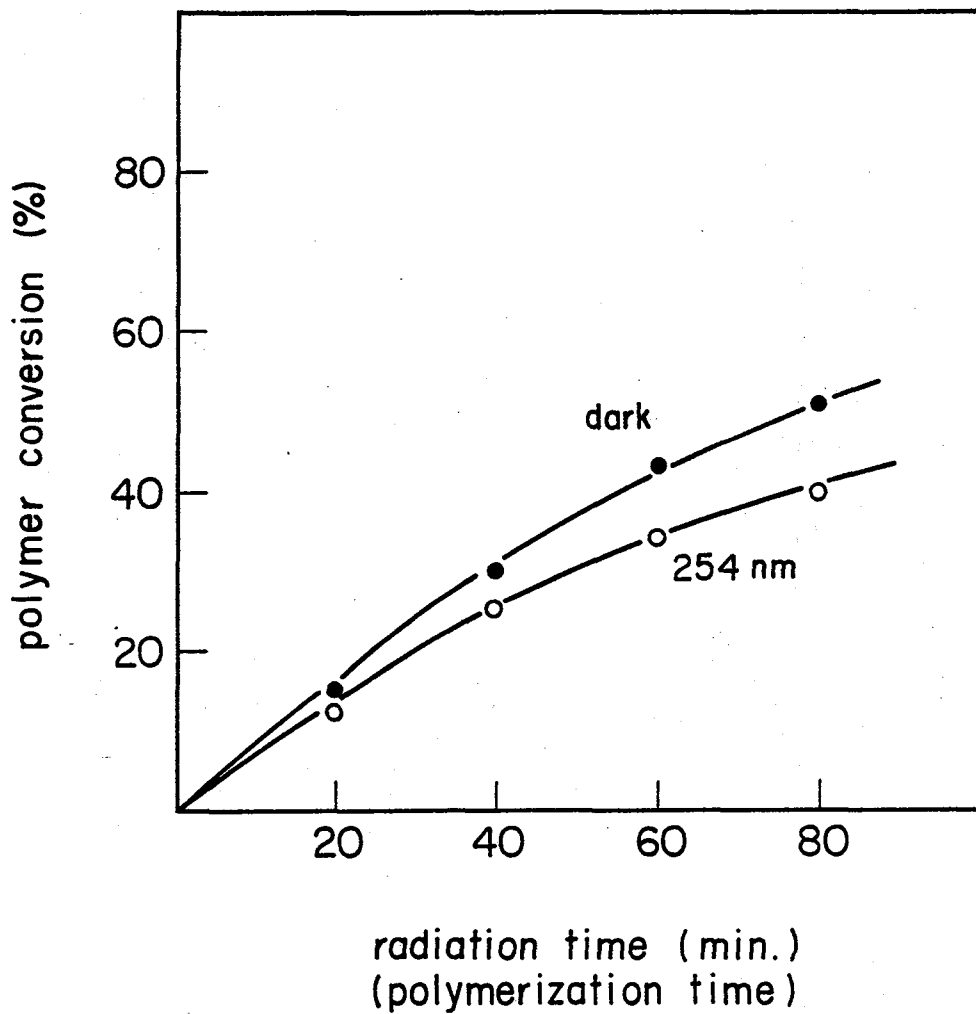
Figure 3   Polymerization of cyclohexene oxide under
   UV radiation.   Al(SA)$_3$/Ph$_3$SiOH (0.01 mol%/0.01 mol/%)
   low pressure mercury lamp.

carbonyl oxygen. Therefore it is anticipated that the interaction between Al(acac)$_3$ and triphenylsilanol is strengthened under UV-radiation.

However, in case of Al(Etaa)$_3$/triphenylsilanol or Al(SA)$_3$/triphenylsilanol, interaction between aluminum complex and silanol is caused between oxygen of Si-OH and aluminum, and between oxygen of Al-O-Si and proton of SiO-H. Probably, such an interaction is not strengthened under UV-radiation. Another reason has to be considered. Since aluminum complex becomes labile under UV-radiation, ligand exchange reaction between aluminum chelate and triphenylsilanol will become to occur easily. Therefore, it is considered that the amount of effective SiOH decreases in polymerization system, and catalyst activity also decreases.

Reference

1. P. Suppan, Principles of Photochemistry, The Chemical
   Society Monographs, No. 22, The Chemistry Society
   Publication (1972); T. Matuura, "Yuki Hikari Kagaku",
   Chemistry Monograph No. 20, p. 179, Kagaku Dojin,
   Kyoto (1976)

Chapter 9   Thermal and Electrical Properties of Epoxy

Resin Cured by Aluminum Complex/Silanol

Catalyst

9-1   Introduction

The present catalyst is developed for the epoxy
resin to be used in electrical appliances. In order to
examine the effect of the catalyst, electrical properties
of the epoxy resin cured with the present catalyst were
measured. The results especially at high temperature were
unexpectedly good. The reason of such excellent electri-
cal properties will be discussed.

9-2   Difference in electrical properties between epoxy

resin cured with BF3 complex catalyst and that

cured with tris(salicylaldehydato)aluminum/diphenyl-

silanediol catalyst

The electrical properties of bisphenol A type epoxy
resin (I) Epikote 828 cured with tris(salicylaldehydato)-
aluminum/diphenylsilanediol((I)-Al(SA)$_3$/DP) were compared
with that cured with BF$_3$ monoethylamine complex catalyst
((I)-BF$_3$·MEA). Figure 1 shows the relation between elec-
trical dissipation factor (Tan δ) and temperature. The
dissipation factor of (I)-BF$_3$·MEA increased remarkably at
the temperature above 130°C. However in case of (I)-
Al(SA)$_3$/DP, the value had a maximum at about 150°C and
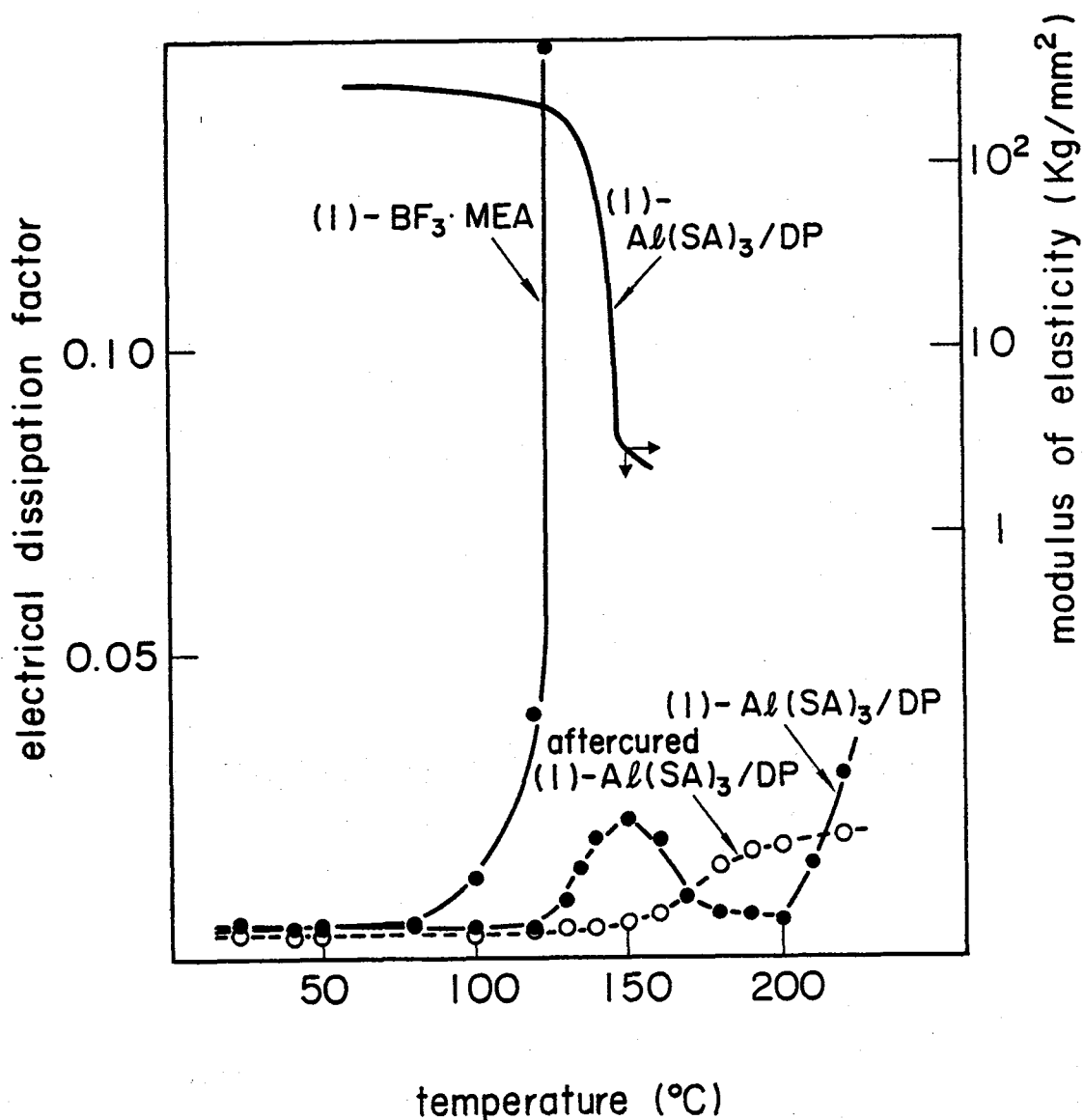
Figure 1   Relation between electrical dissipation factor
   and temperature, and relation between modulus of
   elasticity and temperature.   Sample, thickness 1 mm,
   (I)-Al(SA)₃/DP, Al(SA)₃, 2 phr, DP 2 phr: (I)-BF₃·MEA,
   BF₃·MEA, 3 phr, 150°C, 15 h, aftercure 180°C for 15 h.

increased again gradually at temperature above 200°C.
The maximum point shifted to higher temperature and the
height of peak diminished when (I)-Al(SA)$_3$/DP was after-
cured at 180°C for 15 hours. Figure 1 also shows the mod-
ulus of elasticity. T_g of (I)-Al(SA)$_3$/ DP coincided with
the maximum temperature for Tan δ - temperature curve.
Therefore, the peak is considered to be due to the mobili-
ty of main chain of epoxy resin cured. The dissipation
factor for (I)-BF$_3$·MEA did not have such a maximum. This
could be explained as follows. The conductance loss be-
came a dominant factor at temperature above 130°C, there-
fore, the peak of Tan δ due to the motion of the dipoles
on the main chain was considered to be buried by the in-
crease in the conductance loss. The explanation was sup-
ported by the fact that the relation between ε" and fre-
quency in the logarithmic scale becomes to have a straight
line with slope equal to -1 at temperature above 130°C,
as shown in Figure 2. The following equation is known
between A.C. conductivity and angular frequency.[1]

$$\sigma_a(\omega) = \omega \{ \frac{1}{\omega} \sigma_{ao} + \varepsilon_o \varepsilon''(\omega) \} = \sigma_{ao} + \varepsilon_o \varepsilon''(\omega) \cdot \omega$$

where $\sigma_a(\omega)$: A.C. conductivity

     σ_{ao} : D.C. conductivity

     ω : angular frequency

     ε_o : dielectric constant in vacuum
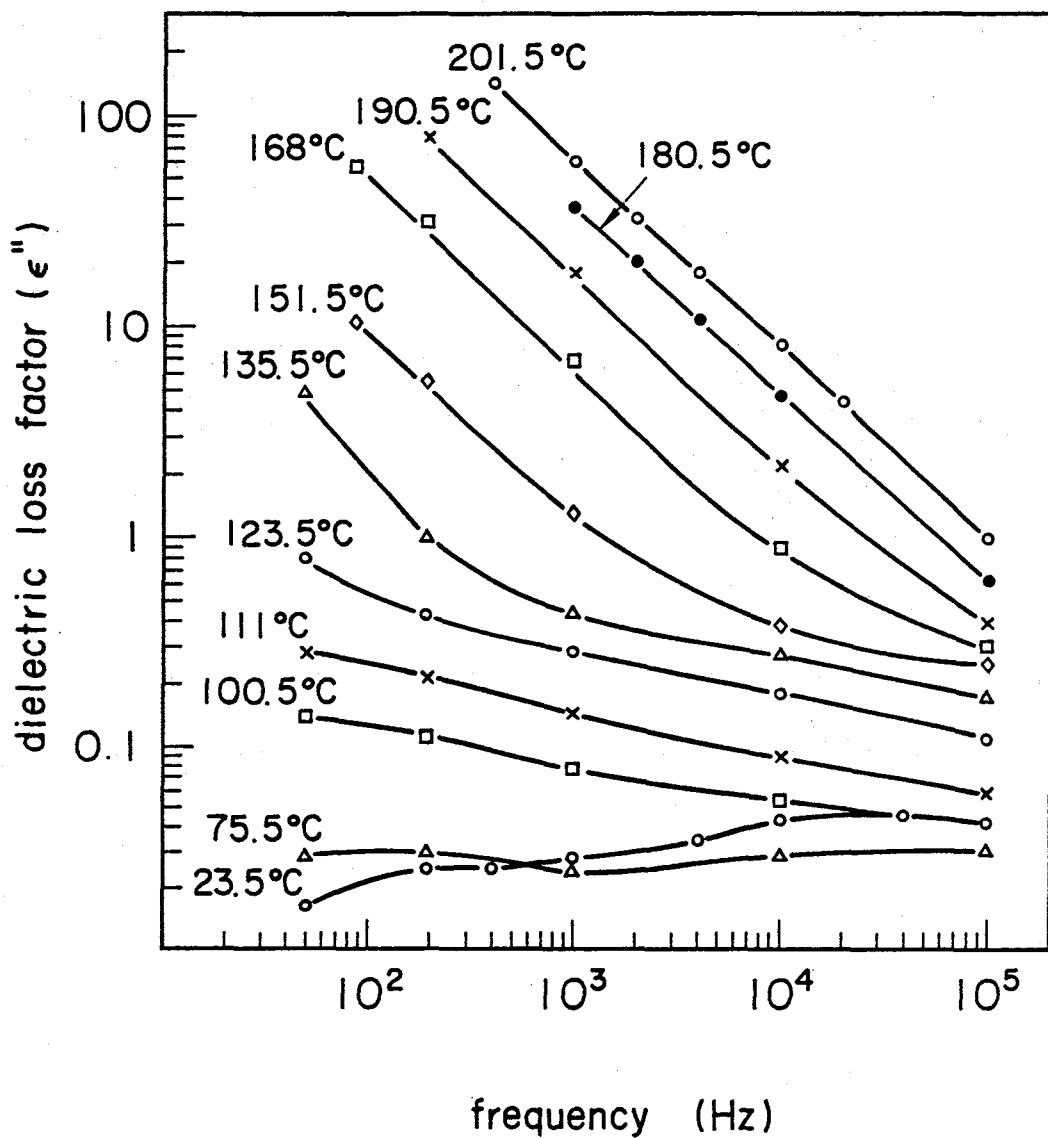
Figure 2   Relation between dielectric loss factor and
frequency: sample, (I)-BF$_3$·MEA.

Therefore, if conductance loss is predominant, $\log \varepsilon''$ would be inversely proportional to $\log f$ (frequency), and the slope would be -1.

The difference in the electrical properties between $(I)-Al(acac)_3/SH6018$ and $(I)-BF_3 \cdot MEA$ was investigated by means of thermal depolarization current method. Figure 3 shows the depolarization current-temperature curve. The curve had a maximum at about $120°C$. Figure 4 shows the relation between the depolarization charge (Q) and the polarizing field (Ep). The depolarization charge for $(I)-Al(acac)_3/SH6018$ was about 10^{-8} coul/cm^2 and that for $(I)-BF_3-MEA$ was about $10^{-6} \sim 10^{-7}$ coul/cm^2. Generally speaking, polarization of dielectrics is classified into heterogeneous polarization and homogeneous polarization[3]. In the former, there are hetero charge which is caused by the macroscopic shift of ionic impurity in dielectrics, and homocharge which is caused by the injection of charge from electrode to dielectric. In the latter, there are orientational polarization charge and hetero charge which is caused by the microscopic displacement of ionic impurity. In the present experiment, the charge was hetero. The depolarization charge was directly proportional to the polarizing field. Therefore, the charge was considered to be due to homogeneous polarization.[4] If the polarization is attributed to the thermal disorder for orientational dipole only, maximum value for orientational
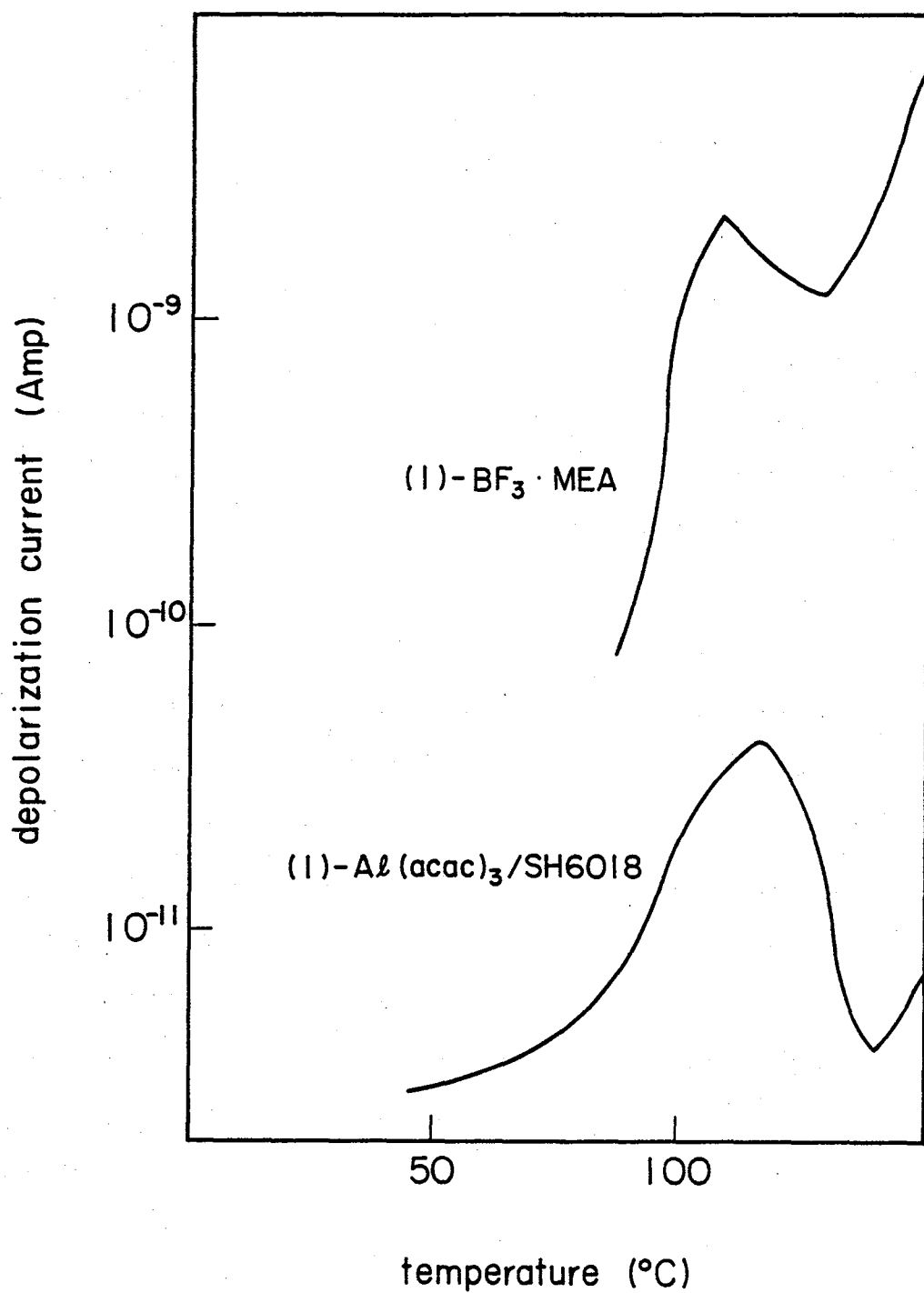
Figure 3   Depolarization current curve.
Condition, see Figure 4.
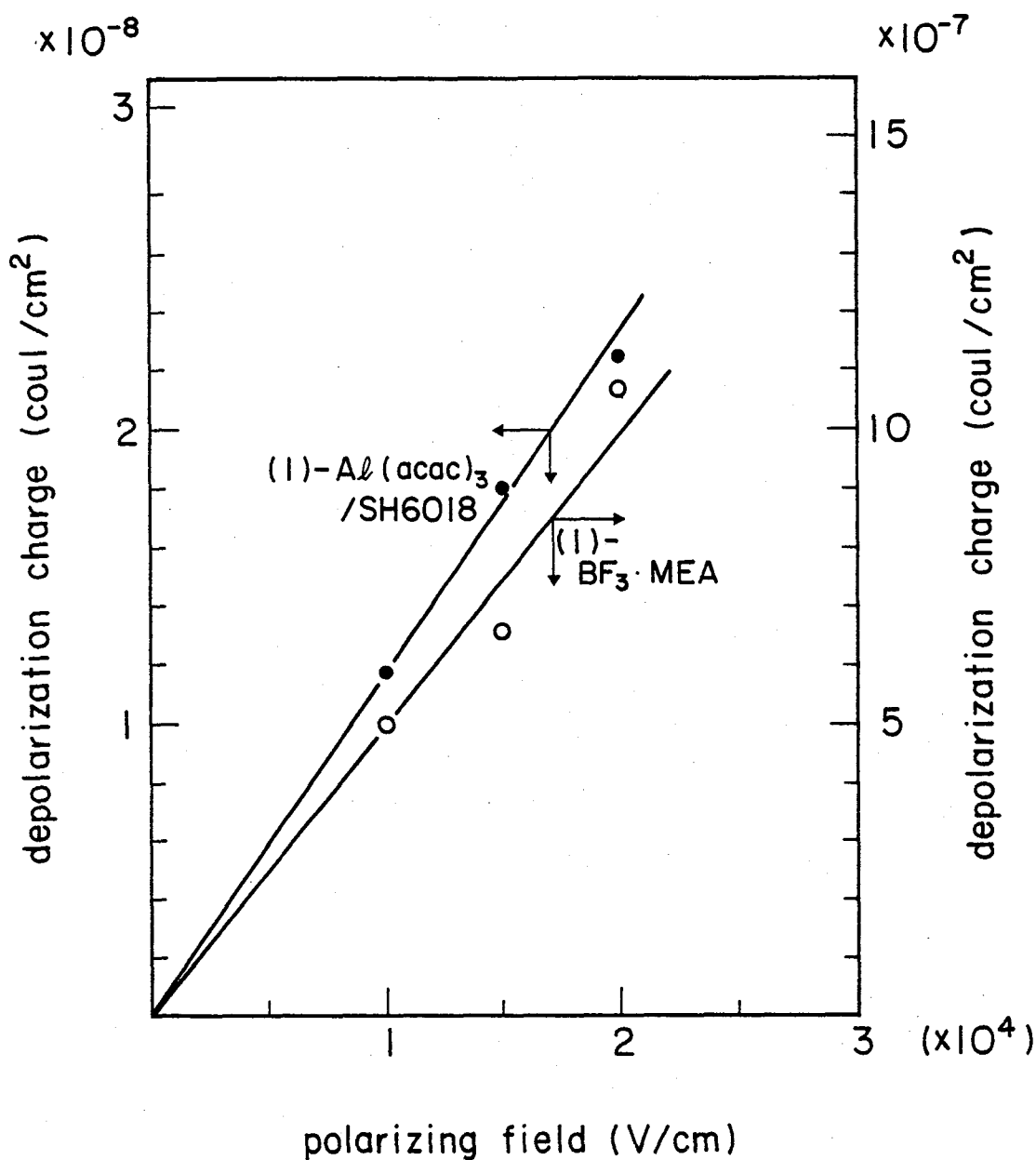
Figure 4 Relation between depolarization charge and
polarizing field. Thickness 1 mm, (I)-Al(acac)$_3$/
SH6018, Al(acac)$_3$ 2 phr, SH6018 3 phr, 150°C, 15 h,
electrode 10 mmφ, 2×10^4 V/cm at 150°C.

polarization charge would be obtained from the following
equation by use of Debye's polarization orientation
theory.[5]

$$P = \frac{N\mu_{eff}^2 E_p}{3kT_p}$$

Where   N   : the number of dipole in 1 cm^3

             μ_{eff}: effective dipole moment

             E_p : polarizing field

             k   : Boltzmann's constant

             T_p : depolarization temperature

Hydroxide and ether linkage are present as the dipole in
the cured epoxy resins. Group moment for alcohol and
ether is about 1.6 - 1.7 Debye. The calculated orienta-
tional polarization charge was about 10^{-10} coul/cm^2, even
if dipole moved freely. The measured depolarization
charge was more than the calculated depolarization charge
by a factor of about 10^2 in case of (I)-Al(acac)$_3$/SH6018
and by a factor of about $10^3 \sim 10^4$ in case of (I)-BF$_3$·MEA.
Therefore the depolarization charge could not be explained
in terms of thermal disordering of dipoles only. However,
when microscopic displacement and trap for ionic impurity
were considered, the experimental results could be ex-
plained. Both of (I)-Al(acac)$_3$/SH6018 and (I)-BF$_3$·MEA
had ionic impurity, however, it was found that the amount
of ionic impurity in (I)-Al(acac)$_3$/SH6018 was smaller

than that in (I)-BF$_3$·MEA.

Dielectric constant for (I)-Al(SA)$_3$/DP was relatively constant throughout the temperature from 25°C to 220°C. However dielectric constant for (I)-BF$_3$·MEA changed remarkably at the temperature above 130°C, as shown in Figure 5.

Figure 6 shows the relation between volume resistivity and temperature. The volume resistivity of (I)-Al(SA)$_3$/DP was higher than that of (I)-BF$_3$·MEA by a factor of about 10^4 times at 150°C. The volume resistivity for (I)-Al(SA)$_3$/DP hold the value of 10^{12} Ωcm at even 200°C.

Break down voltage for (I)-Al(acac)$_3$/SH6018 was compared with that for (I)-BF$_3$·MEA. Figure 7 shows the results. Break down voltage for (I)-Al(acac)$_3$/SH6018 increased gradually with temperature, however, that for (I)-BF$_3$·MEA decreased remarkably at 120°C. These results show that Al(acac)$_3$/SH6018 catalyst system is "clean" electrically, compared with BF$_3$·complex catalyst.

The polymerization was considered to be caused cationically by the proton formed by the interaction between aluminum complex and silanol as mentioned in Chapter 5. Diphenylsilanediol was consumed by self condensation reaction, condensation with secondary alcohol in epoxy resin, and addition to the epoxide as shown in Figure 8. The cationic site is made by the interaction between aluminum complex and silanol. If the silanol is consumed in

- 117 -
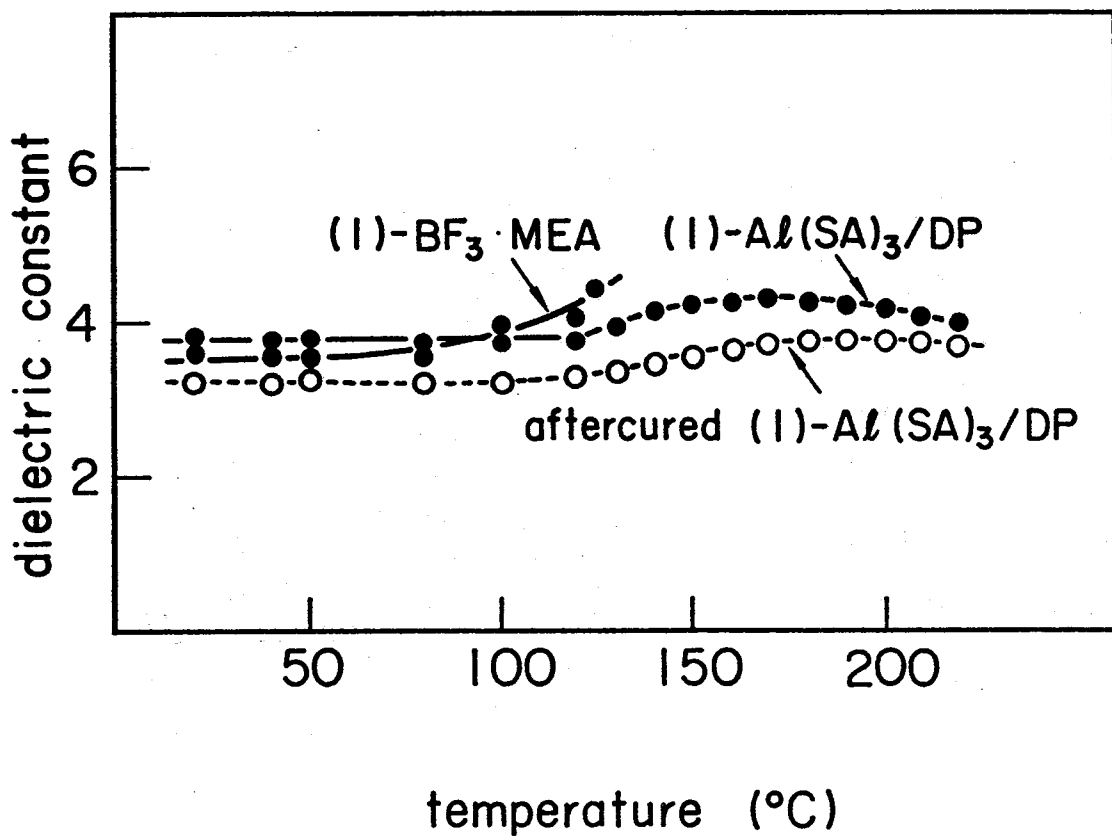
Figure 5   Relation between dielectric constant and
  temperature: aftercure, 180°C for 15 h.
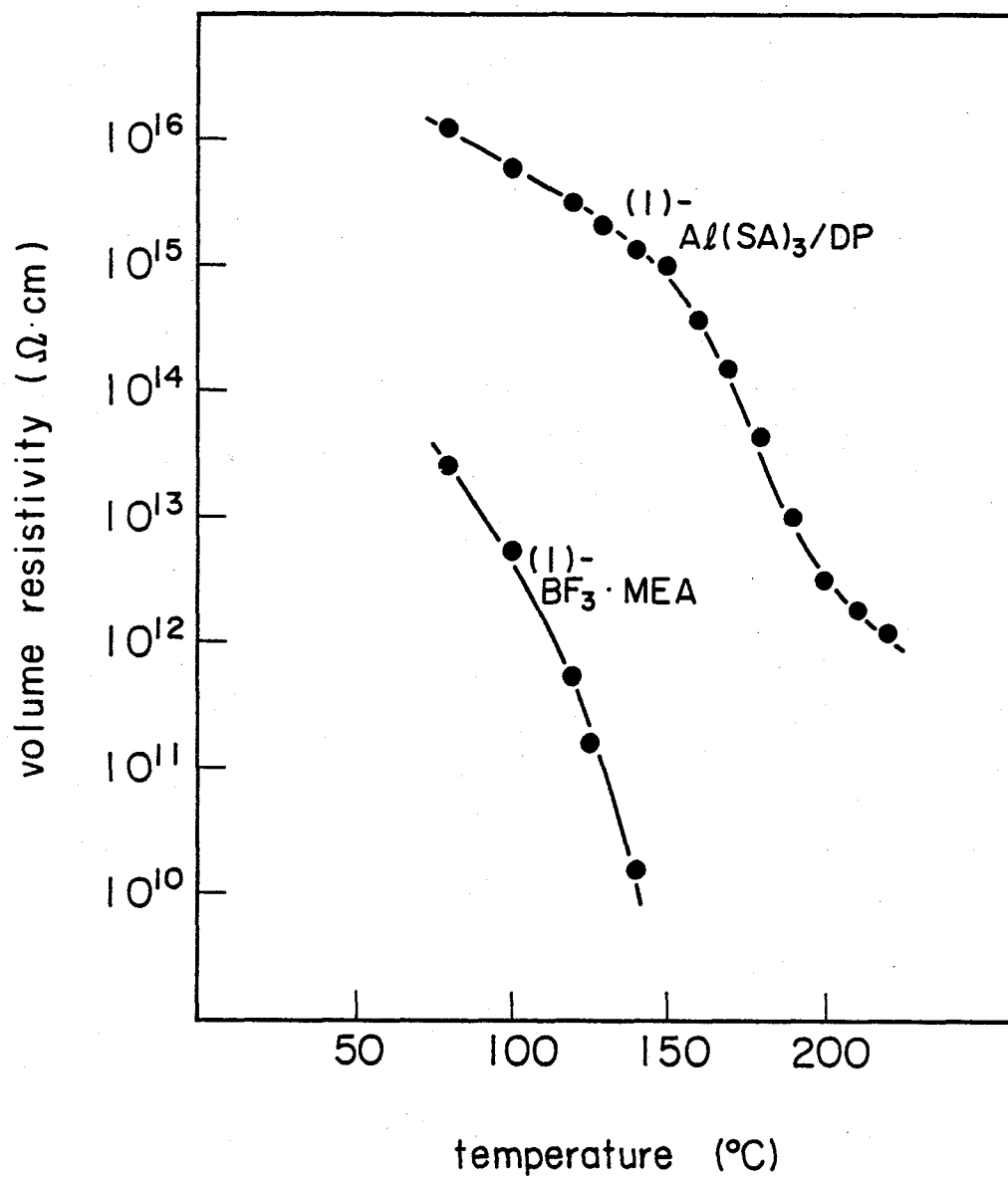
Figure 6   Relation between volume resistivity and
    temperature.
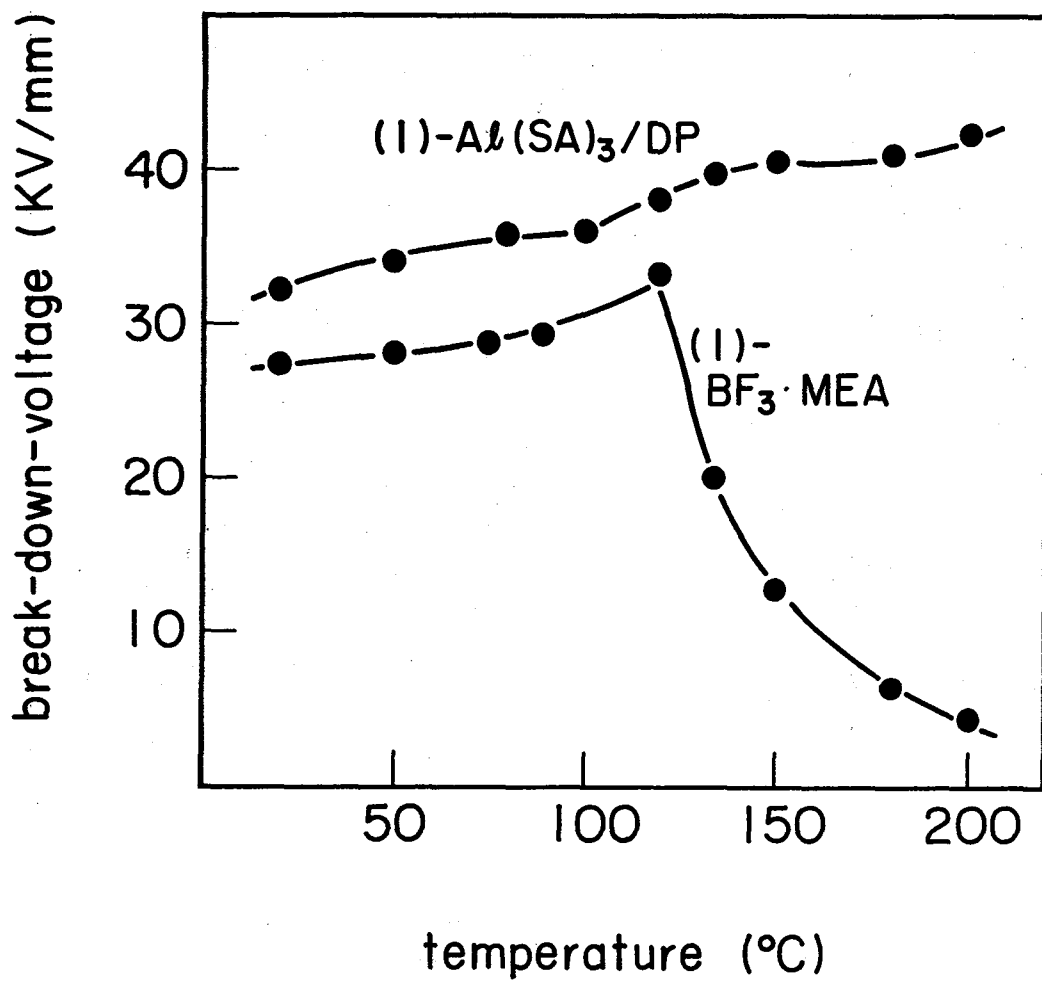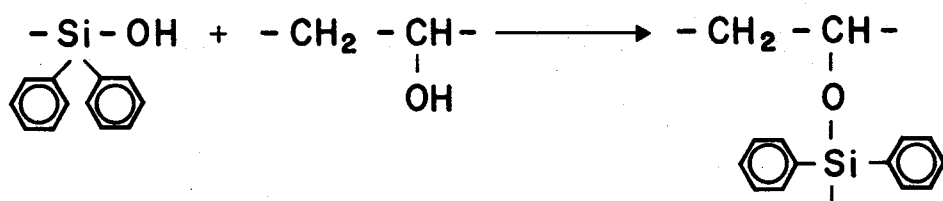
Figure 7   Relation between break-down-voltage and
temperature.
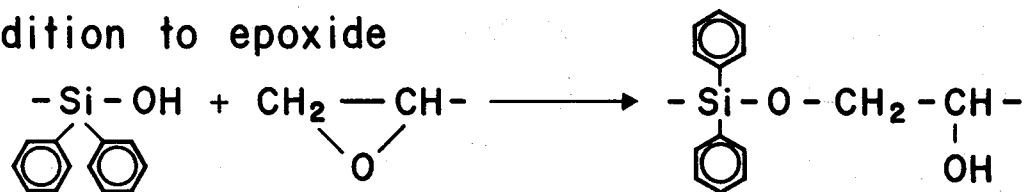
Figure 8

the polymerization reaction, no cationic site exists in the polymerization system. Therefore, the absence of any appreciable ionic species after polymerization will be important for the excellent electrical properties.

The presence of the cationic site in the cured resin matrix was considered to affect the thermal stability. Relation between weightloss of cured resin plate and aging time at 225°C was shown in Figure 9. The ratio of weightloss for (I)-BF_3·MEA was larger than that for (I)-Al(SA)$_3$/ SH6018 (Toray silicone, silicone resin containing SiOH, OH equivalent 400). Ionic species in (I)-BF_3·MEA would accelate the degradation of the polymer chain.

9-3 Dependence of the electrical properties on structure
      of catalyst

The electrical properties depend on the structure of catalyst, as shown in Table 1. When triphenylsilanol was used as the silanol component, the electrical properties at 220°C deteriorated depending on the structure of catalyst, as follows, Al(SA)$_3$ > Al(Etaa)$_3$ > Al(acac)$_3$. Gellation of the epoxide occurred depending on the catalyst, in the following order, Al(SA)$_3$/Ph$_3$SiOH > Al(Etaa)$_3$/ Ph$_3$SiOH > Al(acac)$_3$/Ph$_3$SiOH. The electrical properties improved as curing proceeds.

When Al(SA)$_3$ was used as the aluminum component, the dependence of the electrical properties on silanol struc-
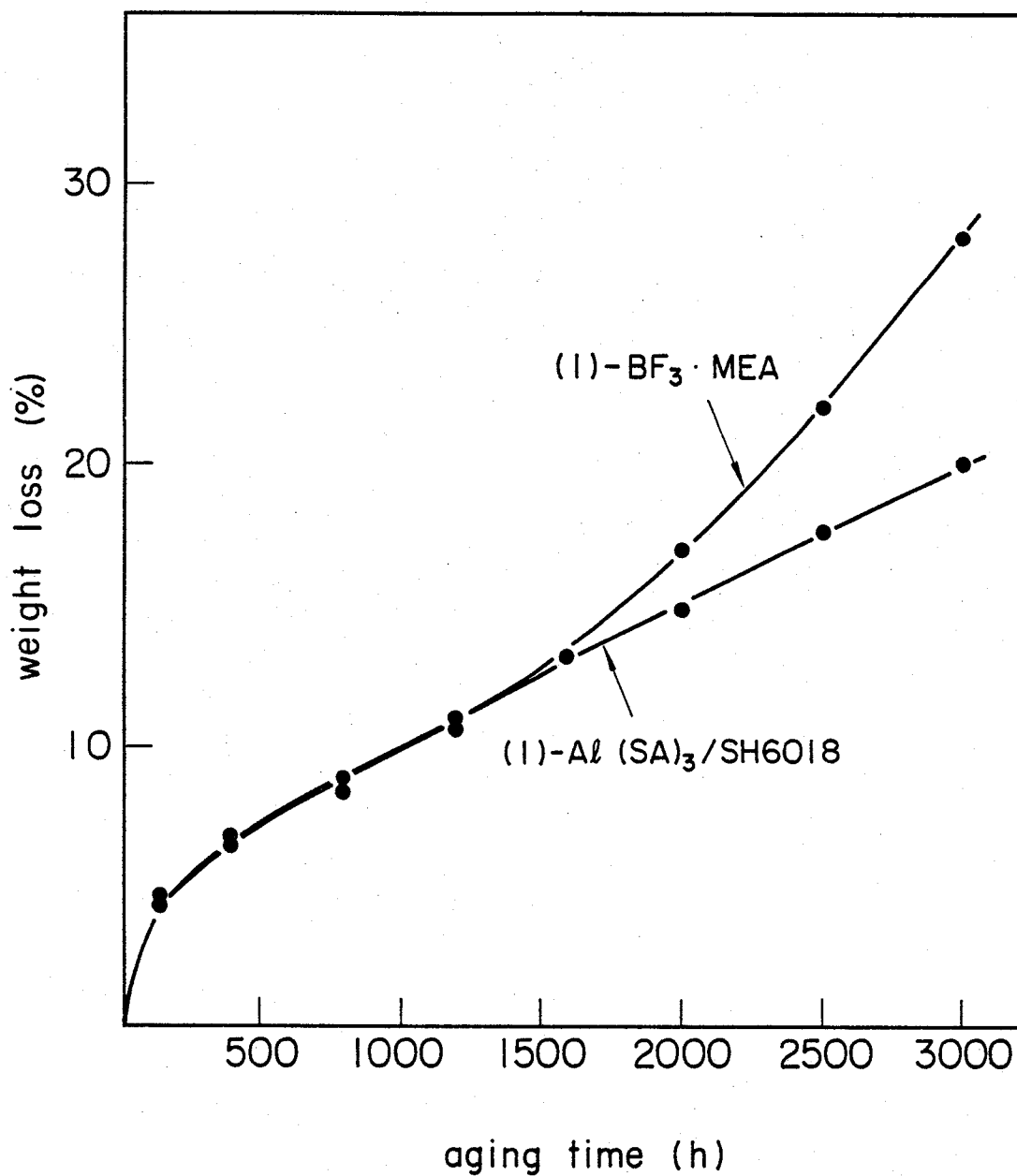
Figure 9   Relation between weight loss and aging time
at 225°C Sample, (I)-Al(SA)$_3$/SH6018, Al(SA)$_3$ 2 phr,
SH6018 2 phr, 150°C, 15 h.

ture was examined. The electrical properties at 220°C lowered as follows, $Ph_3SiOH > SH6018 > Ph_2Si(OH)_2$. The order could be explained as the same way.

Dependence of the electrical properties on the amount of the catalyst was examined. When the amount of the silanol increased, the gellation time of the epoxy resin was faster. However, best electrical properties were obtained in case of aluminum complex/silanol(1/3)(mol/mol). When the ratio of the silanol was too large, silanol would remain in the matrix of the cured epoxy resin, therefore, the electrical properties would deteriorate.

Table 1　　Electrical Properties for Epoxy Resin Cured with
Aluminum Complex/Silanol Catalysts[a]

Al complex	(phr)	Silanol	(phr)	Dissipation factor (%)		Dielectric constant		Volume resistivity (Ωcm)
				25°C	220°C	25°C	220°C	220°C
Al(SA)$_3$	2.4	Ph$_3$SiOH	3.8	0.5	1.2	3.7	3.8	7.2×10^{12}
Al(Etaa)$_3$	2.6	Ph$_3$SiOH	3.8	0.4	2.9	3.9	4.1	3.0×10^{12}
Al(acac)$_3$	2.0	Ph$_3$SiOH	3.8	0.5	6.0	3.7	4.4	9.5×10^{11}
Al(SA)$_3$	2.4	SH6018	5.6	0.5	2.5	3.8	3.9	5.0×10^{12}
Al(SA)$_3$	2.4	Ph$_2$Si(OH)$_2$	3.0	0.5	3.0	3.8	4.0	1.1×10^{12}
Al(acac)$_3$	2.0	Ph$_2$Si(OH)$_2$	1.5	0.8	12.4	3.9	6.1	—
"	"	"	3.0	0.6	8.0	3.7	4.9	—
"	"	"	4.5	0.7	6.2	3.7	4.5	—
"	"	"	6.0	0.7	4.9	3.7	4.0	—
"	"	"	7.5	0.5	5.7	3.9	4.7	—
"	"	"	9.0	0.9	10.0	4.1	5.7	—

a) 150°C for 15 h cure

References

1. H. Mikawa, and S. Kusabayashi, Kobunshi Handotai,

   p. 248, Kodan-sha, printed in Japan (1977);

   Y. Toriyama, Hoden Hand Book, Denki-Gakkai, p.390,

   printed in Japan.

2. P. K. C. Pillai and M. Goel, J. Electrochem. Soc.,

   120, 395 (1973)

3. G. Gross, Phys. Rev., 54, 57 (1940)

4. M. M. Perlman, J. Appl. Phys., 42, 2645 (1971)

5. P. Debye, "Polar Molecules" Reinhold Pub. Co., (1929)

Chapter 10   Latent Catalyst

10-1   Introduction

In this way, "clean" and active catalyst for epoxide polymerization was obtained. For practical use, epoxy resins are provided as a composition containing catalyst. The epoxy resin composition must be stable before use. It must be cured rapidly. Therefore, molecular design is necessary for the active catalyst which is generated by a trigger. Heat or UV-radiation is usually used as the trigger. The catalyst is called as a latent catalyst.

The following latent catalyst were investigated.

1) Aluminum complex/hydrolyzable silicon compound system.

2) Aluminum complex/thermally generated silicon compound system.

3) Aluminum complex/photogenerated silicon compound system.

10-2   Aluminum complex/hydrolyzable silicon compound system

Active site of aluminum complex/silanol catalyst is SiO-H. If the SiOH is protected with alkoxy group, the catalyst activity at room temperature will be inhibited. However, the alkoxy silane will be hydrolyzed by small amount of water contained in epoxy resin monomer at higher temperature, then the catalyst will be active.

$$Si-OR \; + \; H_2O \; \longrightarrow \; Si-OH \; + \; ROH$$

$$catalyst$$

The temperature at which the reaction is carried out (T_h) was examined. Alicyclic epoxy resin (II) shown in Figure 1 was used. Temperature of epoxy resin (II) containing the catalyst was raised at 1.5°C/min and the rise in temperature caused by reaction heats was examined. Table 1 shows the results. The T_h rised in the following order, depending on the structure of alkoxysilane.

$$Ph_2Si(OCOCH_3)_2 \; < \; Ph_2Si(OCH_3)_2 \; < \; Ph_2Si(OEt)_2 \; < \; Ph_3SiOCH_3$$

$$< \; Ph_2(CH_2=CH)SiOEt \; < \; Ph_2Si(OiPr)_2 \; < \; Ph_3SiOEt.$$
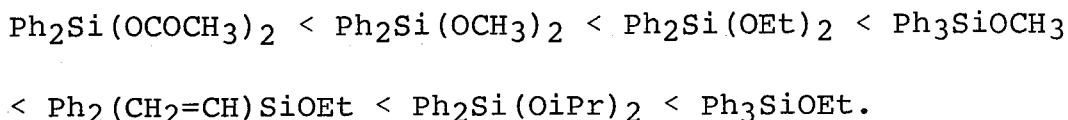
The T_h changed by following factor.

1) Substituent bonding to Si

$$Ph_2Si< \; < \; Ph_2(CH_2=CH)Si- \; < \; Ph_3Si-$$

2) Alkoxide (or esterate)

$$-OCOCH_3 \; < \; -OCH_3 \; < \; -OCH_2CH_3 \; < \; -OCH(CH_3)_2$$
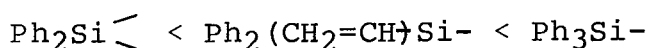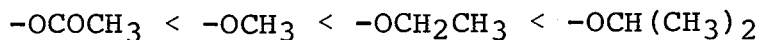
Ease in hydrolyzability for Si-O is determined by bulkiness neighbour Si and O. The tendency of T_h was coincident with that of hydrolyzability.

Table 2 shows the activation energy of gelation from 150°C to 200°C, when Epikote 828 epoxy resin [I] type was
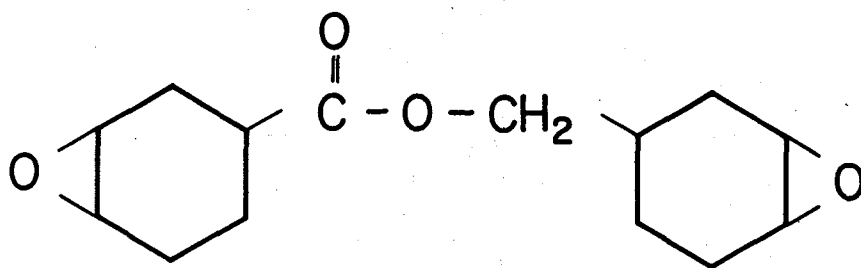
Figure 1   Structure of alicyclic epoxide.
(ERL 4221, UCC)

Table 1   Variation of Catalytic Activity of
Al(acac)$_3$/alkoxysilane.[a]

Alkoxysilane	phr[b]	Temperature (°C)
Ph$_2$Si(OMe)$_2$	0.37	73
Ph$_2$Si(OEt)$_2$	0.41	85
Ph$_2$Si(OiPr)$_2$	0.45	123
Ph$_2$Si(OCOCH$_3$)$_2$	0.45	50
Ph$_3$SiOMe	0.44	95
Ph$_3$SiOEt	0.46	130
Ph$_2$(CH$_2$=CH)SiOEt	0.39	100

a) Program rate 1.5°C/min. epoxide aliphatic epoxide
   (see Figure 1), Al(acac)$_3$ 0.19 mol%, alkoxysilane
   0.38 mol%

b) weight % to epoxy resin.

Table 2   Activation Energy Obtained Using
          Various Silane Catalysts[a]

Alkoxysilane	Activation energy (kcal/mol)
$Ph_2Si(OMe)_2$	23.7
$Ph_2Si(OEt)_2$	28.4
$Ph_2Si(OiPr)_2$	25.6
$Ph_2Si(OPh)_2$	23.3
Ph_2SiOEt	26.0
Ph_3SiOMe	25.5

a) $Al(SA)_3$ 2.4 phr, alkoxysilane 0.123 mol/1000 ml
   of epoxide, measurement of gelation by curast
   meter method.

cured with Al(SA)$_3$/alkoxysilane catalyst. The activation energy increased in the following order.

$$Ph_2Si(OPh)_2 < Ph_2Si(OMe)_2 < Ph_3SiOMe < Ph_2Si(OiPr)_2$$

$$< Ph_3SiOEt$$
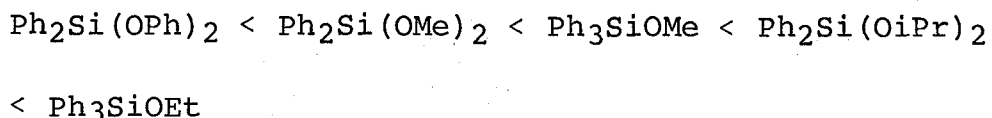
The tendency of order of activation energy was the same as that of T_h.

In the aluminum complex/alkoxysilane catalyst, the alkoxysilane was gradually hydrolyzed even at room temperature and the epoxy resin was gradually reacted. In order to prevent the reaction at room temperature, water in the epoxy resin was eliminated with zeolite 4A. Figure 2 shows the results. The composition was more stable in presence of zeolite. However above 100°C, gelation of the composition in presence of the zeolite was faster.

10-3 Aluminum complex/thermally generated silicon

    compound system

    The silicone compound liberating silanol thermally without H$_2$O was investigated. It is known that the organic compound decomposes by means of β-elimination as follows.[1]

$$HO{(CH_2\underset{\underset{COOC_2H_5}{|}}{\overset{\overset{COOC_2H_5}{|}}{C}})}_nH \xrightarrow{\Delta} H_2O + nCH_2=C(COOC_2H_5)_2$$
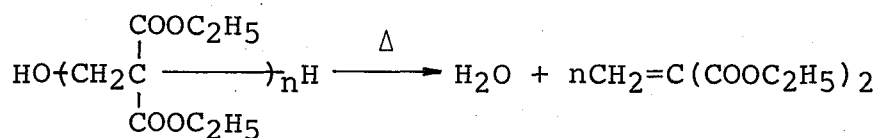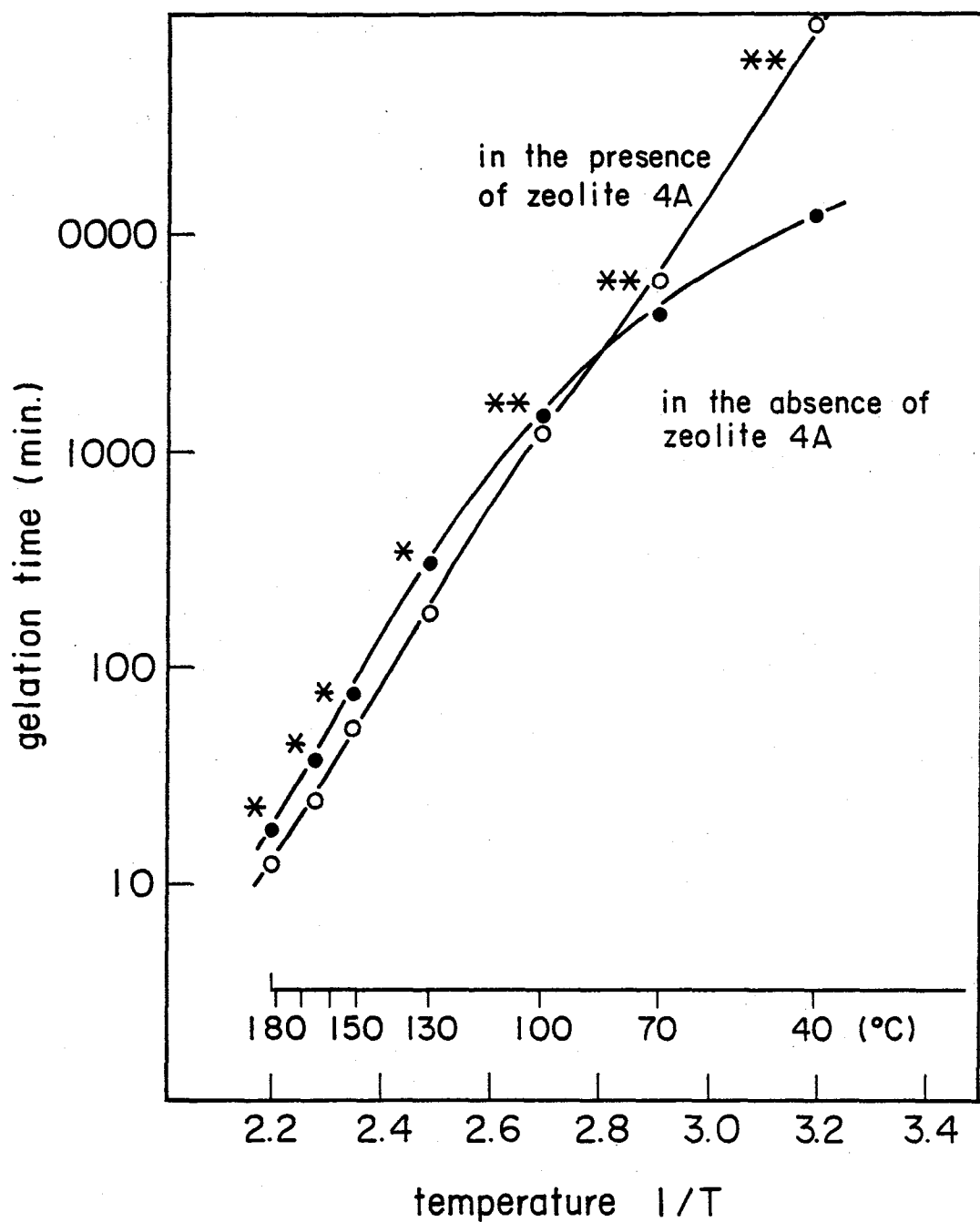
Figure 2   Relation between gelation time and temperature.
Al(SA)$_3$ 4.8 phr, Ph$_2$Si(OMe)$_2$ 2.0 phr, Epikote 828 epoxy
resin, zeolite 4A 10 phr.
* curast meter method, ** test tube method.

$$(HOCH_2)_2C(COOC_2H_5)_2 \xrightarrow{\Delta} H_2O + HCHO + CH_2=C(COOC_2H_5)_2$$
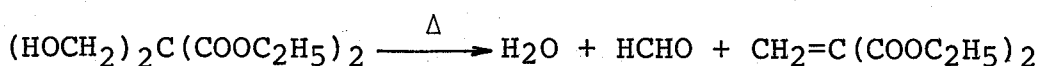
Decomposition of silicon compound by means of the β-elimination was examined. The following compound was found to satisfy the purpose.

$$Ph_2Si(OCH_2\underset{\underset{CH_2OH}{|}}{C}(COOC_2H_5)_2)_2 \longrightarrow Ph_2Si(OH)_2 + CH_2=C(COOC_2H_5)_2$$

(FMSi)   catalyst   + HCHO

                                                              polymer
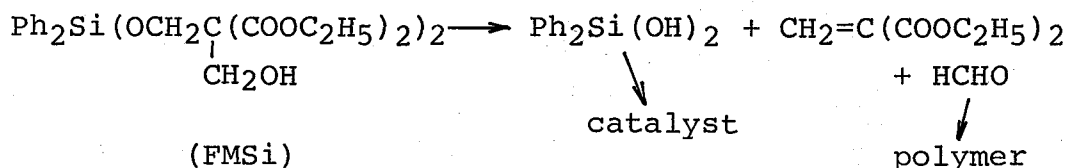
The aluminum complex/FMSi catalyst was more latent than the aluminum complex/hydrolyzable silicon compound catalyst. The results are shown in Table 3. Decomposition of FMSi was slow by itself. However, the aluminum complex accelerated the decomposition. FMSi decomposed within 15 min. at 130°C complately in the presence of $Al(SA)_3$.

10-4 Photogenerated catalyst (I): Aluminum complex/

Ph_3SiCOPh/alcohol system

The catalyst curing epoxy resin with UV radiation have recently attracted interest due to the processability and to the energy saving. The photo-generated catalyst will be most important as latent catalyst, because reaction starts at low temperature, however long pot life is expected in the absence of UV-radiation.

Diazonium salts and some onium salts are known to be effective for the UV curing of the epoxy resins.[2] However

Table 3 Gelation Time of FMSi/Al(SA)$_3$ Latent Catalyst[a]

temperature (°C)	Gelation time (min.)							
	40	100	130	140	150	160	170	180
reference Ph$_2$Si(OEt)$_2$/Al(SA)$_3$	1.4×10^4	4.3×10^3	9.5×10^2	–	60	30	20	17
FMSi/Al(SA)$_3$	7.0×10^5	1.1×10^3	5.0×10^2	1.5×10^2	60	31	20	17

a) Al(SA)$_3$ 4.8 phr, Silyl compound 3 phr, test tube method.

diazonium salts had problems that N_2 gas was evolved, and these catalyst gave ionic species which disturbed insulation.

The UV-curable epoxy resins with good electrical properties may be obtained by use of compounds which produce a component of the present catalyst by photo-reaction. Such photolabile component is implied since A. G. Brook reported that $Ph_3SiCOPh$ had $n-\pi^*$ absorption (424 nm ($\pi = 292$) and $\pi-\pi^*$ absorption (257 nm (16200)), and photo-decomposed to Ph_3SiOH in the presence of H_2O or alcohols.[3] A new catalyst system (aluminum complex/ $Ph_3SiCOPh$/alcohol) was thus investigated.

Figure 3 shows the time-conversion and time-molecular weight curve; the dashed line indicates the polymer conversion curve under UV irradiation and the solid lines indicate conversion curves after UV irradiation was stopped at the point where the dashed line connects with the solid lines. Both polymerization rate and molecular weight increased with photopolymerization time. The polymerization also continued after UV irradiation was stopped. The polymerization rate increased with UV irradiation time. Cyclohexene oxide did not polymerize in the absence of UV irradiation and did not polymerize in the absence of a catalyst component, even under UV irradiation. These facts imply that the catalyst activity results from the interaction between the aluminum complex
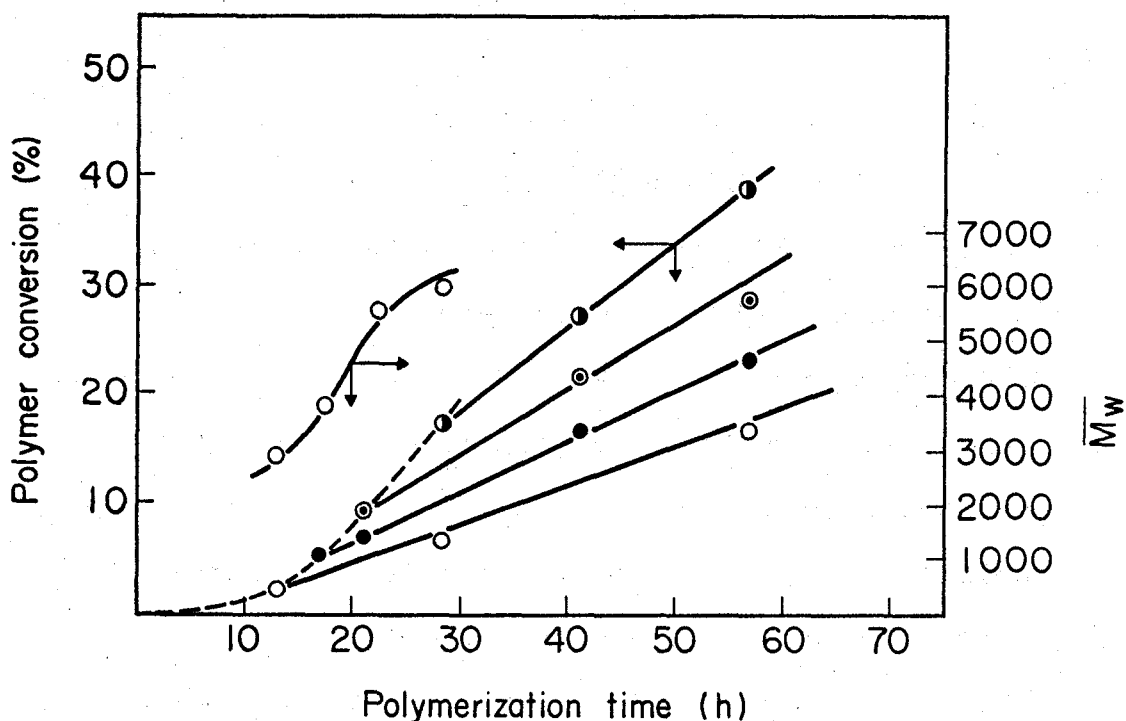
Figure 3　Photopolymerization of cyclohexene oxide.
　Polymerization conditions:　Al(acac)$_3$, 0.1 mol%,
　Ph$_3$SiCOPh, 0.5 mol%, H$_2$O, 1 mol%, polymerization
　temperature, 40°C.　(—O—) molecular weight-poly-
　merization time curve (under UV irradiation);
　(O···●···O···◐) polymer conversion-polymerization time
　curve (under UV irradiation);　(—O—) polymer con-
　version-polymerization time curve after UV irradia-
　tion was stopped at 13 h;　(—●—) polymer conver-
　sion-polymerization time curve after UV irradiation
　was stopped at 17 h;　(—⊙—) polymer conversion-
　polymerization time curve after UV irradiation was
　stopped at 22 h;　(—◐—) polymer conversion-
　polymerization time curve after UV irradiation was
　stopped at 28 h.

and the Ph$_3$SiOH which is a photodecomposition product of Ph$_3$SiCOPh.

The fact that the molecular weight and polymerization rate increased with photopolymerization time could be explained by the presence of alcohol in the polymerization system. In thermal polymerization with Al(acac)$_3$/Ph$_3$SiOH catalyst the polymerization rate was almost constant or decreased with polymerization time and the molecular weight was almost constant. Table 4 shows the polymer conversion and molecular weight in thermal polymerization with Al(acac)$_3$/Ph$_3$SiOH catalyst in the presence of i-PrOH. Addition of 2 mol% of i-PrOH decreased the polymerization rate to 40 % and decreased the molecular weight of the polymer obtained. The polymerization behavior in Figure 3 can be explained as follows: in the initial stage of photopolymerization a large amount of alcohol was present in the polymerization system, but the alcohol diminished as the photodecomposition of Ph$_3$SiCOPh proceeded. Therefore the molecular weight and polymerization rate probably increased with photopolymerization time.

Influence of the structure of alcohol on photopolymerization catalyst activity

In Al(n-Praa)$_3$/Ph$_3$SiCOPh/i-PrOH catalyst the photodecomposition rate of Ph$_3$SiCOPh became greater and polymer conversion increased by increasing the amount of i-PrOH.

Table 4   Influence of Polymer Conversion and Molecular
Weight on the Amount of i-PrOH

i-PrOH (mol%)	Polymerization rate (x 10^{-5}) (mol/min)	M_w	M_n
0	0.20(1.00)[1]	—	—
0.1	0.14(0.70)	29,000	14,000
0.5	0.11(0.55)	24,000	11,000
1.0	0.09(0.45)	18,000	8,000
2.0	0.08(0.40)	15,000	7,300

Note: Polymerization conditions: 40°C, Al(acac)$_3$ 0.05
mol% Ph$_3$SiOH 0.05 mol%, cyclohexene oxide 1 mL.

[1]The values in parenthesis show the relative polymeriza-
tion rate when the polymerization rate in the absence of
i-PrOH was 1.00.

However, the molecular weight decreased because the amount of i-PrOH in the polymerization system increased (Figure 4). Polymer conversion also varied with the identity of the alcohol (Table 5). The catalyst activity decreased in the following order for the OH component: i-PrOH > n-PrOH > i-BuOH > EtOH > MeOH > t-BuOH > H_2O. Three reasons are given for the maximum polymer conversion when using Al(n-praa)$_3$/Ph$_3$SiCOPh/iPrOH catalyst.

(a) Photodecomposition rate of Ph$_3$SiCOPh in THF is influenced by the structure of OH compound and decreased as follows:

MeOH > EtOH > i-PrOH > H_2O > t-BuOH (Table 5, decomposition rate).

(b) Addition of OH compound inhibited the polymerization of cyclohexene oxide with aluminum complex/silanol catalyst. The degree of inhibition varied with the structure of the OH compound and decreased in the following order:

t-BuOH > i-PrOH > EtOH > MeOH > H_2O (Table 5, model thermal polymerization rate).

(c) Ph$_3$SiCOPh has been known to be photodecomposed to Ph$_3$SiOH, Ph$_3$SiOR, Ph$_3$SiOCH(OR)Ph, and other products.[3] Among them only Ph$_3$SiOH became the active catalyst component by interaction with aluminum complex. The formation rate of Ph$_3$SiOH decreased in the following order:
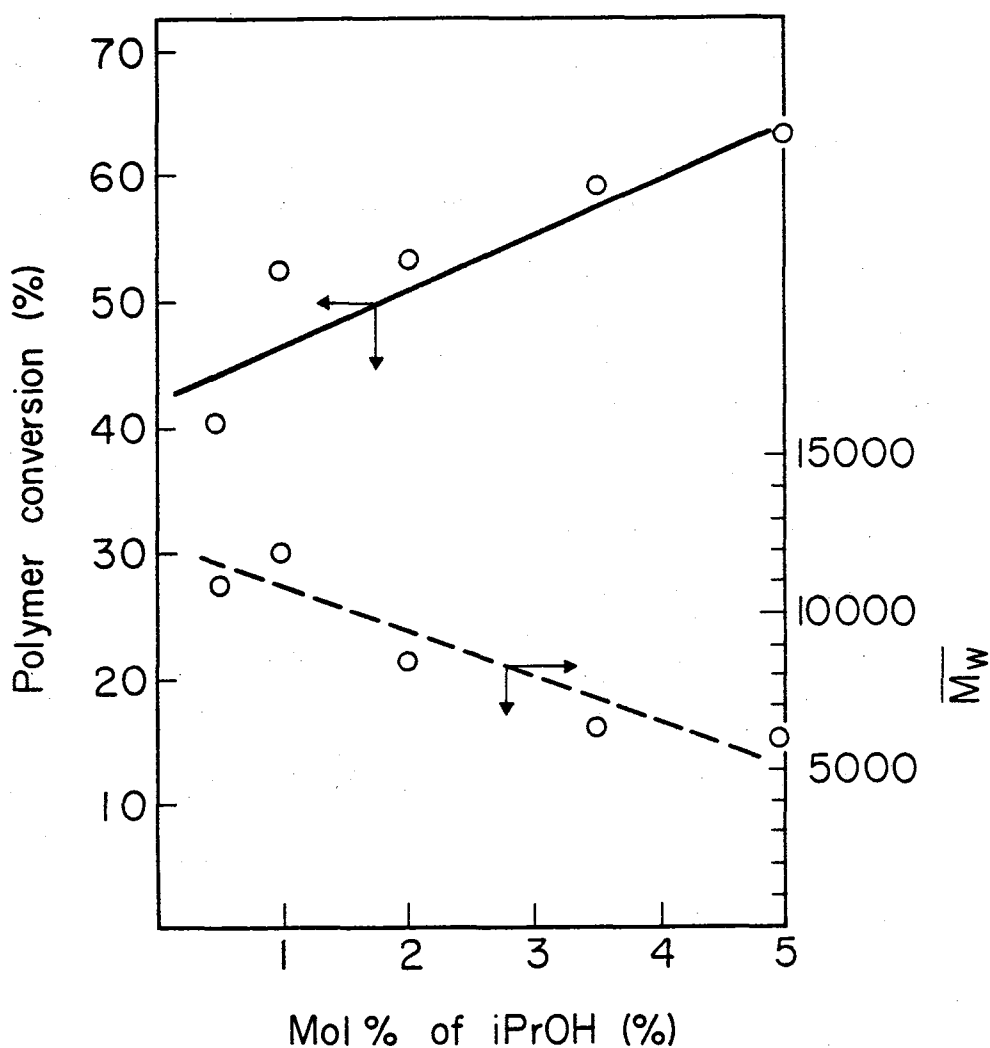
Figure 4   Influence of the amount of i-PrOH on poly-
  mer yield and molecular weight. Polymerization
  conditions: Al(n-Praa)$_3$; 0.1 mol%, Ph$_3$SiCOPh; 0.5
  mol%, polymerization time; 12 h, polymerization
  temperature, 40°C.

Table 5 Influence of polymer conversion on alcohol

OH compound	Polymerization time (h)	$\overline{M_W}$	Conversion (%)	Decomposition[1] rate $\times 10^{-8}$ (mol/min)	Model[2] reaction rate $\times 10^{-5}$ (mol/min)	Ratio of Ph_3SiOH(%)
H_2O	12.5	—	14.3	0.95 (1)	0.54 (1.0)	35
MeOH	10.0	8,800	19.9	6.18 (6.5)	0.92 (1.7)	16
EtOH	10.0	12,000	27.1	2.95 (3.1)	1.08 (2.0)	55
n-PrOH	11.0	8,400	39.4	— (-)	— (-)	-
i-BuOH	11.0	8,500	32.9	— (-)	— (-)	-
t-BuOH	11.0	14,000	14.6	0.38 (0.4)	1.62 (3.0)	43
i-PrOH	11.0	10,500	50.6	0.95 (1.0)	1.24 (2.3)	69

Polymerization conditions ; $Al(nPraa)_3$ 0.1 mol%, $Ph_3SiCOPh$ 0.5 mol%, OH compound, 0.1 mol%, 40°C

1) $Ph_3SiCOPh$ 1.23 $\times$ 10^{-5} mol, OH compound 1.83 $\times$ 10^{-3} mol, THF 2.5 cc

2   $Al(acac)_3$ 0.05 mol%, Ph_3SiOH 0.05 mol%, OH compound 1 mol%, cyclohexene oxide 1.0 ml, 40°C

i-PrOH > EtOH > t-BuOH > H_2O > MeOH (Table 5, ratio

of Ph_3SiOH).

In a combination of these three different orders the best

selection was i-PrOH. The molecular weight was also influ-

enced mainly, by alcohols and decreased in the following

order: t-BuOH > EtOH > i-PrOH > MeOH, which was similar

to the order of the polymerization rate with $Al(acac)_3$/

Ph_3SiOH catalyst in the presence of alcohol.

Dependence of Polymer Conversion and Molecular Weight on
the Amount of $Ph_3SiCOPh$

When the amount of $Ph_3SiCOPh$ was changed from 1 to 4

mol% under the condition that $Al(n-Praa)_3$ and i-PrOH were

1 mol% the polymer conversion increased (Fig. 5). The

degree of increase was large from 1.0 to 2.0 mol% and

small from 2.0 to 4.0 mol%. This molecular weight de-

creased from 12,000 to 9,000 linearly.

Influence of the Structure of Aluminum Complex on Polymer
Conversion

Table 6 shows the dependence of polymer conversion on

the structure of the aluminum complex. The complexes used

were in the following three categories:

(a) β-diketonato aluminum: $Al(acac)_3$, $Al(DPM)_3$,

    $Al(DMH)_3$.

(b) β-ketoesterato aluminum: $Al(Etaa)_3$, $Al(n-Praa)_3$,
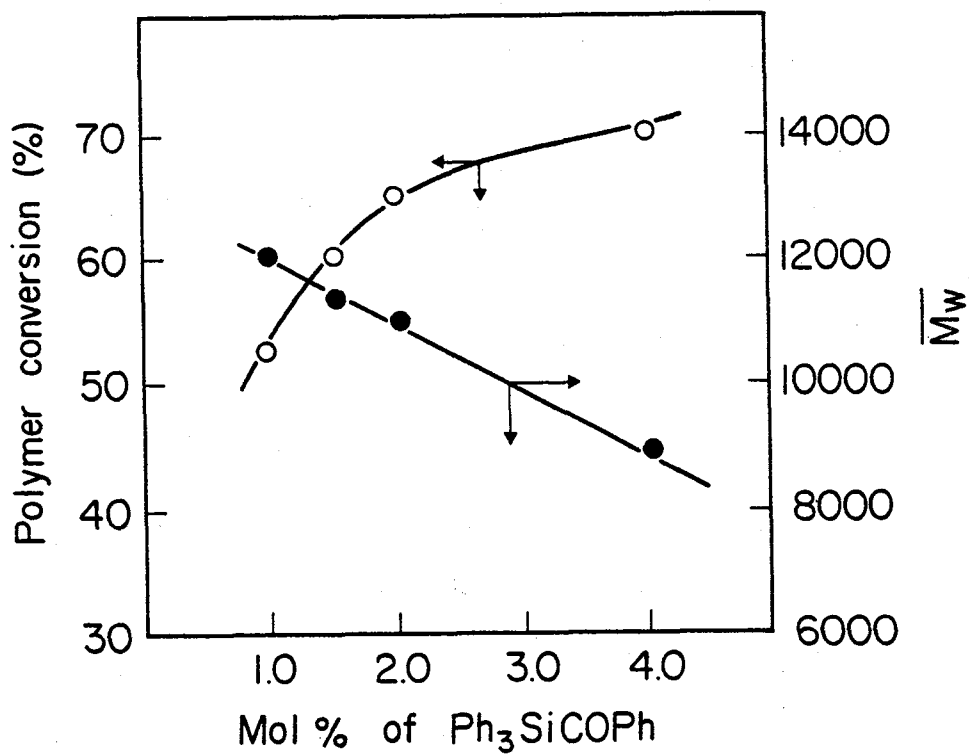
Figure 5   Influence of amount of Ph$_3$SiCOPh on polymer
   yield and molecular weight, Polymerization conditions:
   Al(n-Praa)$_3$, 0.1 mol%, i-PrOH, 1.0 mol%, polymeriza-
   tion time, 12 h, polymerization temperature, 40°C.

Table 6 Influence of Aluminum Compound on Polymer Conversion

Aluminum compound	Polymer conversion (%)	$\overline{M}_W$	Decomposition rate of Ph$_3$SiCOPh[a] $(\times 10^{-8})$ (mol/min)
Al(acac)$_3$	3.1	5300	0.95
Al(DMH)$_3$	4.5	—	—
Al(DPM)$_3$	5.1	8200	0.94
Al(Etaa)$_3$	15.5	8000	0.98
Al(nPraa)$_3$	19.3	8000	0.95
Al(iBuaa)$_3$	22.6	—	—
Al(SA)$_3$	11.0	8300	0.85
Al(ASA)$_3$	14.0	—	—

Note: Polymerization conditions: aluminum compound, 0.1 mol%, Ph$_3$SiCOPh, 0.5 mol%, i-PrOH, 1.0 mol%, polymerization temperature, 40°C, polymerization time, 9.5 h.

a) Ph$_3$SiCOPh 4.92×10^{-3}M, i-PrOH 0.73M and aluminum complex, 1.85×10^{-3} in THF. See Experimental section, photolysis.

Al(iBuaa)$_3$.

(c) Orthocarbonylphenolato aluminum: Al(SA)$_3$, Al(ASA)$_3$. Although the catalyst system that contained β-diketonato aluminum had low activity, activity in the catalyst system that contained β-ketoesterato aluminum was high. Among the catalyst systems that contained β-diketonato aluminum the catalyst activity decreased in the sequence Al(DPM)$_3$ > Al(DMH)$_3$ > Al(acac)$_3$, which was coincident with the activity order of the aluminum complex in the thermal polymerization with aluminum complex/Ph$_3$SiOH catalyst. Among the catalyst systems that contained β-ketoesterato aluminum the same trend was recognized: Al(i-Buaa)$_3$ > Al(n-Praa)$_3$ > Al(Etaa)$_3$.
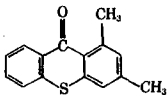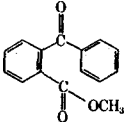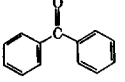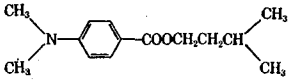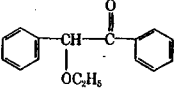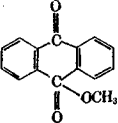
Orthocarbonylphenolato aluminum had high activity in thermal polymerization with Ph$_3$SiOH. In photopolymerization, however, the activity was not high. The lower photoactivity can be explained: orthocarbonylphenolato aluminum has strong absorption in the UV region. Therefore photodecomposition of Ph$_3$SiCOPh would be inhibited to some extent in the presence of orthocarbonylphenolato aluminum. As shown in Table 6 (decomposition rate), the photodecomposition rate of Ph$_3$SiCOPh in the presence of orthocarbonylphenolato aluminum was slower than that in the presence of the other aluminum complexes.

The Photosensitizer

A. G. Brook reported that pyridine was effective as a sensitizer in photodecomposition of $Ph_3SiCOPh$.[3] In the present experiment the following three categories of sensitizers were used in the $Ph_3SiCOPh/Al(nPraa)_3/i-PrOH$ catalyst system (Table 7): (a) benzophenones, (b) amines, (c) benzoin ether. Among them, benzophenone derivatives were the most useful for the photodecomposition of $Ph_3SiCOPh$ and catalytic polymerization. Compared with the decomposition rate in the absence of sensitizer, photodecomposition was accelerated 10.7 times in the presence of methyl benzoylbenzoate and polymer conversion was 2.6 times larger. Benzophenone was most effective and polymer conversion increased 3.2 times. When the amount of benzophenone was large the polymer conversion increased with no decrease in molecular weight. Amines were not effective and the decomposition rate was only 1.2 or 1.3 times larger. Moreover, the polymer conversion was lower than that in the absence of amines. The effects of amines can be explained: (a) the polymerization is probably cationic; therefore the presence of amine would retard the polymerization. (b) When amine was used as a sensitizer the amount of Ph_3SiOH in the photodecomposition products of $Ph_3SiCOPh$ was extremely low. When the amine with low basicity was used at low concentration inhibition of polymerization was negligible

Table 7 Dependence of Photosensitizer on Polymer Conversion

Sensitizer	Mole %	Polymerization time (h)	Polymer conversion	$\overline{M}_w$	Decomposition rate of Ph$_3$SiCOPh[a] ($\times 10^{-8}$) (mol/min)
[2,4-dimethylthioxanthone structure]	—	7	8.5	4,200	0.95 (1.0)[b]
	0.5	7	13.8	3,700	4.47 (4.7)
[o-benzoylbenzoic acid methyl ester structure]	0.5	7	22.0	3,400	10.17 (10.7)
[benzophenone structure]	0.5	7	26.8	3,400	—
NEt$_3$	0.4	12	3.5	—	0.95 (1.0)
Pyridine	0.4	12	3.1	—	1.24 (1.3)
[(CH$_3$)$_2$N–C$_6$H$_4$–COOCH$_2$CH$_2$CH(CH$_3$)$_2$ structure]	0.01	9	12.2	—	1.14 (1.2)
``	0.05	9	6.6	—	—
``	0.10	9	5.5	—	—
[benzoin ethyl ether structure]	0.5	7	11.5	3,500	3.14 (3.3)
[anthraquinone carboxylic acid methyl ester structure]	0.08	7	18.1	3,500	—
``	0.41	7	20.0	3,400	—
``	0.83	7	23.2	3,600	—
``	1.67	7	25.1	3,600	—

Note: Polymerization conditions: 40°C, Al(n-Praa)$_3$, 0.1 mol %, Ph$_3$SiCOPh, 0.5 mol %, i-PrOH, 1.0 mol %.

[a] Ph$_3$SiCOPh 4.92 $\times$ 10^{-3}M, i-PrOH, 0.73M in THF. See Experimental section, photolysis.

[b] The values in parentheses show the relative decomposition rate of Ph$_3$SiCOPh when the rate in the absence of sensitizer was 1.0.

but became apparent as the concentration increased.

Benzoin ether photodecomposed at the fastest rate but the decomposition rate of $Ph_3SiCOPh$ in the presence of benzoin ether was not larger than that in the presence of benzophenone. Therefore polymer conversion with benzoin ether was lower than that with benzophenone.

10-5   Photogenerated catalyst (II): Aluminum complex/ ortho-nitrobenzylsilyl ether system

Some silicon compounds which isomerize to silanols directly under UV radiation were also investigated. A compound with a hemiacetal structure, SiOCH(OH)-, formed by photolysis was considered to be suitable for the present purpose. If the hemiacetal is formed under UV-radiation, the silicon compound will decompose rapidly even at room temperature, forming silanol, as follows.

$$
\boxed{} \xrightarrow{\; h\nu \;} (Si\text{-}O\text{-}\underset{\underset{OH}{|}}{CH}\text{-}R) \xrightarrow[\substack{\text{room} \\ \text{temperature}}]{\Delta} SiOH + O{=}\underset{\underset{H}{|}}{C}\text{-}R
$$
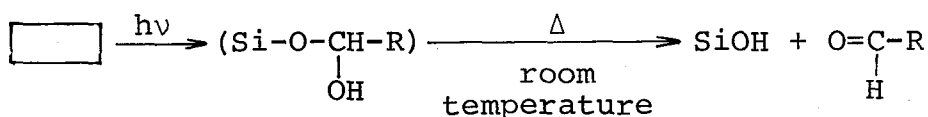
The hemiacetal compound might be produced by photo-oxidation of $Si\text{-}O\text{-}CH_2\text{-}Ph$ with an aromatic nitro compound, since it is known that p-methoxytoluene is photodecomposed to p-methoxybenzylalcohol, as follows.[4]

$$
CH_3\text{-}C_6H_4\text{-}OCH_3 \xrightarrow[\substack{\text{aromatic nitro} \\ \text{compound}}]{h\nu} HOCH_2\text{-}C_6H_4\text{-}OCH_3
$$
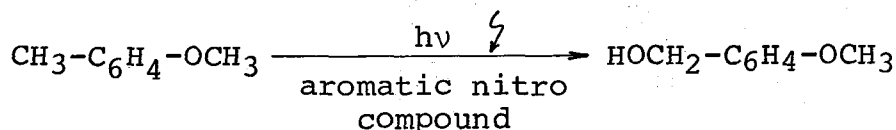
The photo-polymerization catalyst, aluminum complex/ triphenylbenzyl ether/aromatic nitro compound system, polymerized cyclohexene oxide under UV-radiation. Table 8 shows the results. The catalytic activity increased with introduction of a methoxy group to the benzene ring of the benzyl ether group, and increased with introduction of a nitro group to nitrobenzene. It is known that photodecomposition rate of methoxytoluene is increased by introduction of a methoxy group to the benzene ring of the benzyl ether group. The reason is explained by the fact that introduction of the methoxy group increases electron density of methoxytoluene, then, the electron transfer from methoxytoluene to nitrobenzene readily takes place[4]. The substitution effect on the catalyst activity could be explained in the same way.

When the amount of nitrobenzene was varied, maximum yield was obtained at 2.0 mol%. Nitrobenzene in concentration higher than 2.0 mol% will retard the thermal polymerization after photolysis because of prevention of the interaction between aluminum complex and silanol.

Introduction of a nitro group to benzene ring of nitrobenzene increased the catalyst activity. The reason could be explained by the above donor-acceptor theory.

Thus, the aluminum complex/methoxybenzyl(triphenyl)-silyl ether/nitrobenzene catalyst was found to have catalyst activity.

In order to obtain more active catalyst, ortho-nitro-
benzylsilyl ether, where a neighboring effect was antici-
pated, was investigated. Ortho-nitrobenzyl ether was used
as alcoholic hydroxy protector group of peptides, necleo-
sides and saccharides.[5] Following photodecomposition was
anticipated.

$$
Ph_3Si\text{-}O\text{-}CH_2\text{-}C_6H_4(NO_2) \xrightarrow{h\nu} \left(Ph_3Si\text{-}O\text{-}\overset{H}{\underset{OH}{C}}\text{-}C_6H_4(NO) \right)
$$

(ONBSi)

$$
Ph_3SiOH + \left(\overset{O}{\underset{H}{C}}\text{-}C_6H_4(NO) \right)
$$

$$
\downarrow \quad\quad\quad \downarrow
$$

$$
catalyst \quad\quad C_6H_4(COOH)\text{-}N=N\text{-}C_6H_4(COOH)
$$
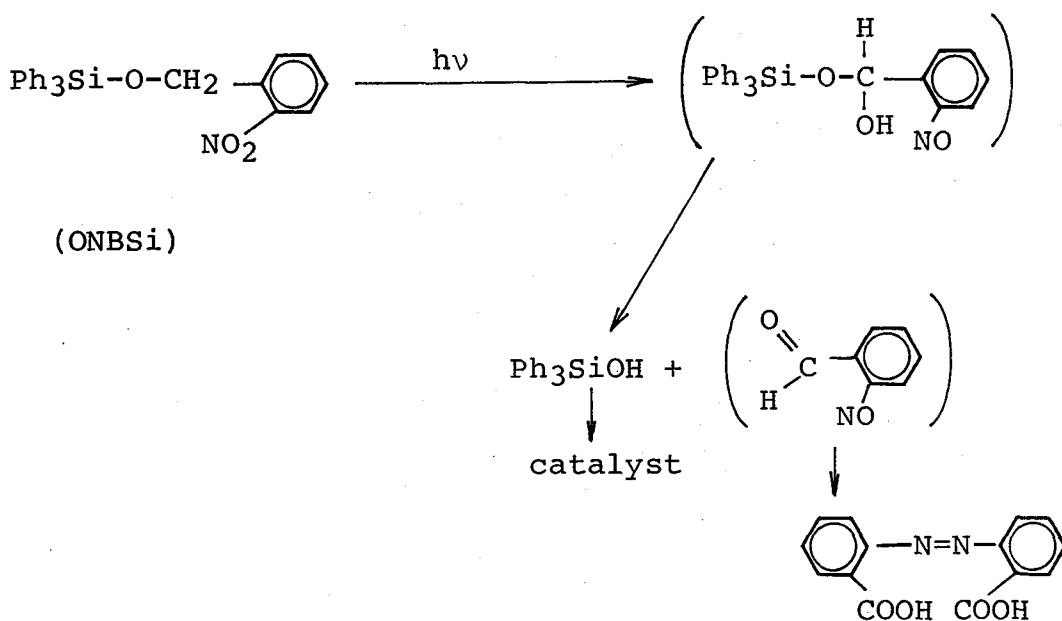
Photodecomposition of ortho-nitrobenzyl(triphenyl)-
silyl ether (ONBSi) was thus examined. Figure 6 shows the
results. The photodecomposition was carried out under
irradiation of 254 nm, 365 nm and > 390 nm UV-light. Table
9 shows the quantum yield of the photodecomposition. 254
nm light was most active for the photodecomposition. The
quantum yield decreased with radiation time. The reason
was explained by the fact that the decomposed azo compound
absorbed the effective UV-light and retarded the photodecom-
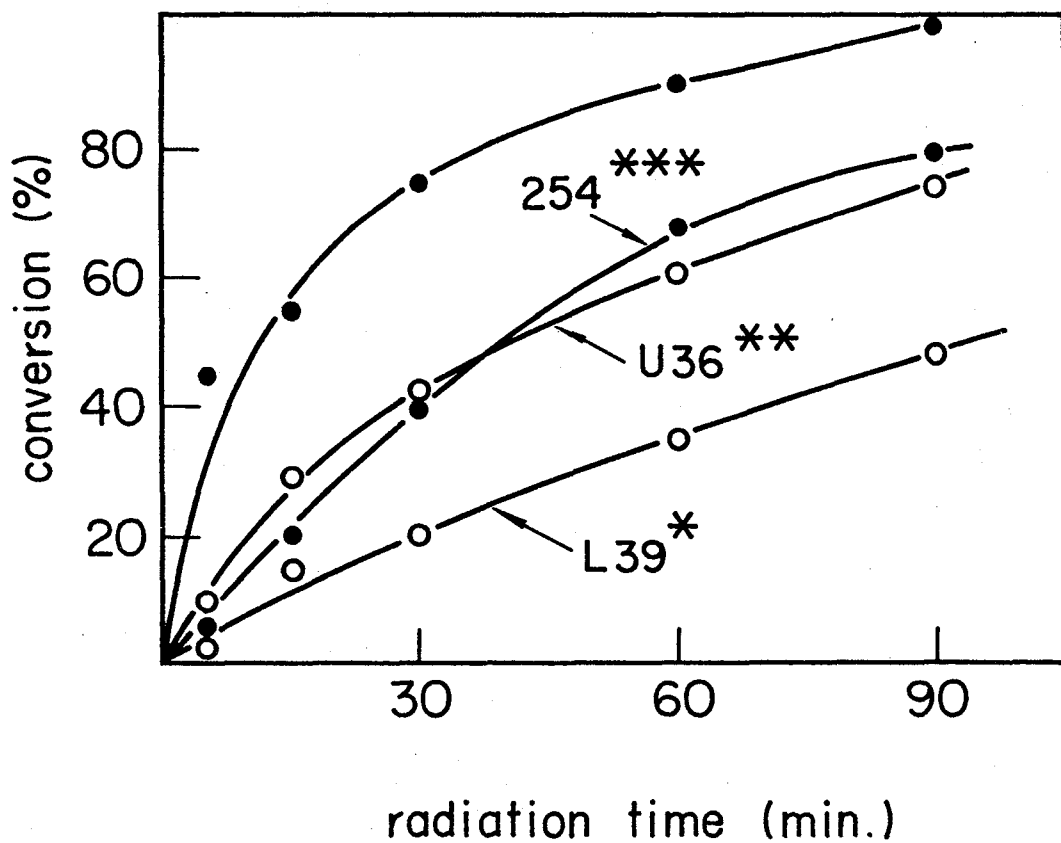
Figure 6   Photo-decomposition of ONBSi.
   * > 390 nm, ** 365 nm, *** low-pressure-mercury
   lamp ONBSi, 0.0221 M in CH$_3$CN

Table 8   Polymerization of Cyclohexene Oxide with Al Complex/Silyl Ether/Aromatic Nitro Compound Catalyst.[a]

Silyl ether	mol%	Nitro compd.	mol%	Time (h)	Yield (%)
Ph_3SiOCH_2Ph	0.1	$C_6H_5NO_2$	0.5	8	0
"	0.3	"	2.0	8	0
$Ph_3SiOCH_2C_6H_4-OCH_3$	0.2	"	2.0	7	9
$Ph_3SiOCH_2C_6H_3(OCH_3)_2$	0.2	"	2.0	7	14
$Ph_3SiOCH_2C_6H_2(OCH_3)_3$	0.1	"	0.5	7	5
"	0.1	"	1.0	7	10
"	0.1	"	2.0	7	32
"	0.1	"	4.0	7	21
"	0.15	$m-C_6H_4(NO_2)_2$	1.0	10	19
"	0.15	$C_6H_5NO_2$	1.0	10	14

a) 40°C, $Al(Etaa)_3$ 0.02 mol% to monomer, 400W-high pressure mercury lamp.

Table 9   Quantum Yield for ONBSi[a]

Filter	Radiation time (min.)				
	5	15	30	60	90
L39[1]	0.1	0.1	0.1	0.1	0.1
U36[2]	0.2	0.2	0.1_5	0.1	0.1
254[3]	0.3	0.4	0.4	0.3	0.3

a) 40°C in acetonitrile, 1) over 390 nm, 2) 365 nm (400W-high pressure mercury lamp), 3) low pressure mercury lamp, ONBSi 0.0221 M.

position, where, as the extent of decomposition was confirmed to be about 100 % by means of separation with column chromatography, triphenylsilanol forms by decomposition of the ONBSi.

In order to use the ONBSi as a photogenerated catalyst, the silyl ether must be used with an aluminum complex. Therefore decomposition of the silyl ether in the presence of an aluminum complex was examined. Al(acac)$_3$, Al(Etaa)$_3$ and Al(SA)$_3$ were used as aluminum complex. Table 10 shows the results. The decomposition rate decreased in the following order.

$$\text{non} > \text{Al(acac)}_3 > \text{Al(Etaa)}_3 > \text{Al(SA)}_3$$
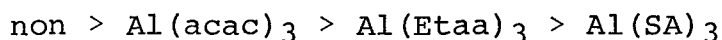
The decomposition rate of ONBSi under 365 nm light was higher than that under 254 nm light in the presence of Al(Etaa)$_3$ (Table 11). The Al(Etaa) had UV-absorption at about 270 nm, $\varepsilon = 10^4$, therefore the dependence of the photodecomposition rate on the structure of the aluminum complex and on wave number of UV-light was explained by the fact that the absorption of the aluminum complex overlapped with that of ONBSi (Figure 7) therefore, ONBSi could not absorb the effective UV-light.

Table 12 shows the photopolymerization results for cyclohexene oxide with Al(Etaa)$_3$/ONBSi. The maximum catalytic activity was obtained at the concentration of 0.05 mol% in the case of ONBSi and 0.02 mol% in the case of

Table 10   Photodecomposition of ONBSi in the
Presence of Aluminum Complex.[a]

aluminum complex	ratio of decomposition (%)				
time (min.)	5	15	30	60	90
non	43	71	88	97	99
Al(acac)$_3$	25	61	83	93	96
Al(Etaa)$_3$	23	56	79	93	96
Al(SA)$_3$	23	53	62	80	91

a) ONBSi 0.0258 M, aluminum complex 0.012 M in
   acetonitrile.
   400W-high pressure mercury lamp.

Table 11 Quantum Yield for Decomposition of o-nitrobenzyl(triphenyl)-silyl ether in the presence of aluminum complex

UV light	254[1]			365[2]		
Radiation time (min.)	10	20	40	10	20	40
Conversion (%)	3.7	10.5	21.3	17.5	32.0	43.0
Quantum yield	0.1_2	0.1_7	0.1_7	0.2	0.1_8	0.1_2
QE-Al(acac)$_3$/QE-non[3] (%)	34	45	47	95	90	92
Conversion (%)	7.8	17.2	28.5	16.0	28.3	39.0
Quantum yield	0.2_5	0.2_7	0.2_3	0.1_8	0.1_6	0.1_1
QE-Al(Etaa)$_3$/QE-non[3] (%)	71	71	64	85	80	84

1) Low pressure mercury lamp, 2) High pressure mercury lamp, filter U-36,
3) Ratio of quantum yield of o-nitrobenzyl(triphenyl)silyl ether in the presence and absence of aluminum compound.
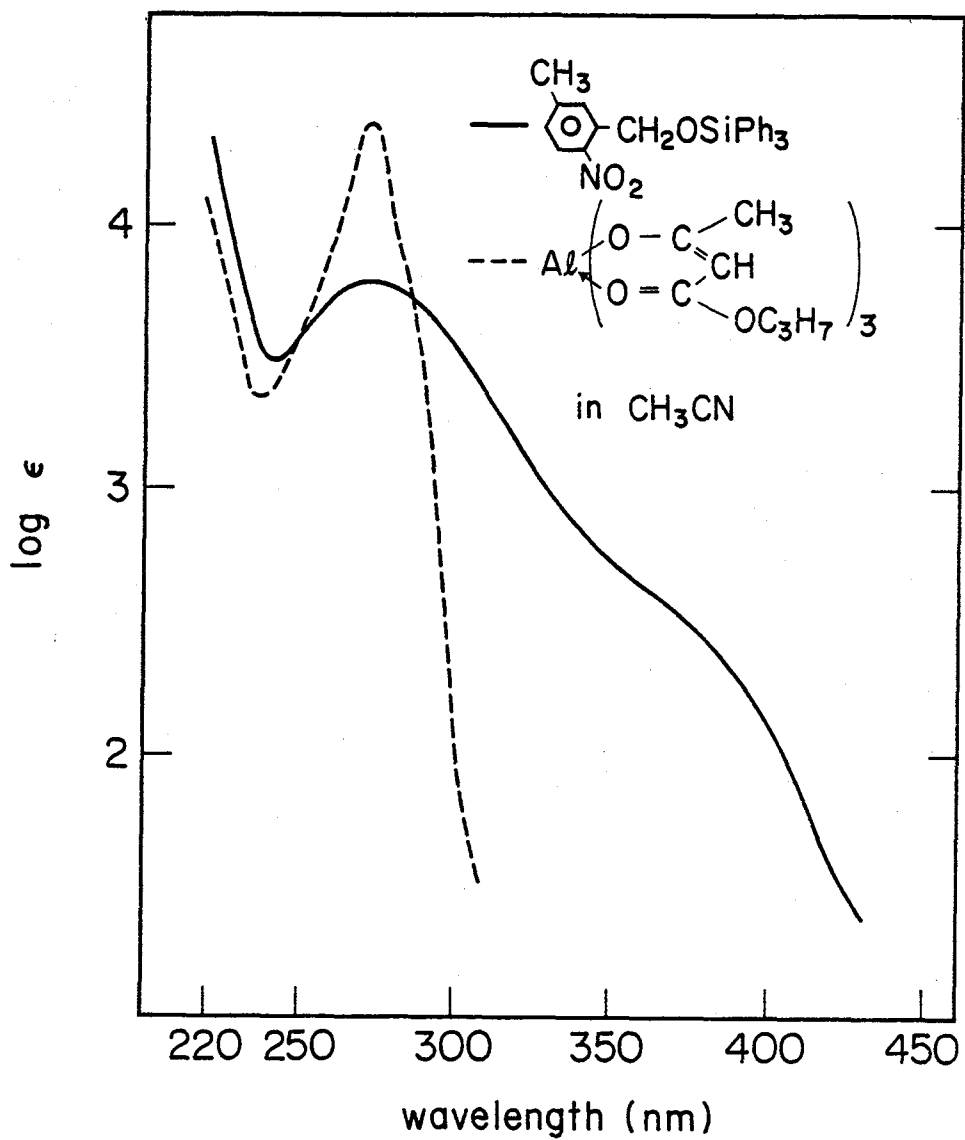
Figure 7   UV spectra of components of the catalyst.

Table 12 Photopolymerization of Cyclohexene Oxide
with Al(Etaa)$_3$/ONBSi catalyst

Al(Etaa)$_3$ mol%	ONBSi mol%	radiation time(min.)	yield (%)
0.1	0.01	5	5
0.1	0.02	5	9
0.1	0.05	5	73
0.1	0.10	5	64
0.1	0.25	5	60
0.1	0.02	50	20
0.5	0.02	50	10
0.02	0.02	50	28
0.005	0.02	50	25

40°C, 400W-high pressure mercury lamp

Al(Etaa)$_3$.

The dependence of the catalytic activity on the concentration of ONBSi will be explained by the fact that the decomposition rate of ONBSi have a maximum value at the concentration of ONBSi, because rise of the concentration of catalyst disturbs the transparence of UV light to inner of test tube. The dependence of the activity on the concentration of Al(Etaa)$_3$ will be explained as follows. Two factors were needed for the explanation.

1) Photodecomposition rate of ONBSi in the presence of Al(Etaa)$_3$

2) Thermal polymerization rate with Al(Etaa)$_3$/triphenylsilanol.

The rate decreased with increased in Al(Etaa)$_3$ concentration, and the rate increased with increase in Al(Etaa)$_3$ concentration under such a low concentration as about 0.005 mol%. 0.02 mol% of Al(Etaa)$_3$ will be most suitable point on consideration of 1) and 2).

Dependence of the catalyst activity on the structure of the aluminum complex was examined. The results are shown in Figure 8. At initial step, the activity increased in the following order,

$$Al(acac)_3 < Al(SA)_3 < Al(Etaa)_3$$
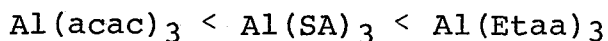
however at the last step, the activity was as follows.

$$Al(acac)_3 < Al(Etaa)_3 < Al(SA)_3$$
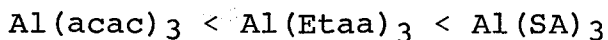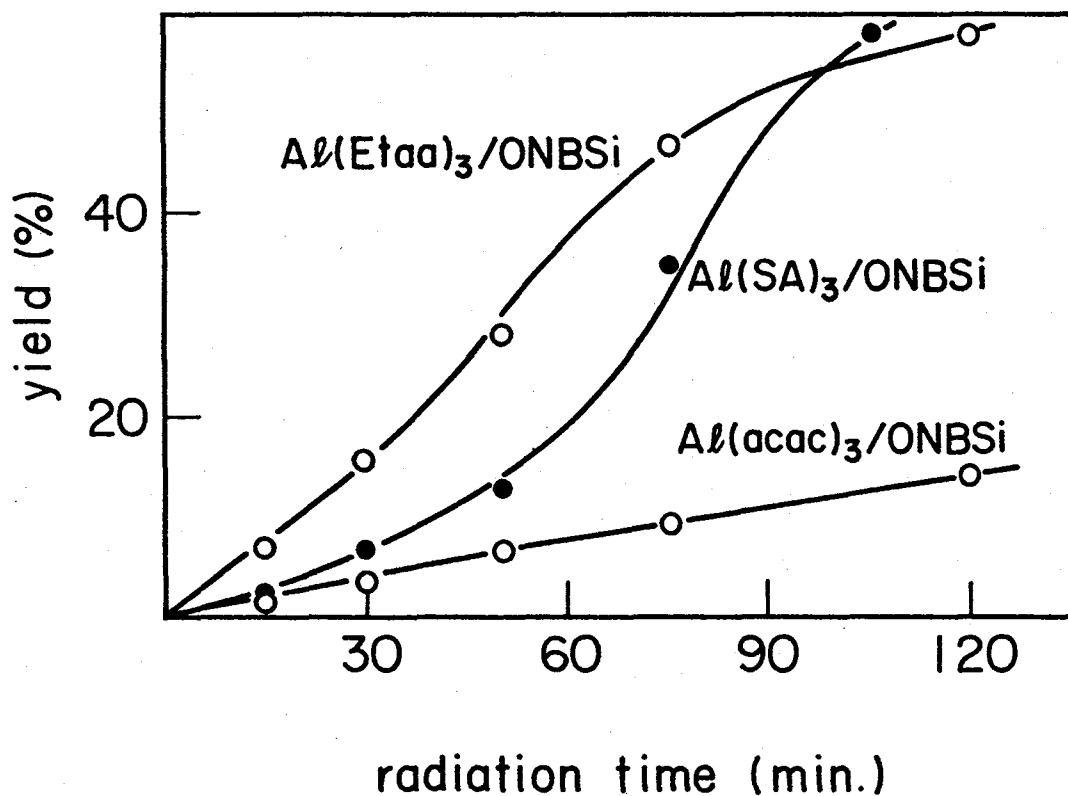
Figure 8   Photo-polymerization of cyclohexene oxide
   with Aluminum complex/ONBSi catalyst 40°C, Al 0.02
   mol%, ONBSi 0.02 mol% 400W-high-pressure-mercury
   lamp.

The phenomena could be also explained by 1) photodecomposition rate and 2) thermal polymerization rate. Namely, photodecomposition rate of ONBSi in the presence of the aluminum complex increased in the following order,

$$Al(SA)_3 < Al(Etaa)_3 < Al(acac)_3$$
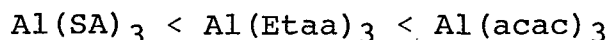
however thermal polymerization rate of cyclohexene oxide was as follows.

$$Al(acac)_3 << Al(Etaa)_3 < Al(SA)_3$$
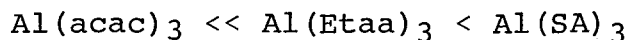
The photopolymerization rate at initial stage will be affected by the photodecomposition rate of ONBSi mainly, and the rate at the last stage will be mainly affected by the thermal polymerization rate.

Dependence of the catalyst activity on wavelength of UV light was examined (see Table 13). 365 nm UV light was found to be most active. The reason will be explained as the same way as the explanation for the photodecomposition in the presence of aluminum complex.

Dependence of the catalyst activity and photodecomposition rate on the structure of silyl ether was investigated. The results are shown in Table 14 and 15. Introduction of a methoxy group to the benzene ring of silylether decreased the photodecomposition rate and the photopolymerization rate. On the other hand, introduction of a methyl or a chloro group to the benzene ring of silyl

Table 13   Photopolymerization of Cyclohexene
Oxide with Aluminum Complex/ONBSi Catalyst.

filter	aluminum complex	radiation time(min.)	conversion (%)
U36	$Al(acac)_3$	20	4
"	$Al(Etaa)_3$	20	27
"	$Al(SA)_3$	20	2
L39	$Al(acac)_3$	45	2
"	$Al(Etaa)_3$	45	12
"	$Al(SA)_3$	45	1
254	$Al(acac)_3$	35	1
"	$Al(Etaa)_3$	35	7
"	$Al(SA)_3$	35	5

a) 40°C, aluminum complex 0.03mol%, ONBSi 0.03mol%
   400W-high pressure mercury lamp.

Table 14   Photopolymerization of Cyclohexene Oxide

silyl ether	conversion (%)		
radiation time	10min.	40min.	100min.
Si-I	13	51	100
Si-II	4	10	22
Si-III	6	12	26
ONBSi	9	21	55
Si-IV	16	18	19*
Si-V	32	36	18*
Si-VI	18	20	22*
Si-VII	12	43	86
Si-VIII	4	8	16
Si-IX	4	6	10

a) catalyst, $Al(Etaa)_3$ 0.02mol%,   silyl ether   0.02mol%,   * 0.01 mol%,
polymerization temperature 40°C,   400W high pressure mercury lamp
abbreviation;   see experimental

Table 15   Photodecomposition of Silyl ethers

silyl ether		decomposition (%)				
	radiation time (min.)	2	5	10	20	40
Si-I		37	55	74	88	96
Si-II		5	14	20	50	71
Si-III		51	60	71	82	90
ONBSi		5	27	52	89	92
Si-IV		20	29	55	75	86
Si-V		22	48	67	83	94
Si-VI		8	27	55	73	89
Si-VII		57	71	85	93	97
Si-VIII		0	13	20	37	40
Si-IX		11	33	67	93	94

a) silyl ether 0.0221M in CH_3CN, 40°C, 400W high pressure mercury lamp
   abbreviation; see experimental

ether increased the both rates.

Alicyclic epoxide (II) (Figure 1) with Al(Etaa)$_3$/ONBSi catalyst could be photo-cured by high-pressure-mercury-lamp (80 W/cm). The epoxide photo-cured within 20 second.

As mentioned above, the catalyst activity of the aluminum complex/ortho-nitrobenzyl silyl ether catalyst was high and was sufficiently high for practical use.

10-6 Electrical properties of epoxy resins cured by the latent catalysis

Table 16 shows electrical properties of epoxy resin cured with latent catalysts.

Dependence of the electrical properties on the structure of alkoxysilane was examined. The electrical properties deteriorated in the following order.

Ph$_2$Si(OMe)$_2$ $\gtrsim$ Ph$_3$SiOMe > Ph$_2$Si(OPh)$_2$ > Ph$_2$Si(OEt)$_2$

> Ph$_3$SiOEt $\gtrsim$ Ph$_3$Si(OiPr)$_2$
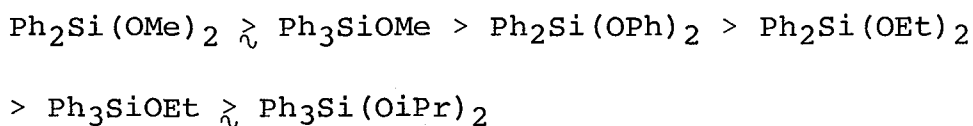
The order was almost coincident with that of activity of the catalyst.

Epoxy resin cured with the latent catalysts, namely, hydrolyzable catalyst, thermally generated catalyst and photogenerated catalyst had excellent electrical properties, compared with that with BF$_3$·monoethylamine catalyst.

Table 16   Electrical Properties of Epoxide
            Cured with the Latent Catalyst.

catalyst	phr[a)	tan δ at 200°C (%)
$Ph_2Si(OMe)_2$	3.0*	0.8
$Ph_2Si(OPh)_2$	4.5*	1.0
Ph_3SiOMe	3.7*	1.3
$Ph_2Si(OEt)_2$	3.5*	1.5
Ph_3SiOEt	4.5*	4.0
$Ph_2Si(OiPr)_2$	3.9*	8.2
FMSi	6.0*	1.2
o-nitrobenzyl (triphenyl)silyl ether	3.0**	2.0

* $Al(SA)_3$ 2.4 phr, cured at 165°C for 15h, Epikote
    828 resin.
** 80A/cm, high pressure mercury lamp, distance from
    sample 15 cm, radiation time 60 sec., catalyst
    $Al(Etaa)_3$ 0.5phr, alicyclic epoxy resin
    (see Figure 1)
a) weight % to epoxy resin.

References

1. U. Michel and S. Tchelitcheff, Bull. Soc. Chim. Fr., 2230 (1964)

2. J. V. Crivello, J. H. W. Lam, J. E. Moore and S. H. Schroster, J. Radia. Curing, $\underline{5}$, 2 (1978); J. V. Crivell and J. H. W. Lam, Macromolecules, $\underline{10}$, 1307 (1977): J. V. Crivello and J. H. W. Lam, J. Polymer Sci., Polym. Chem. Ed., $\underline{17}$, 2877 (1979); ibid., $\underline{17}$, 1047 (1979); ibid., 1021 (1980); ibid., $\underline{17}$, 977 (1979); ibid., $\underline{16}$, 2441 (1969)

3. A. G. Brook, J. Am. Chem. Soc., $\underline{82}$, 5102 (1960); ibid., $\underline{91}$, 355 (1969)

4. J. Libman, J. Chem. Soc., Chem. Comm., 868 (1977); R. Hurley, A. C. Test, J. Am. Chem. Soc., $\underline{88}$, 4330 (1966); J. A. Barltop and N. J. Bunce, J. Chem. Soc., (C), 1467 (1968)

5. A. Patchornik, B. Amit and R. B. Woodward, J. Am. Chem. Soc., $\underline{19}$, 6333 (1970); E. Ohtsuka, T. Wakabayashi, S. Tanaka, T. Tanaka, K. Oshie, H. Hasegawa and M. Ikehara, Chem. Pharm. Bull., $\underline{29}$, 318 (1981); P. M. Collins and V. R. N. Munasinghe, J. Chem. Soc., Chem. Commun., $\underline{1981}$, 362

Chapter 11   Selective Synthesis of Structually Isometric

          Poly-β-ester and Poly-δ-ester from β-(2-

          acyloxyethyl)-β-propiolactone with Al-H_2O

          and Zn-H_2O Catalysts

11-1   Introduction

     The polymerization of β-substituted-β-propiolactones
has been studied in view of stereoregular polymerization
in a systematic manner.[1] In the course of studies it was
found that organoaluminum catalyst $(EtAlO)_n$ which is ob-
tained from Et_3Al and H_2O tends to give stereoregular
polymers while a related organozic catalyst $(Et(ZnO)_2ZnEt)$
which is called $ZnEt_2$-H_2O catalyst has little capability
for stereoregulation.[1] In the preceding study[1] it was
shown that the Al-catalyst strongly coordinates with the
lactone group in the monomer while Et_2Zn cannot coordinate
with this group.

     The new observations herewith reported by employing
β-(2-acetoxyethyl)-β-propiolactone (1) revealed a remark-
able difference in the catalytic behaviors of the two
catalysts. Namely, the Al-catalyst catalyzes normal
polymerization leading to poly-β-ester, and the Zn-catalyst
forms isomerized poly-δ-ester as main product.

     These observations have a dual significance that (i)
a new route of isomerization polymerization is opened up,
and (ii) the Al-catalyst prefers the lactonic ester group

predominantly, but the Zn-catalyst attacks on the linear
ester group rather than lactonic ester group. The site-
selective interactions can be used for interpretation of
the difference in behaviors of the two catalysts in a
more detailed manner. This seems of value in view of that
these catalysts are the active entities of widely used
$AlEt_3-H_2O$ and Et_2Zn-H_2O catalytic systems.

There remained two major questions in this new poly-
merization behavior: (1) Whether the phenomenon is
general for the cases of β-(2-acyloxyethyl)-β-propiolactone
series? (2) What are the effects of substituent groups at
the terminal of the side-chain ester group on the polymer-
ization behaviors, especially at the stage of cyclic in-
termediate? In order to answer these questions we chose
two special monomers containing $(CH_3)_2CHCOO-$ and $(CH_3)Cl-$
CHCOO- groups and compared the results of these monomers
with that obtained by CH_3COO-monomer.

I offer the experimental results of polymerization
behaviors, structure of the polymers formed, and coordina-
tion behaviors of the two types of catalyst with the
monomer. The structures and designations are shown in
Scheme 1.

11-2 Polymerization of β-(2-acetoxyethyl)-β-propiolactone

    (monomer 1)

    Polymerization Behaviors:

Scheme 1

Designation of monomer:

$$CH_2-CH_2-O-COR$$

$$\begin{array}{c} H \\ | \\ O \underline{\hspace{1cm}} C=O \end{array}$$

$\underset{\sim}{1}$: $R = -CH_3$

$\underset{\sim}{2}$: $R = -CH(CH_3)_2$

$\underset{\sim}{3}$: $R = -CHCl(CH_3)$
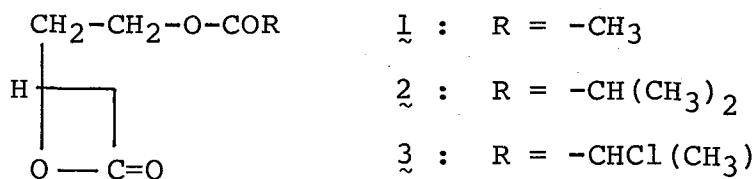
Designation of polymer:

Monomer	Catalyst	Polymer
$\underset{\sim}{1}$	$(EtAlO)_n$	$poly(\underset{\sim}{1})-Al$
$\underset{\sim}{2}$	$(EtAlO)_n$	$poly(\underset{\sim}{2})-Al$
$\underset{\sim}{3}$	$(EtAlO)_n$	$poly(\underset{\sim}{3})-Al$
$\underset{\sim}{1}$	$Et(ZnO)_2ZnEt$	$poly(\underset{\sim}{1})-Zn$
$\underset{\sim}{2}$	$Et(ZnO)_2ZnEt$	$poly(\underset{\sim}{2})-Zn$
$\underset{\sim}{3}$	$Et(ZnO)_2ZnEt$	$poly(\underset{\sim}{3})-Zn$

The polymerization profiles in respect to time-conversion and time-MW relations are shown in Figure 1 for the Al- and Zn-catalyses. The new polymerization behaviors with the Al catalyst were similar to the polymerization of a series of β-alkyl-β-propiolactones reported previously,[1] i.e., gradual increase of polymer yield with almost constant MW. Polymerization behavior with the Zn catalyst, however, can be characterized by a drastic increase of polymer yield and MW after a considerably long induction period. Table 1 shows the selected polymerization results giving better yields, when a variety of polymerization factors was changed. Lower catalyst concentration, lower polymerization temperature, or solvent other than tabulated gave generally lower polymer yields.

1-2.   Polymer structures:

^{13}C-NMR Spectra of Poly (1): For convenience the following designations are used hereafter for the polymers: poly(1)-Al for the polymer formed with $(EtAlO)_n$ catalyst, and poly(1)-Zn for one formed with $Et(ZnO)_2ZnEt$ catalyst. The polymers obtained by Al- and Zn-catalyses showed almost identical IR spectra (Figure 2), indicating the presence of ester structures in both polymers. No significant difference was also observed in ^{1}H-NMR spectra of both polymers (Figure 3).
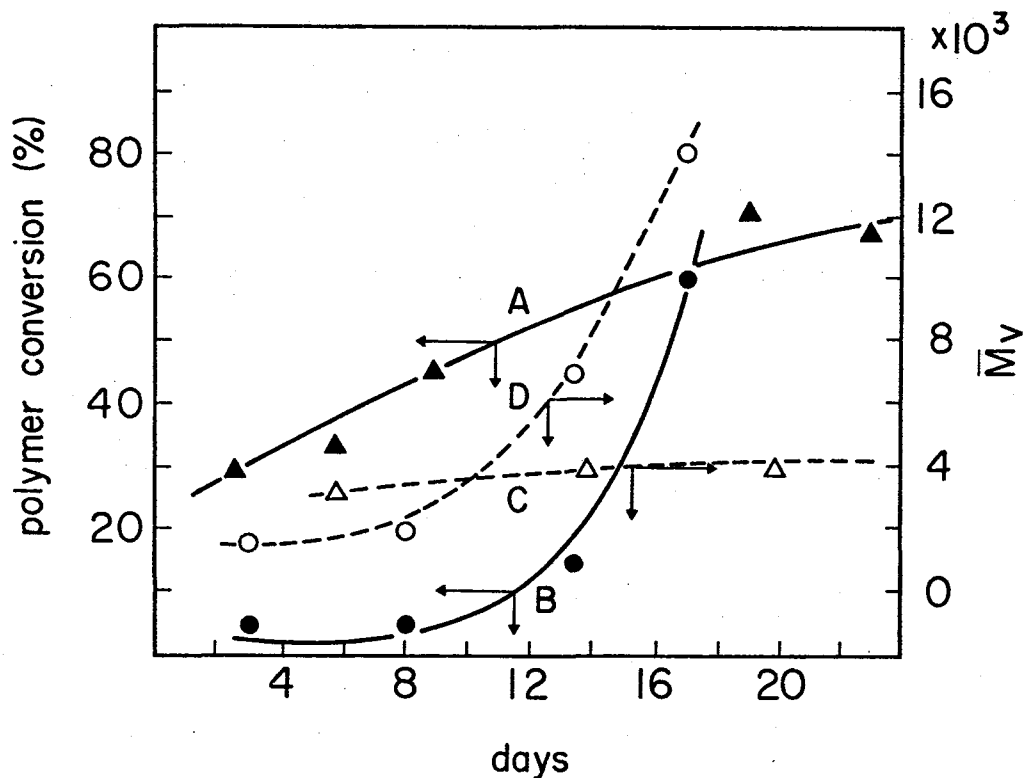
Figure 1   Time-dependent polymerization profiles of
monomer (1) with (EtAlO)$_n$ and Et(ZnO)$_2$ZnEt catalysts.
A: Polymer conversion in Al-catalysts, B: Polymer
conversion in Zn-catalysis, C: $\overline{M}_V$ for polymer obtained
with the Al catalyst, D: $\overline{M}_V$ for polymer obtained with
the Zn catalyst. Polymerization conditions: monomer,
1 ml; solvent toluene 1 ml, catalyst, 4 mol% of
monomer, polymerization temperature, 60°C for Al-
catalysis and 30°C for Zn-catalysis.
Values of $\overline{M}_V$ were obtained from GPC standardized with
authentic polysyrene samples.

Table 1   Selected Polymerization Results of (1)[a]

Catalyst	Catalyst concentration (mol% of monomer)	Polymerization			Polymer yield (%)
		Temp. (°C)	Time (days)	Solvent	
Al	2	63	30	$PhCH_3$	61
Al	4	63	30	$PhCH_3$	52
Al	7	63	13	$PhCH_3$	62
Al	11	63	6	$PhCH_3$	60
Zn	2	65	4	$PhCH_3$	61
Zn	4	65	4	$PhCH_3$	68
Zn	4	30	34	CH_2Cl_2	77
BF_4OEt_3	1	30	25	$PhCH_3$	46[b]
$SnCl_4$	2.5	30	9	$PhCH_3$	43[b]

a) Monomer 2 mℓ, solvent 2 mℓ.

b) Low molecular weight polymers. An example of GPC
   is shown in Figure 5.
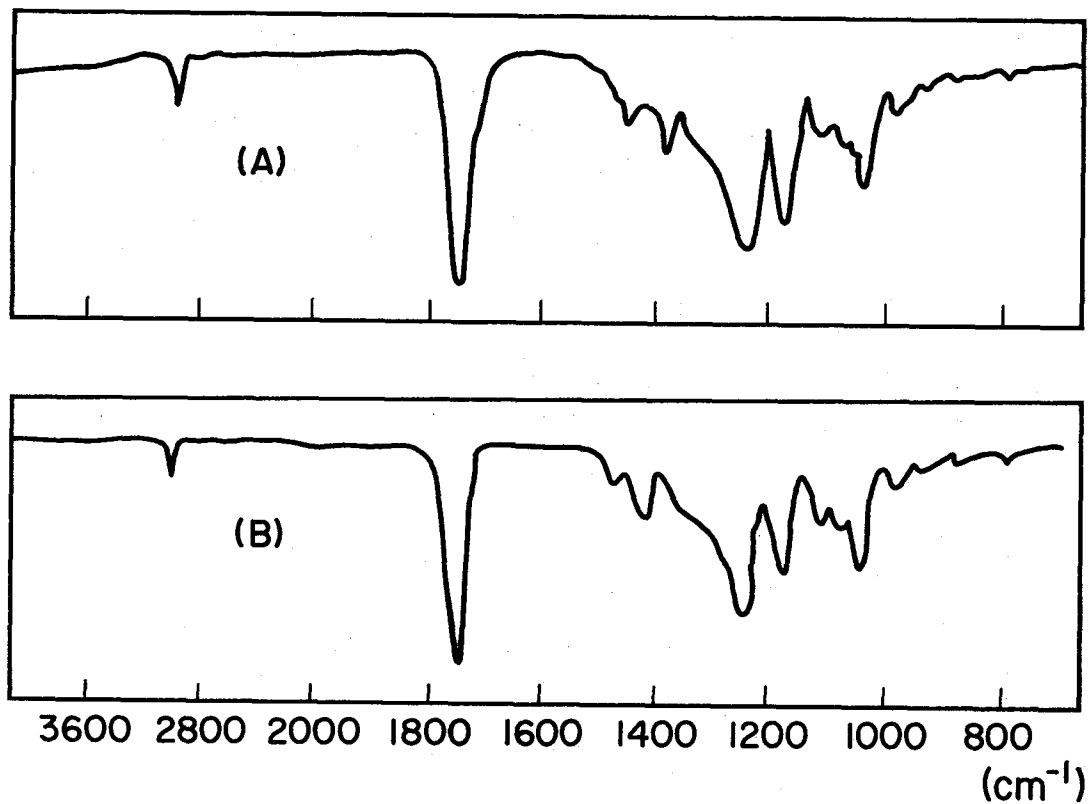
Figure 2   IR-Spectra of Poly(1)-Al and Poly(1)-Zn.
(A): Poly(1)-Al, (B): Poly(1)-Zn, (KBr disc)
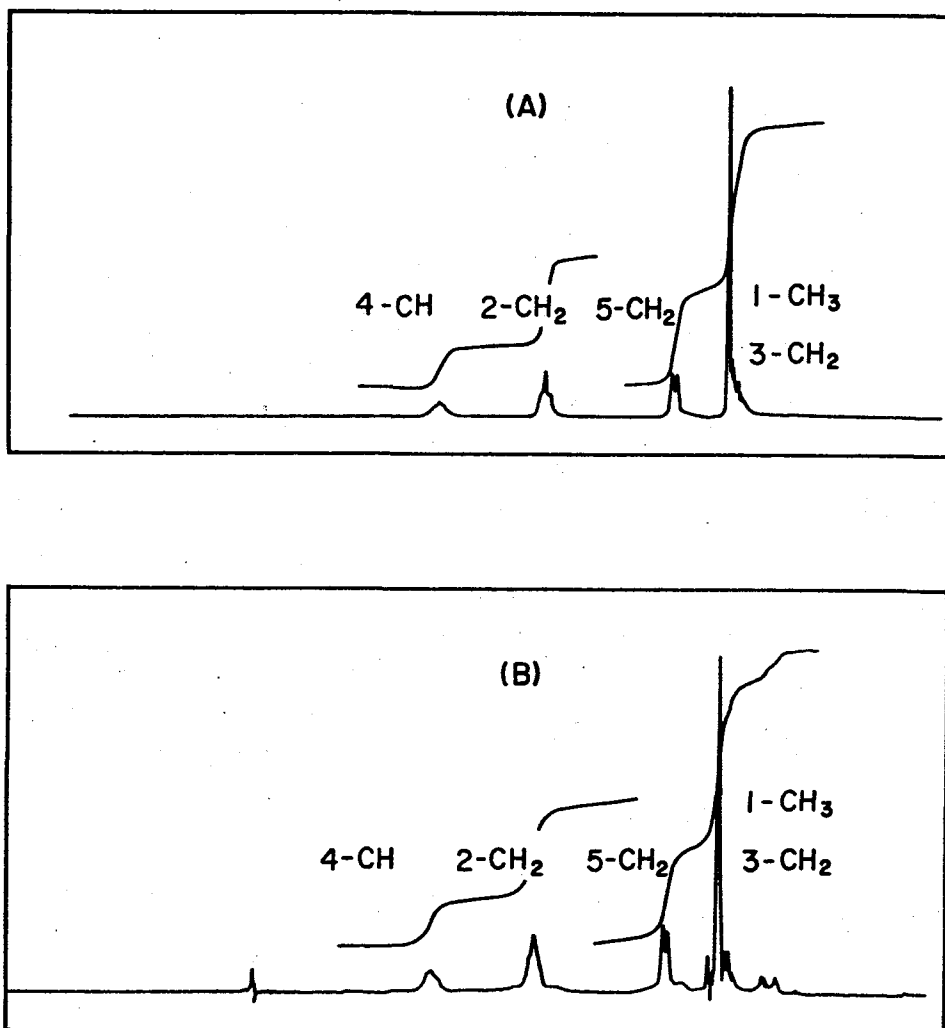
Figure 3 ^{1}H-NMR spectra of Poly($\underset{\sim}{1}$)-Al and Poly($\underset{\sim}{1}$)-Zn
in CDCl$_3$. (A): Poly($\underset{\sim}{1}$)-Al, (B): Poly($\underset{\sim}{1}$)-Zn.
Numbering of protones is made from monomer structure
$\overset{1}{C}H_3 - \overset{2}{C}O - O - \overset{3}{C}H_2 - CH_2 -$ for side chain, and
for ring-originated protons. Chemical shift values
for poly($\underset{\sim}{1}$)-Al are 1, 1.97; 2, 4.03; 3, (1.97); 4,
5.19; 5, 2.56 ppm and for poly($\underset{\sim}{1}$)-Zn are 1, 2.01; 2
4.11; 3, (2.01); 4, 5.25; 5, 2.60 ppm. Coupling
constants J_{23}, J_{43}, J_{54}, can be estimated as $\sim$6.0 Hz
for both polymers.
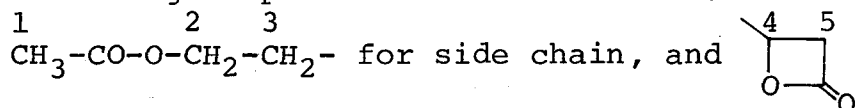
However, a characteristic difference in the polymer structure for poly(l)-Al and poly(l)-Zn was implied by ^{13}C-NMR spectra (Figure 4). Assignment of the signals was performed by off-resonance technique and the numberings are noted in the Figure caption. Four sets of double-singlet resonance were observed at the carbonyl carbons (2,7) and the carbons adjacent to ether-oxygen atoms (3-CH$_2$ and 5-CH carbons). Importantly, relative intensity of each set of the double-singlet signals in poly(l)-Al and poly(l)-Zn was reversed. Upon mixing the two types of polymer, a complete additiveness of the signals was confirmed, i.e., the four sets of double-singlet resonance with expected relative intensities were observed. Since the polymer samples have an identical range of MW (12,000 and 10,000) and both have monodisperse molecular weight distributions (Figure 5), these double-singlet resonances are not due to the oligomeric impurity.

The possibility of that the double-singlet signals might arise from tacticity separation is excluded on the following basis. It has been already reported that signal separation of poly(β-alkyl-β-propiolactones) by dyad tacticity can be observed in ^{13}C-NMR with ∿0.1 ppm separation in the presence of a shift reagent, Eu(dpm)$_3$.[1] This order of magnitude was held for a variety of higher series of analogous polymers,[2] and in the absence of the shift reagent the tacticity separation was only slight. In con-
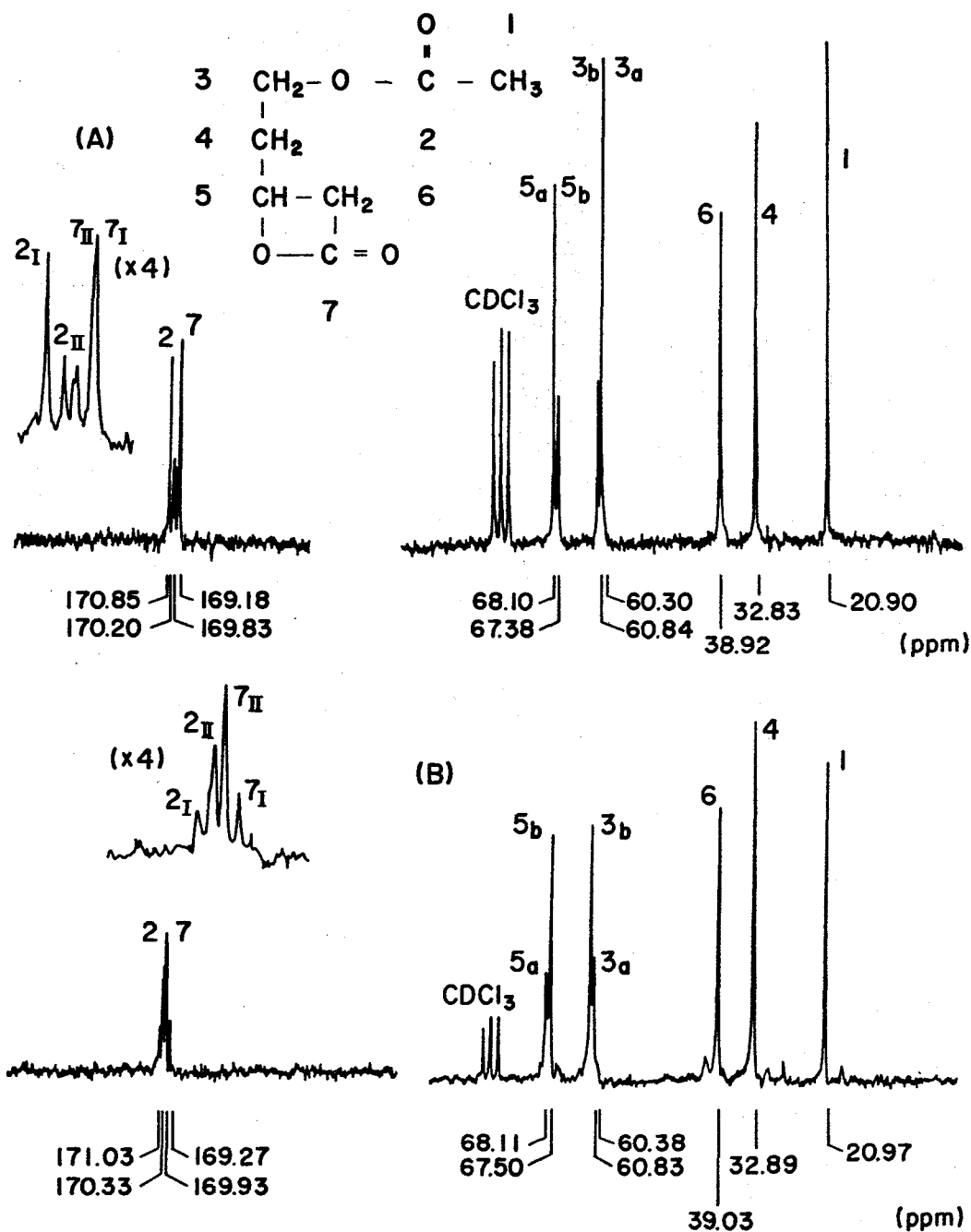
Figure 4 ^{13}C-NMR spectra of poly(1)-Al and poly(1)-Zn in CDCl$_3$.   (A): Poly(1)-Al, M$_w$ = 12000, (B): Poly(1)-Zn, M$_w$ = 10000.   Numbering of the signals should be referred to the above structure.
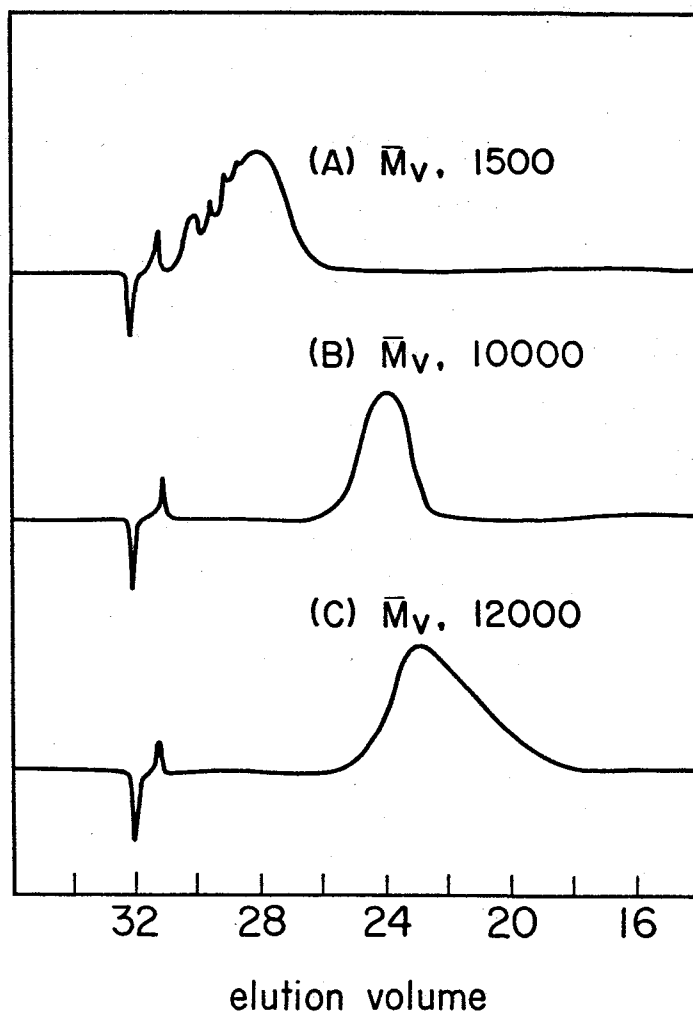
Figure 5　GPC curves of Poly(1)-Al and Poly(1)-Zn.
(A): Poly(1)-SnCl$_4^a$, $\bar{M}_V$ = 1500, (B): Poly(1)-Al^b,
$\bar{M}_V$ = 10000, (C): Poly(1)-Zn^c, $\bar{M}_V$ = 12000.
Polymerization conditions: a) Monomer 1 ml;
toluene 1 ml; temperature 30°C; catalyst 0.01 mol%/
mol-monomer. b) Monomer 1 ml; toluene 1 ml, tempera-
ture 30°C; catalyst 0.04 mol/mol-monomer. c) Monomer
1 ml; toluene 1 ml; temperature 65°C; catalyst, 0.04
mol/mol-monomer. GPC conditions: THF at 45°C.

sistent to this fact, the signal separation of each set of double-singlet resonances of poly($\underset{\sim}{1}$)s was an order of 0.5 - 0.6 ppm. Hence, we conclude that the Al catalyst and Zn one form polymers with different chemical structures in the monomeric units, though both of them are polyesters and their relative contents differ.

T_1 Measurement by ^{13}C-NMR: The relative relaxation time (T_1) of poly($\underset{\sim}{1}$)-Zn was measured in CDCl$_3$ for each carbon signal in the ^{13}C-NMR, at four limited time intervals: 0.05, 0.1, 0.5 and 3s. The value listed in Table 2 indicate the time intervals during which the signal loss occurs. The suffix a and b in carbons are used in order to distinguish the two types of structure (See Figure 4).

The structure (a) is characterized by a larger T_1 value at ^3C_a and a small value at ^5C_a carbons, while the structure (b) has an opposite property: $^5C_b > {}^3C_b$. Since T_1 values in ^{13}C-NMR can be related to segmental mobility of a molecule,[3] we can discuss the difference in structures (a) and (b) in view of the length of side chain and the number of atoms constituting the main-chain unit. The extremely large T_1 value of ^1C-carbon (CH$_3$ in acetyl) corresponds to that this carbon situates at the terminal of side chain. The structure (a), which dominates in poly($\underset{\sim}{1}$)-Al, can reasonably be deduced as "normal" poly-β-ester when considered its shorter main-chain unit (carry-

Table 2 T_1 Values of Each Carbons in Poly$(\underset{\sim}{1})$[a]

Carbon No.	T_1 (second)[b]
^1C	0.72 ∿ 4.32
^3C_a	0.14 ∿ 0.72
^3C_b	< 0.07
^4C	0.07 ∿ 0.14
^5C_a	0.07 ∿ 0.14
^5C_b	0.14 ∿ 0.72
^6C	0.07 ∿ 0.14

a) 33 % solution of Poly$(\underset{\sim}{1})$-Zn in $CDCl_3$ was measured with a 25.16 MHz ^{13}C-NMR apparatus, accumulated with 2000 scans.

b) Time intervals during which signal loss was observed are shown.
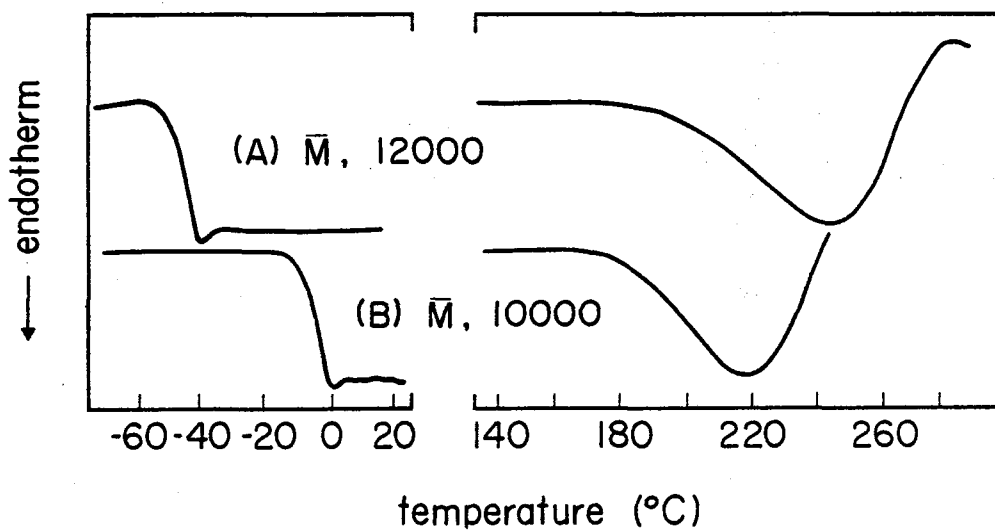
Figure 6 T_g and decomposition measurement with DSC.
(A): Poly($\underset{\sim}{1}$)-Al, $\overline{M}_V$ = 12000, (B): Poly($\underset{\sim}{1}$)-Zn, $\overline{M}_V$ = 10000.   Program rate: 10°C/min.

ing ^5C_a and ^6C carbons) and its larger side chain length (^4C exists at the neck of the chain, and ^3C_b at the second position from the main-chain).

The structure (b), which predominates in poly(1)-Zn, becomes reasonable when considered a longer main-chain unit (carrying ^3C_b, ^4C, ^5C_b and ^6C carbons) and a shorter side chain containing only acetoxy group. Partial double bond character of the main-chain CO-O bond plays a stiffening role of the main-chain. The relatively high mobility of the ^5C_b carbon, judged from the T_1 value, seems to be reasonable in view of that there are four carbon atoms intervening the successive CO-O groups, i.e., poly-δ-ester structure.
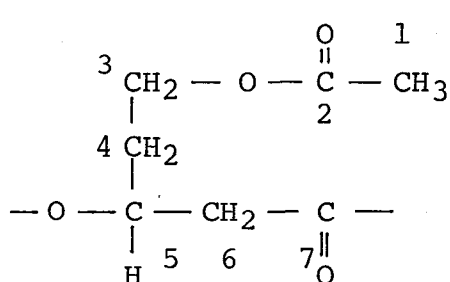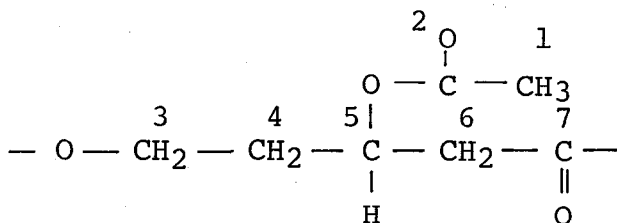
          structure a   structure b
      (poly-β-ester)   (poly-δ-ester)

Thermal Behaviors of Poly(1)s: The conclusion concerning the chemical structures of poly(1)-Al and poly(1)-Zn derived from the T_1 measurement is supported by thermal experiments. Figure 6 shows the results of DSC measurements. T_g of the poly(1)-Al sample (-60°C ∿ -40°C) was lower than that of the poly(1)-Zn sample (-10°C ∿ 0°C).

These results indicate that the former carries longer side chains which cause a weaker interchain interaction, and the latter has shorter side chains which cause a stronger interchain interaction. T_{decomp} of the poly(1)-Al sample (ca. 240°C) was higher than that of the poly(1)-Zn sample (ca. 218°C). These facts also correspond to that the mainchain of higher mobility (poly-δ-ester) decomposes more readily than that of lower mobility (poly-β-ester).[4]

Thermal decomposition of the poly(1)-Zn sample at 218°C gave 5,6-dihydro-2-pyrrone in a high yield. The product was identified by ^{1}H-NMR and IR by comparing the authentic sample prepared separately. On the other hand, when the poly(1)-Al sample was decomposed at 240°C, $CH_3COOCH_2CH_2-CH=CHCO_2H$ and 5,6-dihydro-2-pyrrone were confirmed to present in the decomposition product (Figure 7). These results are consistent with that the poly-δ-ester can more readily cyclize during main-chain scission, while the cyclization from the poly-β-ester type requires a regular movement of a long side chain to attack a predetermined position in the main chain. It is well known that poly-β-esters decompose into acrylic acid and poly-δ-ester into δ-valerolactone in pyrolysis.[5]

Polymerization Mechanism

Supposed Polymerization Scheme: Based on the analyses

$$
\underset{\text{poly-}\delta\text{-ester}}{-(O-CH_2CH_2\overset{\overset{\displaystyle OCOCH_3}{|}}{CH}CH_2CO)_n-} \xrightarrow{\Delta} \left[\underset{\underset{O}{\overset{\|}{C}}-CH_2}{\overset{CH_2CH_2}{O}}CH-OCOCH_3 \right] \longrightarrow \underset{O}{\bigcirc}{=}\hspace{-0.5em} +CH_3CO_2H
$$

$$
\underset{\text{poly-}\beta\text{-ester}}{-(O-\overset{\overset{\displaystyle CH_2CH_2OCOCH_3}{|}}{CH}-CH_2CO)_n-} \xrightarrow{\Delta} CH_3COOCH_2CH_2CH=CHCO_2H
$$
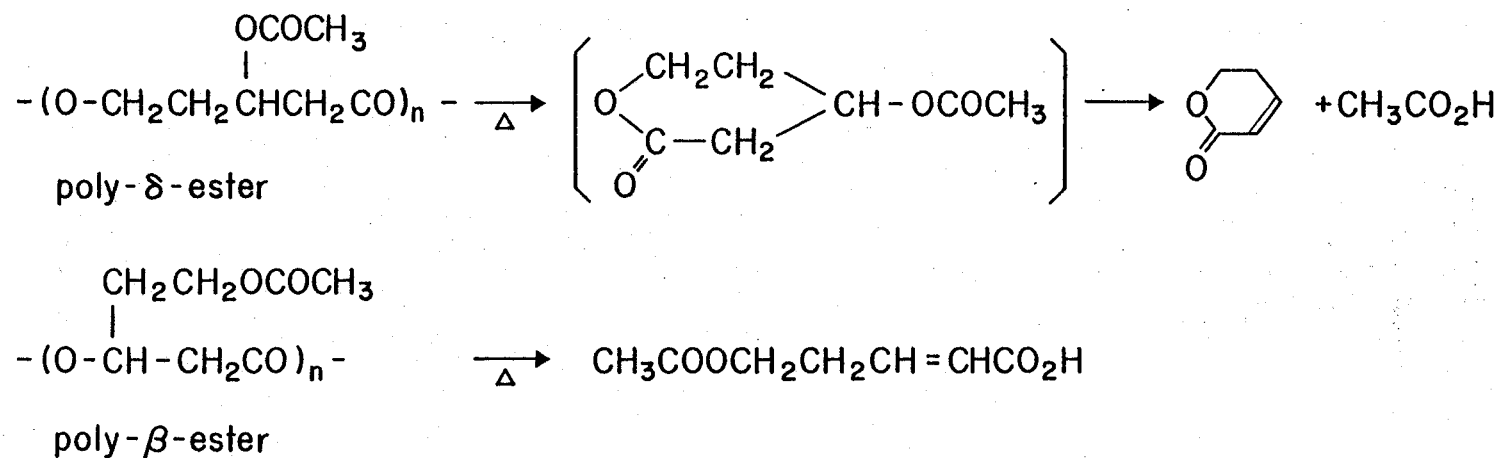
Figure 7   Thermal decomposition products of poly-δ-ester
and poly-β-ester.

of the polymer structures produced by the Al catalyst and the Zn catalyst, one can suppose polymerization schemes for Al-catalyzed "normal" polymerization and for Zn-catalyzed "isomerization" polymerization (Figure 8).

The "normal" polymerization involves simple ring-opening of the lactone ring without significant participation of the side chain ester group. In contrast, the "isomerization" polymerization involves a strong participation of the side chain ester group in the transition stage in a manner of forming a six-membered cyclic intermediate, followed by ring-opening through acyl migration. In order to verify the reaction mechanisms two types of experiment were carried out. First, a model polymerization using β-methyl-β-propiolactone in the presence of ethylacetate as a competing ester species. Second, elucidation of coordination stages of the 1 monomer with the Al- and Zn-compounds, by employing ^{13}C-NMR technique.

Model Polymerization Systems: Ethylacetate ($CH_3COOCH_2CH_3$) is a model of the side chain of 1 monomer (CH_3COOCH_2CH-). Then, if the proposed mechanism shown in Figure 7 is true, the ethylacetate would interfere the polymerization catalyzed by the Zn-compound rather than that catalyzed by the Al compound. The polymerization of β-methyl-β-propiolactone was carried out in ethylacetate solvent and was compared with the behaviors in toluene
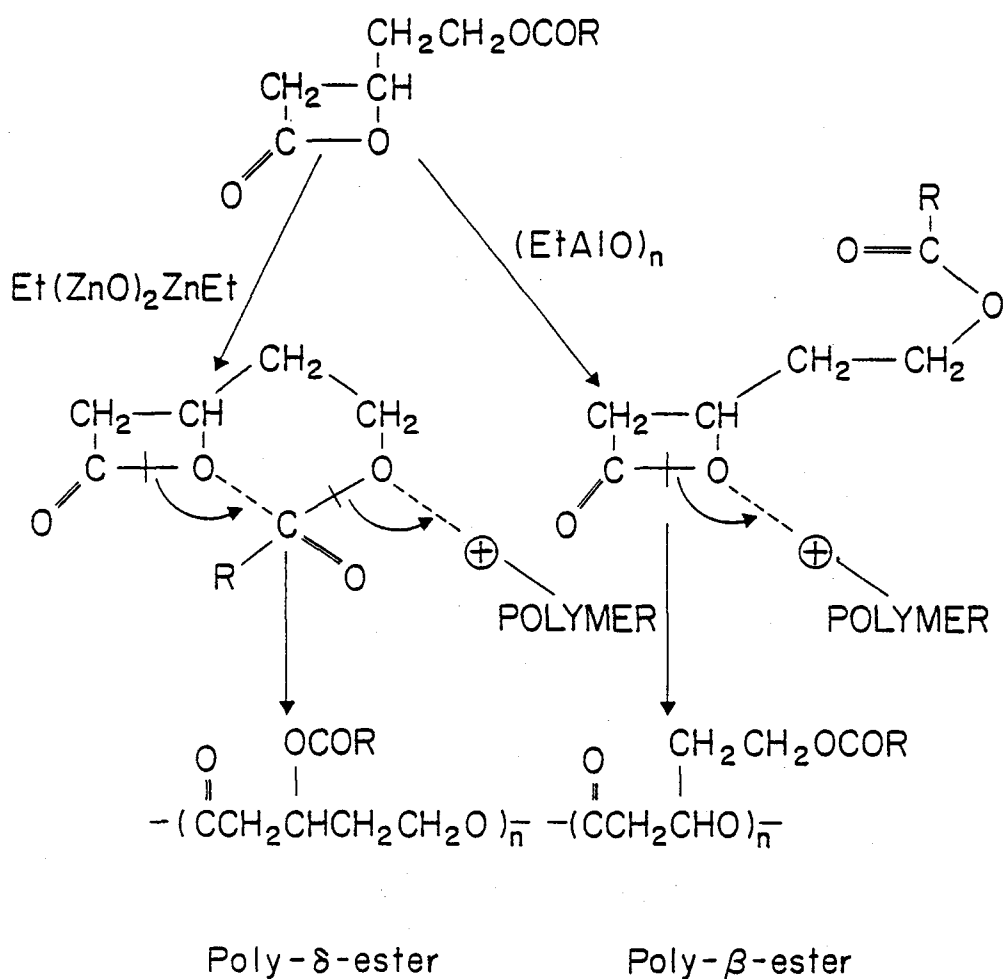
Figure 8   Reaction scheme in the polymerization.

solvent. Figure 9 shows time-dependent profiles of polymerization in ethylacetate, and Figure 10 shows the corresponding results obtained in toluene.

Clearly, the polymerization reactions in ethylacetate were considerably suppressed. In the case of Al-catalysis the rate of polymerization decreased and MW of the polymer tended to decrease after a maximum. The MW of the polymer was still high in ethylacetate keeping a range of value >20,000. In the Zn-catalysis, however, the MW of the polymer decreased to an oligomeric region as the polymerization time exceeds ca. 10 days. The polymer yield also decreases during a prolonged time, indicating decomposition of the polymer once formed. From these experiments it can be concluded that subsequent chain transfer of ethyl acetate occurs more readily in the Zn-catalysis than in the Al-catalysis.

Coordination of the Monomer 1 with Al- and Zn-compounds: The proposed intermediate stage shown in Figure 8 suggests that the structure of the monomer is different at the stages of coordination with Al-catalyst and with Zn-catalyst. ^{13}C-NMR is a powerful tool for elucidating this problem. Since the rate of polymerization with the Al-catalyst is slow enough below 20°C, the coordination stage with the $(EtAlO)_n$ compound could directly be observed. The Zn-catalysis is much faster even
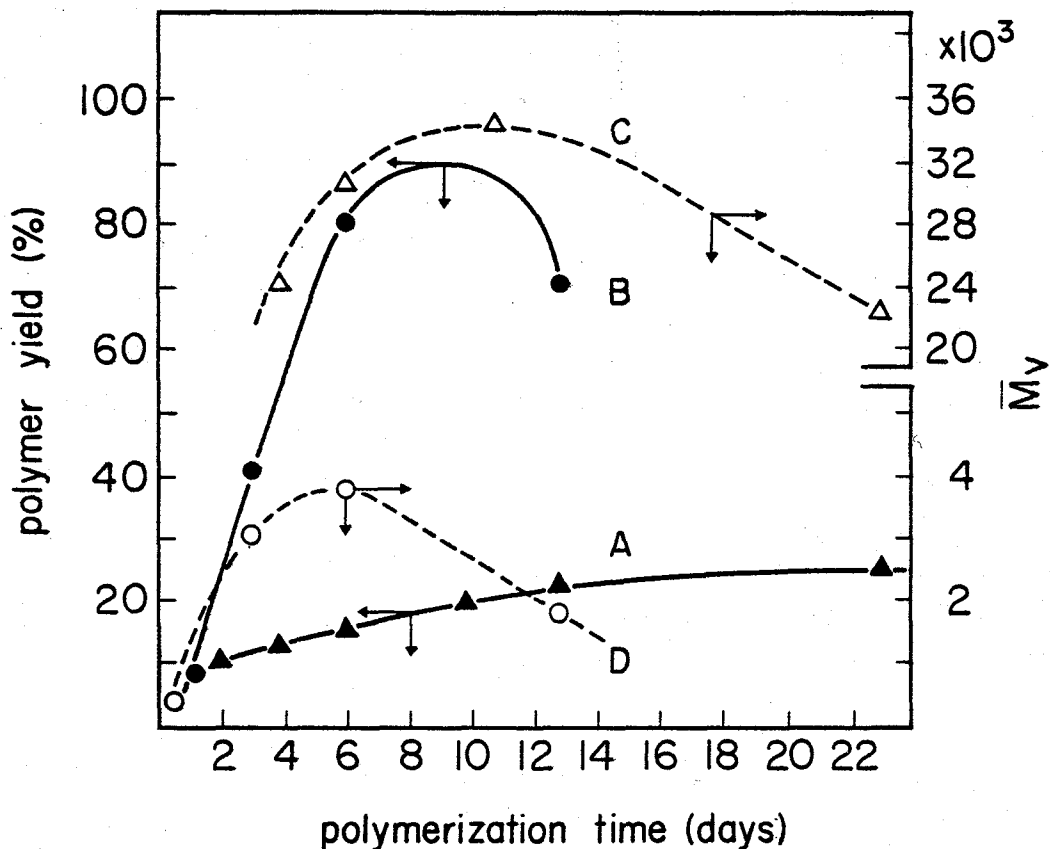
Figure 9   Time dependence of polymer yield and molecular
weight for the polymerization of β-methyl-β-pro-
piolactone in ethyl acetate-toluene mixed solvent.
A: Polymer yields in $(EtAlO)_n$ catalysis, B: polymer
yields in $Et(ZnO)_2ZnEt$ catalysis, C: $\overline{M}_v$ for polymers
obtained with $(EtAlO)_n$ catalyst, D: $\overline{M}_v$ for polymers
obtained with $Et(ZnO)_2ZnEt$ catalyst.
Polymerization conditions: Monomer, 1 ml; toluene,
0.38 ml; ethylacetate 0.62 ml; catalyst, 0.04 mol/
mol-monomer; temperature 60°C for $(EtAlO)_n$ catalysis
and 30°C for $Et(ZnO)_2ZnEt$ catalysis. Values of $\overline{M}_v$
were obtained from GPC calibrated by standardization
with polystyrene samples.
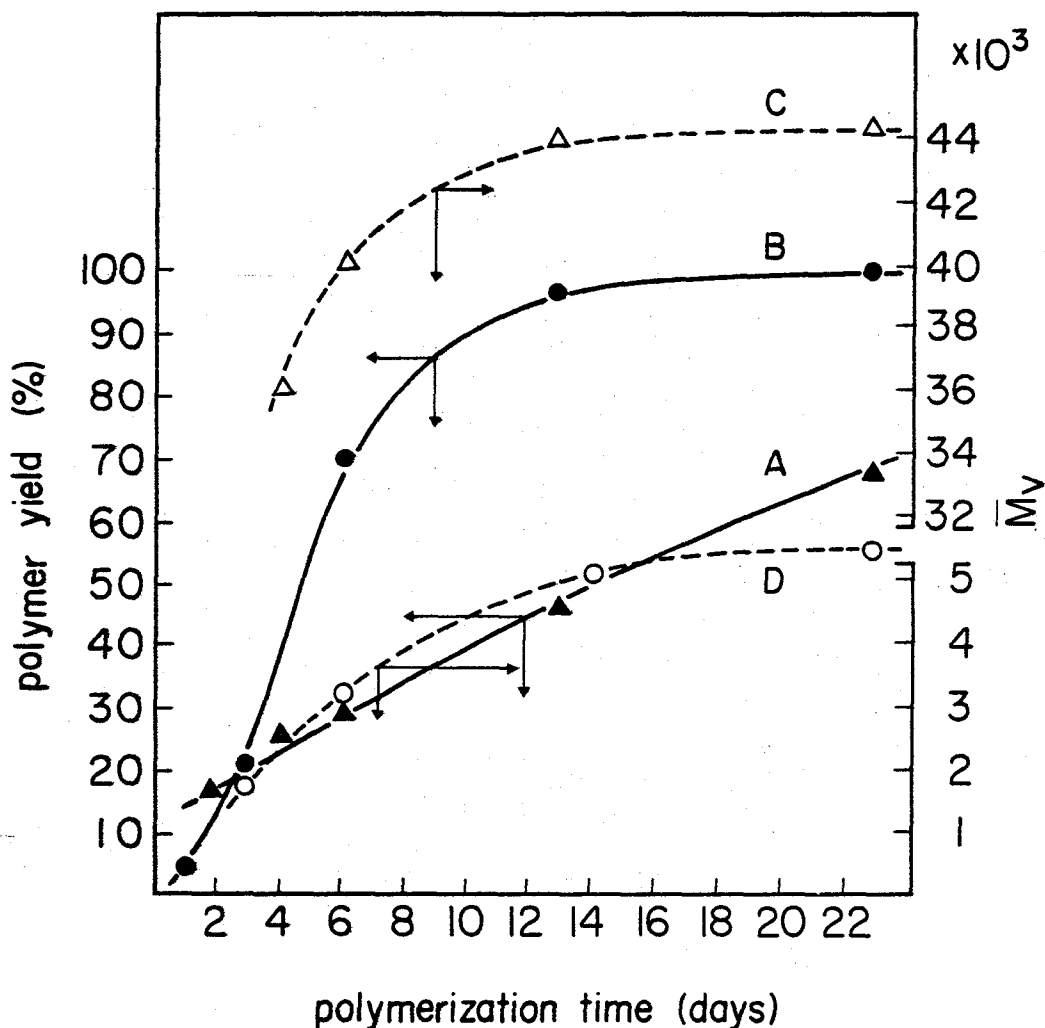
Figure 10　Time dependence of polymer yield and molecular
weight for the polymerization of β-methyl-β-pro-
piolactone in toluene.
A: Polymer yields in (EtAlO)$_n$ catalysis, B: polymer
yields in Et(ZnO)$_2$ZnEt catalysis, C: $\overline{M}_V$ for polymers
obtained with (EtAlO)$_n$, D: $\overline{M}_V$ for polymers obtained
with Et(ZnO)$_2$ZnEt. Polymerization conditions are
identical as shown in Figure　9 except for toluene
(1 ml) was used.

at low temperatures, and Et_2Zn was used instead of the
$Et(ZnO)_2ZnEt$ compound.

^{13}C-NMR spectra of an equimolar mixture of monomer,
1 and $(EtAlO)_n$ compound were taken in toluene-d_8 by
changing the temperature from -50 to +20°C and the change
of the chemical shift (δ) of each carbon was plotted in
Figure 11. The corresponding results obtained with an
equimolar mixture of the monomer 1 and Et_2Zn compound are
shown in Figure 12. In the Al-system a large change in
the chemical shift was observed for the ring-carbonyl
carbon (C7) and the ring methine carbon (C5), while the
side chain carbonyl (C2) was relatively unaffected. In
contrast, the chemical shift change in the Zn-system was
remarkable only for the side chain carbonyl carbon (C2),
while the ring carbons (C7, C5) were almost unaffected.
These observations are consistent with the idea that the
Al-compound interacts more strongly with the lactone ring
moiety in the monomer molecule, but the Zn-compound more
strongly with the side chain ester group rather than
lactone ring. This idea is a key for understanding the
polymerization routes whether the "normal" formation of
poly-β-ester or the "isomerized" product poly-δ-ester is
predominant.

Other Factors Affecting Polymerization Courses: The
discussions above are made by assuming that the nature of
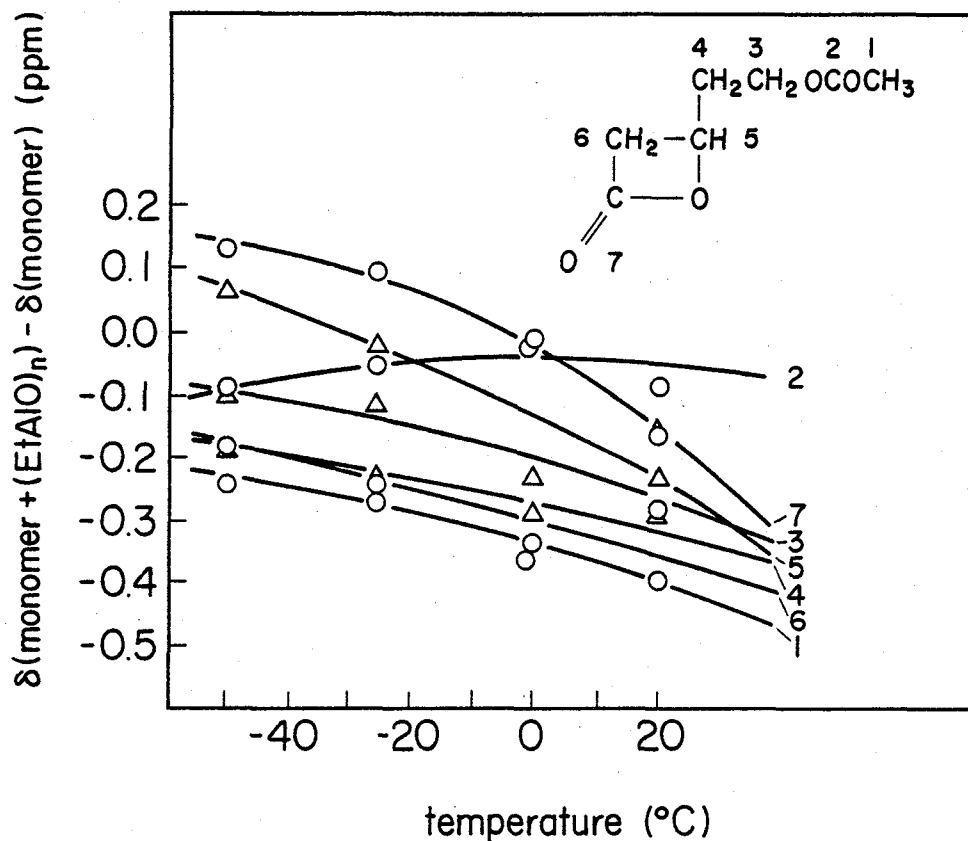
Figure 11 Temperature dependence of ^{13}C-NMR chemical shift value of (1) in the presence and absence of (EtAlO)$_n$. Accumulated with 200 scans. Chemical shift values (ppm) are internally standardized from d$_8$-toluene-ring carbon signal. (1) 1 ml; d$_8$-toluene 2 ml and equimolar amount of (EtAlO)$_n$ to (1) were used.
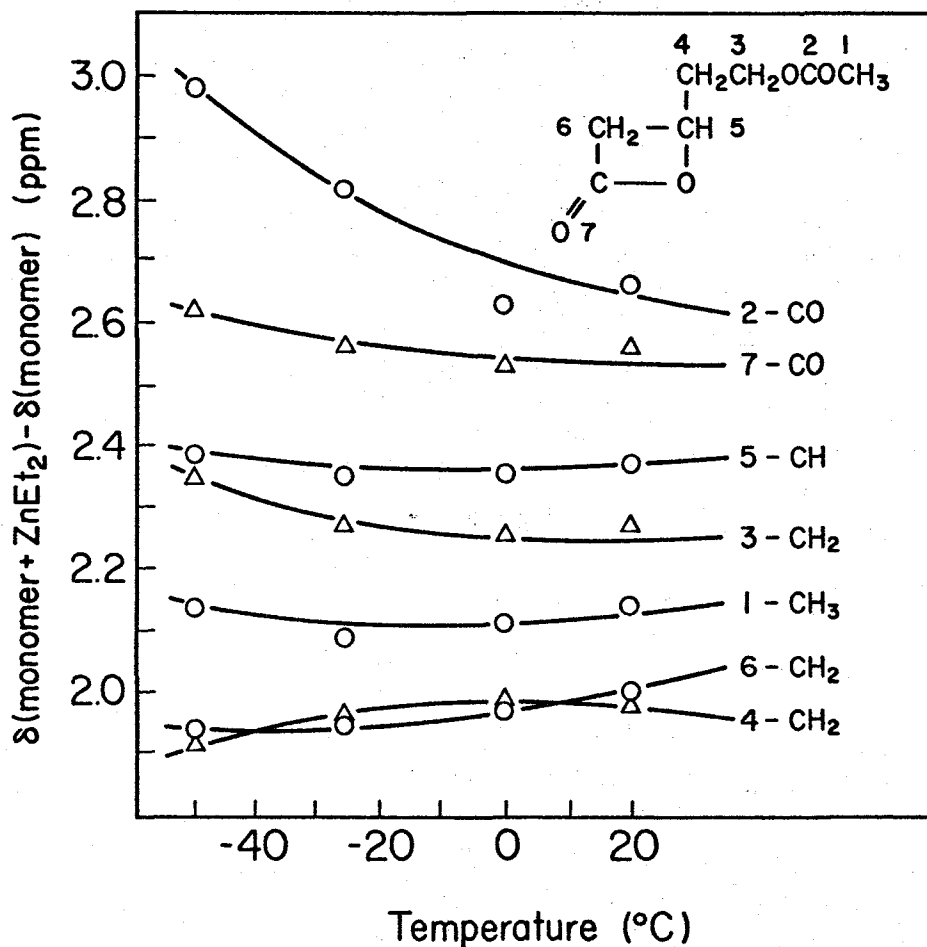
Figure 12   Temperature dependence of ^{13}C-NMR chemical
shift value of (1) in the presence and absence of Et$_2$Zn.
(1) 1 ml and d$_8$-toluene 2 ml for the measurement of
δ(monomer); (1) 1 ml, ZnEt$_2$ 0.72 ml and d$_8$-toluene,
1.28 ml for δ(monomer + ZnEt$_2$).
Other conditions: see Figure 11.

catalyst is a major determining factor for the polymeriza-
tion routes. This assumption was verified by the results
shown in Table 3, where the isomer ratio obtained with a
given catalyst is almost independent of polymerization
temperature and catalyst concentration.

A typical cationic catalyst, $SnCl_4$, behaves simi-
larly to the Zn catalyst in view of the predominant for-
mation of the poly-δ-ester structure (cf. Table 1),
although the product is a mixture of lower M_w compounds
(Figure 5). In this respect, the Zn catalyst appears to
act cationally. Since the Al catalyst has also been sug-
gested as cationic in nature[1], the difference in electro-
philic properties of the Al and Zn atoms seems to be re-
sponsible for the site-selective interactions leading to
the two types of polymer.

Stereoregularity of Poly($\underset{\sim}{1}$)-Al: Although the Al
catalyst is more stereoregulating than the Zn catalyst,
the poly($\underset{\sim}{1}$)-Al was an atactic polymer as evidenced by (i)
its amorphous X-ray diffraction pattern and (ii) by ^{13}C-
NMR showing further ~ 0.1 ppm separations at ^7C_a and ^7C_b
carbons, respectively. As shown in the coordination
study and the model polymerization system with ethyl-
acetate, the side chain ester group cannot be completely
free from coordination to the Al catalyst. This factor
seems to inhibit the regular arrangement of the monomer

Table 3　Isomerization Ratio in the Polymerization
　　　　　of (1)a)

Catalyst	Polymerization temperature (°C)	Catalyst concentration (mol%)	Isomerization ratio (%)
Al	63	2	25
Al	63	4	33
Al	45	7	32
Al	63	7	31
Al	63	11	30
Zn	30	2	75
Zn	65	2	71
Zn	30	4	68
Zn	50	4	71

a) Monomer 2 mℓ, toluene 2 mℓ.

molecules on the catalyst during the propagation reaction, through some competition between the side-chain ester group and the lactone ring.

Relation with Stereoregulation in the "Normal" Type Polymerization: The difference of the interacting site in the monomer molecule toward the Zn and Al catalysts may be used to interpret the difference in the stereo-controlling properties of the two types of catalyst in the "normal" type polymerization of β-alkyl- and β-chloro-alkyl-β-propiolactones.[1,6] For example, the Al catalyst coordinates predominantly with the lactone ring of a monomer, whereas the Zn catalyst interacts with the poly-ester chain rather than with the attacking monomer. This leads to the former catalyst as being more stereoregulat-ing than the latter. The Zn catalyst becomes stereoregu-lating only when an appropriate structure is possible be-tween the attacking monomer and the growing chain end, as in the case of polymerization of α-methyl-β-propiolactone.[7]

In conclusion, the mistery of behaviors of Al-type and Zn-type catalyses for the stereoregulation in a va-riety of ring-opening polymerization can be solved when a simple but basic concept is applied; i.e., the strength of interaction between the catalyst and the growing chain end is of prime importance. Hence, early discussions widely made on the basis of whether a catalyst is cationic

or anionic will be only significant in considering the
structure of an active end of the growing polymer chain.
It should be noted, however, an effective stereoregulation
in the cationic polymerization is limited where the grow-
ing chain end can effectively coordinate to the metal
catalyst, and this situation is relatively restricted
compared to in anionic polymerization in general.

11-3   Polymerization of β-(2-isopropylcarboxyethyl)-β-
      propiolactone (2) and β-(2-(1-chloroethyl)carboxy-
      ethyl)β-propiolactone (3)

The reason of the choice of the monomers 2 and 3 is
that (1) These two are higher analogs of the monomer 1 but
they are the smallest members with significant steric
factor, and (2) Electronic effect of $(CH_3)_2CH-$ and
$(CH_3)ClCH-$ groups operates in opposite ways in keeping
the steric effects being almost identical.[1] The relative
Taft's factors (σ^*)[8] for $(CH_3)_2CHCOO-$ and $(CH_3)ClCHCOO-$
groups can be estimated as -0.19 and $+0.95$ (-0.10 for
addition of one CH_3 and $+1.05$ for addition of one Cl),
respectively, when standardized by CH_3COO- as 0.00.
(3) These monomers can be prepared in similar procedures
as the case of the monomer 1, and can be obtained in al-
most identical purities. This factor seems important for
comparison of polymerization behaviors of different type
of monomers in the organometallic catalyses.

2-1. <u>Polymerization Results</u>: Polymerization of the mono-
mers 2 and 3 was found to proceed in a similar manner as
the case of the monomer 1. The results are tabulated in
Tables 4 and 5 for monomers 2 and 3, respectively, and
typical results with the monomer 1 are also included. The
polymer yields were determined from the amount of polymers
isolated by precipitation then washing with ether. The
polymerizability of the monomers evaluated from the poly-
mer yields was found to be 1 > 2 >> 3 for the Al-catalysis
and 1 ≥ 2 >> 3 for the Zn-catalysis in toluene solvent.
These results indicate that the increase of steric factors
in the monomers 2 and 3 relative of 1 is more apparently
reflected in the Al-catalysis rather than in the Zn-cata-
lysis. This is in accord with the fact that the stereo-
regulation of the polymerization for β-alkyl- and β-chloro-
alkyl-β-propiolactone series is much effective in the Al-
catalysis than in the Zn-catalysis.[1] Similarity in the
polymer yields from 1 and 2 in the Zn-catalysis suggests
that there is no significant steric factors to produce a
reaction intermediate in the presence of Zn atom. Remark-
able decrease of the polymerizability of monomer 3 com-
pared with that of monomer 2 is largely due to electronic
factor of the Cl group in the former since the steric
factors of the monomers 2 and 3 are almost identical.
Hence, decrease of the electron density in the side-chain
ester group of the Cl-containing monomer causes drastic

Table 4   Polymerization Results of Monomers 1 and 2.[a]

Monomer	Catalyst[b]	Catalyst concn. (mol%)	Solvent[c]	Temp. (°C)	Time (days)	Polymer yield (%)[d]
1	Al	4	toluene	63	30	52
1	Zn	4	toluene	65	4	68
2	Al	4	toluene	80	28	43
2	Al	4	toluene	65	32	41
2	Zn	4	toluene	65	21	45
2	Zn	4	toluene	35	32	70
2	Zn	4	CH_2Cl_2	30	31	30
2	Zn	6	toluene	30	28	60
2	BF_4OEt_3	1	toluene	30	30	16

a) The results of monomer 1 are selected from Table 1.

b) Al denotes $(EtAlO)_n$ and Zn denotes $Et(ZnO)_2ZnEt$.

c) Monomer/solvent ratio, 1/1 (v/v).

d) Determined by weight of isolated polymer.

Table 5   Polymerization Results of Monomer 3.[a)]

Catalyst	Catalyst concn. (mol%)	Temp. (°C)	Time (days)	Polymer yield (%)
Al	4	65	31	21
Al	6	65	21	29
Zn	4	30	9	21
Zn	4	65	23	11
Zn	6	30	40	10
BF_4OEt_3	1	30	31	5

a) Toluene was used as solvent, monomer/solvent ratio
   1/1 (v/v). Notes described in Table 1 should be
   referred to.

decrease in the polymerizability. Such a effect seems to consistent with the previous observation that the side-chain ester group interacts with the catalyst, especially with Zn, in a manner of competition against "normal" ring-opening process of the lactonic ester group. For Al-catalysis decrease of the polymerizability of monomer 3 is observed, but the extent is considerably smaller than for Zn-catalysis.

2-2. Polymer Structure: The polymer structures were ex-amined with ^{13}C-NMR as was the case of poly(1)s. Figure 13 shows the spectra of poly(2)-Zn, poly(2)-Al, poly(3)-Zn, and poly(3)-Al of molecular weight 4,000. The assignment of the signals can be made straightforeward by refering the results of poly(1). The signals of C-3 and C-5 carbons, which correspond to the side-chain O-CH$_2$ and the ring CH carbons, respectively, split in an essentially similar fashion as were observed in poly(1)-Zn and poly(1)-Al samples. Clearly, the intensity ratios of the C-3$_a$ (in poly-β-ester unit) to the C-3$_b$ (in poly-δ-ester unit) and C-5$_a$ (in poly-β-ester unit) to C-5$_b$ (in poly-δ-ester unit) differ with the nature of the catalyst used. These spec-tral evidences indicate that ring-opening isomerization polymerization occurs also in the cases of monomers 2 and 3.
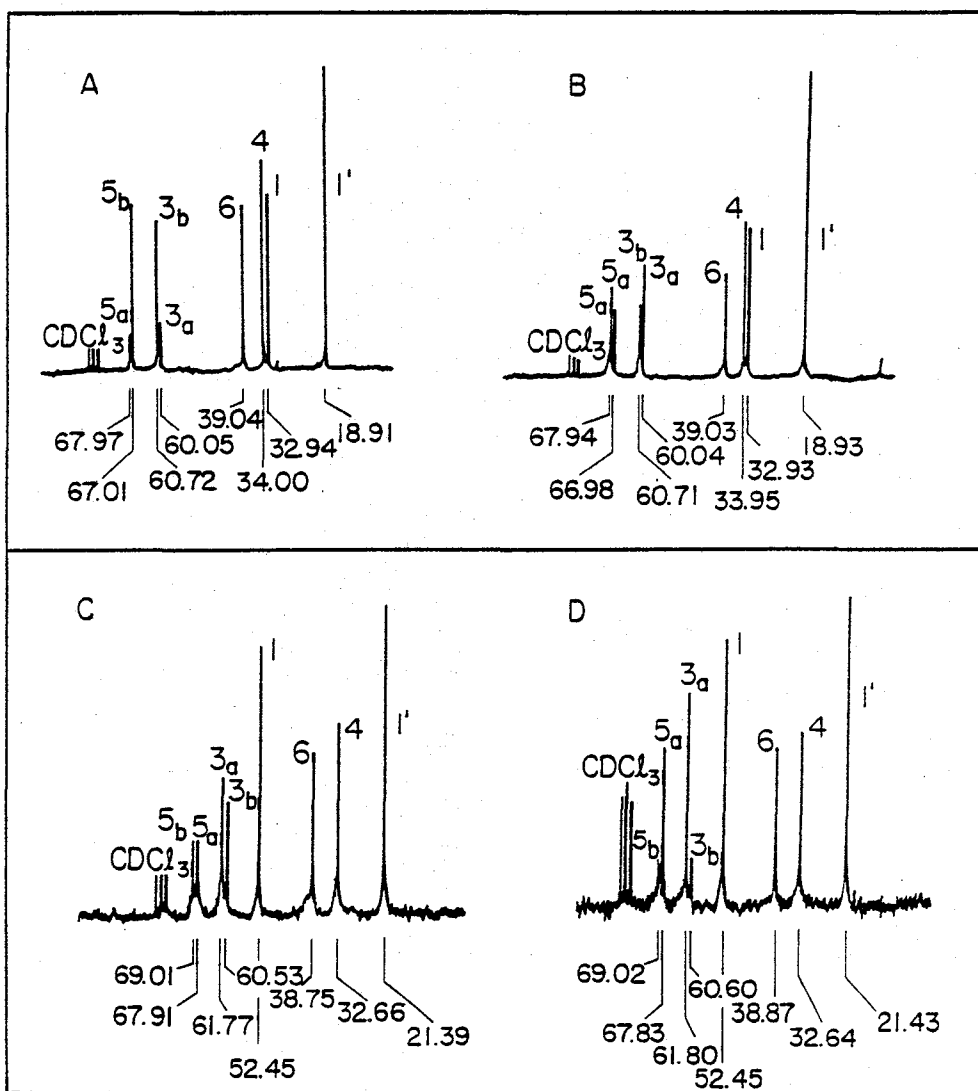
Figure 13 ^{13}C-NMR spectra of Poly(2) and Poly(3) samples
in CDCl$_3$.   A: Poly(2)-Zn, B: poly(2)-Al, C: poly(3)-Zn,
D: poly(3)-Al.   Numbering of the signals should be
referred to the following monomer structure.   The
carbonyl signals are omitted in the Figures.   Suffix a
shows the signals of the poly-β-ester unit, and suf-
fix b that of the poly-δ-ester unit.   The assignments
were referred to the spectrum of poly(1).

2-3. <u>Relative Amount of Isomerization Polymerization</u>:
The intensity ratios of the C-3$_a$/C-3$_b$ and C-5$_a$/C-5$_b$ sig-
nals reflect the relative amounts of isomerized product
to the normal polymerization product. The relative
amounts of poly-δ-ester and poly-β-ester units in the
polymers thus estimated are summarized in Table 6, in
comparison with the results of monomer 1.

For the cases of monomers 2 and 3 the isomerization
ratios were higher for the Zn-catalysis than for the Al-
catalysis. This trend is common for all of the monomers
studied here. The monomer 2 showed a considerably high
isomerization ratio where the Zn-catalysis afforded about
80 % of isomerized poly-δ-ester unit, and even in the Al-
catalysis almost equimolar amounts of poly-δ-ester and
poly-β-ester units were formed. The Cl-containing monomer
3 converts less readily to poly-δ-ester unit compared with
the monomers 1 and 2.

<u>Thermal Behaviors of Polymers</u>: It has been already
shown that the polymer enriched with poly-δ-ester struc-
ture, which is consisted of longer main-chain units and
shorter side-chains, shows higher T$_g$ value than the poly-
mer enriched with poly-β-ester structure (shorter main-
chain units and longer side-chains, therefore weaker in-
terchain interaction). Further, the former has lower de-
composition temperature because of its relative feasibility

Table 6   Isomerization ratio of polymers.

Monomer	Catalyst	Isomerization ratio (%)
1	Al	25-33
1	Zn	68-75
2	Al	42-54
2	Zn	76-84
3	Al	20-25
3	Zn	∿50

in producing a pyrolysate as 2-dihydropyrrone rather than the latter which gives substituted acrylic acid as main pyrolysate. For instance, the poly(1)-Zn and poly(1)-Al with molecular weight of ca. 10,000 showed significant differences in T_g and T_{decomp} values as cited in Table 7. Similar trends were observed for poly(2) and poly(3) samples, though the differences of the T_g values were not so remarkable. The closeness of T_g values in Zn-polymers and Al-polymers may be due to lower molecular weight and to the presence of branched side-chains which reduce the inter-chain interactions operating in both types of polymer. The difference of T_{decomp} values between poly-δ-ester rich and poly-β-ester rich samples was significant for poly(2) and poly(3) series as shown in Table 7.

Transition State of Isomerization Polymerization:
The observed trend of isomerization polymerization, i.e., monomer 2 > monomer 1 > monomer 3, can be interpreted on the basis of reaction scheme shown in Figure 8.

The isopropyl group in the monomer 2 gives rise to the highest electron density at the side-chain carboxyl moiety. Since the Zn atom can coordinate with both of carboxyl groups in the side-chain and lactone ring (in preference at the side-chain), the interaction of the Zn atom with the $(CH_3)_2CHCOO-$ group would be strongest in due course. This effect will exert to bring the side-

Table 7   Thermal Properties of Polymers.

Polymer	M.W.	T_g (°C)	$T_{decomp.}$ (°C)
poly(1)-Al	12000	$-60 \sim -40$	245
poly(1)-Zn	10000	$-10 \sim 0$	220
poly(2)-Al	4000	$-30 \sim -18$	260
poly(2)-Zn	4000	$-27 \sim -12$	215
poly(3)-Al	4000	$-25 \sim -14$	250 - 270
poly(3)-Zn	4000	$-22 \sim -10$	220 - 250

chain ester group near to the lactonic oxygen atom with-
out significant resistance, giving rise to a simultaneous
coordination of Zn with both of the ester group.   Since
the Zn atom was present at the terminal carboxyl group of
the growing chain, the entity of this stage is likely to
constitute a coordination state comprised of three types
of ester oxygen atoms: one from growing chain, one from
the side-chain, and the remainer from the lactone group.
This provides a favorable condition to afford a bicyclic
intermediate suitable for isomerization polymerization
producing poly-δ-ester structure.

$$
\begin{array}{c}
\text{O-CH}_2\text{-CH}_2\text{-CH-CH}_2\text{-CO} \\
| \quad\quad\quad / \\
\text{O} \\
|\text{- -Zn} \\
\text{CO} \\
| \\
\text{iPr}
\end{array}
\;+\;
\begin{array}{c}
\text{O} \\
\| \\
\text{C}-\text{CH}_2 \\
| \quad | \\
\text{O}-\text{CH} \\
| \\
\text{CH}_2 \\
| \\
\text{O} \quad \text{CH}_2 \\
\| \quad | \\
\text{iPrCO-CH}_2
\end{array}
\longrightarrow
\begin{array}{c}
\text{iPr} \\
\backslash \\
\text{C=O} \\
\backslash \\
\text{O} \\
\text{CH} \\
| \\
\text{CH}_2 \\
\text{C}^{+} \\
\|\\
\text{O}
\end{array}
\begin{array}{c}
\text{O=C}-\text{CH}_2 \\
| \quad | \\
\text{O}-\text{CH} \\
\backslash \\
\text{Zn COiPr CH}_2 \\
| \quad / \\
\text{O}-\text{CH}_2
\end{array}
$$
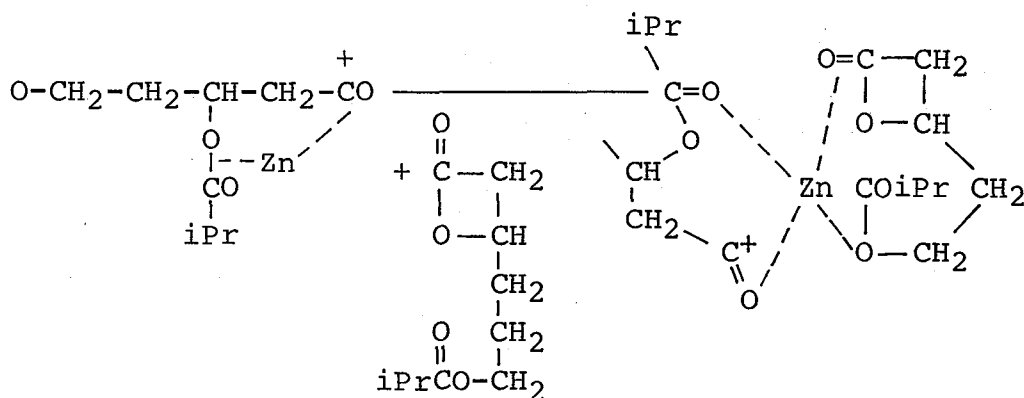
     The situation of monomer 3 where $(CH_3)ClCHCOO-$ group
is present differs considerably because of great decrease
in the electron density at the side-chain ester group (cf.
$\sigma^* = +0.95$ for $(CH_3)ClCHCOO-$).   Hence, the interaction of
the Zn atom with the side-chain ester group becomes week-
ened, and the polymerization will tends to proceed by
spoiling the side-chain group.   This mechanism is sub-

stantially a "normal" ring-opening polymerization mecha-
nism of β-substituted-β-propiolactone.

Our results indicate that even in the Al-catalysis,
an increase in the electron density at the side-chain
ester group in monomer 2 causes a significant increase in
contribution of bicyclic intermediate to afford poly-δ-
ester structure in almost an equal probability as to form
poly-β-ester structure. This result suggests that the
preference of Al-catalysis for "normal" type polymeriza-
tion stands on a delicate balance of the electron density
at the lactone and the side-chain groups, which partici-
pates at the coordination stage.

Kinetic Behaviors of Polymerization: The time-
conversion profiles of polymerization of the monomers 2
and 3 (Figure 14), which were obtained by monitoring the
monomer conversion in the NMR tube, indicate that there
are general trends in the isomerization polymerization
and in the normal polymerization also in view of kinetic
behavior. One exception was polymerization behavior of
the monomer 2 in Al-catalysis, which has the highest
isomerizability.

The poly-δ-ester forming isomerization polymerization
which favors the bicyclic intermediate shown in Figure 8
occurs relatively rapidly after a considerably long induc-
tion period. The long induction period may be due to
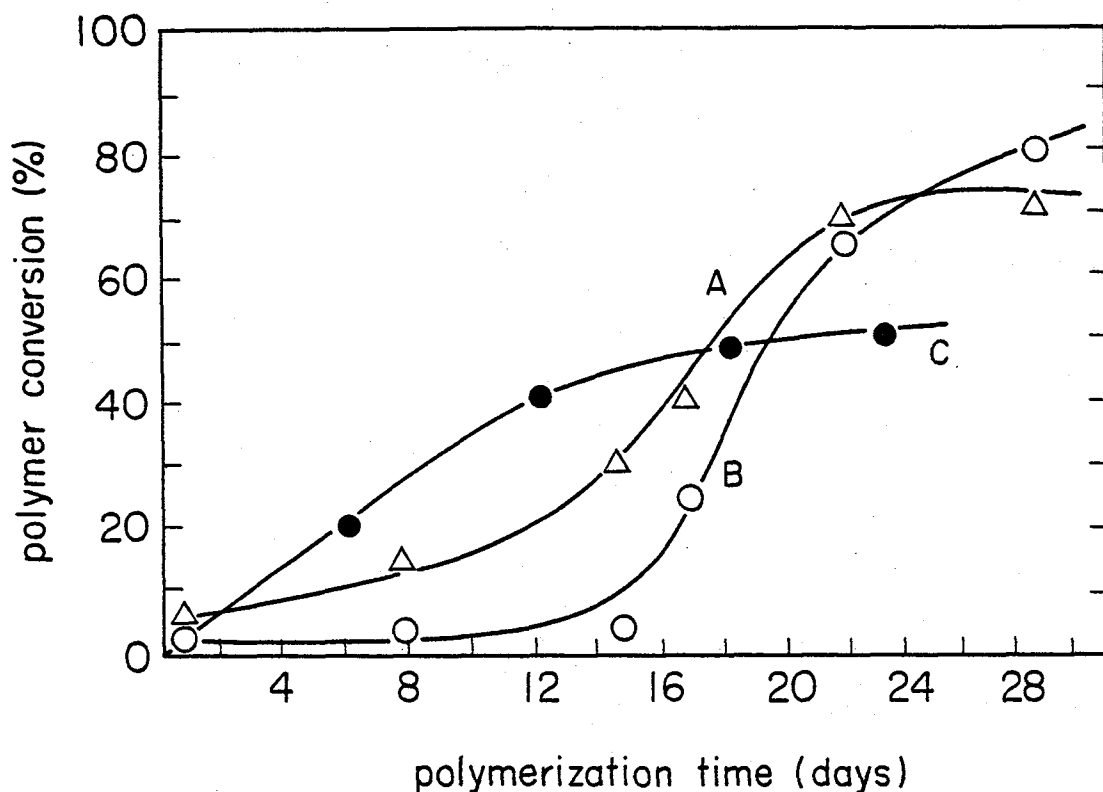
Figure 14 Kinetic profiles in polymerization of monomer
(2) and (3).
A: (2) in Al-catalysis, B: (2) in Zn-catalysis, and
C: (3) in Al-catalysis. Polymerization was carried
out in a sealed NMR tube, and conversion was deter-
mined from relative intensity of methine signals of
monomer and polymer. Polymerization conditions:
monomer/toluene ratio, 1/1 (v/v); catalyst/monomer
ratio, 4 mol%, temperature, 60°C for Al-catalysis
and 30°C for Zn-catalysis.

requirement of movement of the long side-chains in the monomer to give a proper geometry in the bicyclic intermediate.

In contrast, the poly-β-ester forming "normal" polymerization proceeds relatively monotoneously with time as were observed in a variety of substituted β-propiolactones in the presence of the Al-catalyst.[1] The behavior of the monomer 2 in Al-catalysis resembles to the Zn-type one kinetically. This is probably associated with the fact that the polymerization proceed in an almost equal probability of poly-δ-ester and poly-β-ester forming mechanisms. High contribution of the former mechanism seems to result in a net kinetic behavior to have an isomerization-type (Zn-type) profile.

Equibinary Copolymer: It must be noted that the poly(2)-Al and poly(3)-Zn samples contain almost equimolar amounts of poly-β-ester and poly-δ-ester units as shown in Table 6. These polymers are statistically equibinary copolymers of two different monomeric units. Although there remains a possibility that these are alternate copolymer, I have no decicive evidence for this possibility. Rather, it is safe in this stage that the equibinary copolymers are not complete alternate copolymer, since the isomerization ratios differ within a small range by the polymerization conditions, e.g., batch con-

ditions, and in addition no remarkable characteristics in the physical properties of the equibinary copolymer when compared with other copolymers. However, it is still interesting that this type of equibinary copolymers can be synthesized by the new isomerization polymerization.

References

1. K. Teranishi, T. Araki and H. Tani, Macromolecules, 5, 660 (1972); H. Tani, S. Yamashita and K. Teranishi, Polym., J., 3, 417 (1972); K. Teranishi, M. Iida, T. Araki, S. Yamashita and H. Tani, Macromolecules, 7, 421 (1974); M. Iida, T. Araki, K. Teranishi and H. Tani, Macromolecules, 10, 275 (1977); M. Iida, S. Hayase and T. Araki, Macromolecules, 11, 490 (1978).

2. T. Araki, M. Iida and S. Hayase, Polym. Prepr. Jpn., 26, 140 (1977); T. Araki, M. Iida, S. Hayase and A. Nakamura, Preprts. 38th Annual Meeting of Chem. Soc. Jpn., Vol.III, p.1208, 1978, Oct. 16, Nagoya, Japan.

3. D. Shaw, "Fourier Transform N. M. R. Spectroscopy", Elsevier Scientific Publishing Company, p. 297 (1967)

4. R. D. Lunberg and E. F. Cox, "Kinetics and Mechanism of Polymerization", Vol. II, "Ring Opening Polymerization" edited by K. C. Fresch and S. L. Reegen, 1969, Marcel Dekker, New York and London, Chapter 6, p. 247

5. H. Mark and G. S. Whitby, "High Polymers", Vol. 1, "The Collected Papers of W. H. Carothers", Wiley Interscience, New York, 1940, p.81 - 140.

6. J. R. Shelton, D. E. Agostini and J. B. Lando,

   J. Polymer Sci., Part A-1, <u>9</u>, 2789 (1971).

7. T. Araki, M. Iida and S. Hayase, unpublished results.

8. R. W. Taft, Jr., "Separation of Polar, Steric, and

   Resonance Effects in Reactivity" in Steric Effects

   in Organic Chemistry (M. S. Newman, ed.), John Wiley

   and Sons, Inc., New York, 1956, p.590 - 594.

Chapter 12   Experimental

Part I.   A new catalyst for polymerization of epoxide

Material

Cyclohexene oxide was dried over CaH_2, distilled, and
stored in a nitrogen atmosphere.

Silicon compound: Silanols were prepared by methods de-
scribed in the literature.[1] Alkoxysilanes were synthe-
sized from chlorosilane and alcohol, in the same manner
as silanols[1]. Benzylsilylether and ortho-nitrobenzyl-
silylether were purified by means of column chromatography
(ODS silica) and recrystallization from chloroform. Char-
acterizations of new compounds are shown in Table 1.
Other alkoxysilanes were purified by means of distillation.
Oligomers of diphenylsilanediol were prepared by frac-
tional recrystallization of a hydrolysis mixture of
Ph_2SiCl_2[2]. Polymeric silanol compound, SH6018, was ob-
tained from Toray Silicone Co., Ltd. (average OH equiva-
lent, 400).

Syntheses of diphenyl(4-vinylphenyl)silanol: The solution
of 4-bromostyrene(12.0 g) and ethyl bromide(0.4 g) in ab-
solute tetrahydrofurane(30 ml) was added dropwise to
Mg(3.2g) suspended in absolute tetrahydrofurane(10 ml).
The reaction started immediately. The addition took 10
minutes, then it was stirred for 30 min. 20 ml of absolute

Table 1   Characterization of New Silyl Ethers.

	Sample	H^1-NMR (ppm)	IR (cm^{-1})	UV$\lambda_{max}^{CH_3CN}$nm(ε)	Elemental analysis (%) found (calcd.)			
					C	H	N	Cl
Si-I	4-chloro-2-nitrobenzyl	5.25	3060	218(34700)	67.62	4.31	3.06	7.88
	(triphenyl)silyl ether	7.32 - 8.08	1535	252(3600)	(67.33)	(4.52)	(3.14)	(7.95)
			1435	258(4900)				
			1120	263(4700)				
				271(3600)				
				306(1500)				
Si-II	4,5-dimethyoxy-2-nitrobenzyl	3.84	3050	214(32800)	68.45	5.08		
	(triphenyl)silyl ether	3.93	1510	221(32400)	(68.77)	(5.34)		
		5.34	1320	242(10600)				
			1280	265(2300)				
		7.36 - 7.69	1085	271(2400)				
				297(4300)				
				346(6300)				
Si-III	3-methyl-2-nitrobenzyl	2.26	3050	219(27600)	73.46	5.45	3.05	
	(triphenyl)silyl ether	4.93	1540	253(2400)	(73.39)	(5.45)	(3.29)	
			1435	260(2500)				
		7.05 - 7.68	1120	265(2500)				
			718	272(2100)				
ONBSi	2-nitrobenzyl	5.30	3060	221(29000)	72.97	4.76	3.40	
	(tripheny)silyl ether	7.36 - 8.10	2920	254(5300)	(72.97)	(5.14)	(3.47)	
			1520	257(5700)				
			1340	260(6100)				
			1125	265(6200)				
				270(5500)				
				306(1700)				
Si-IV	di(5-chloro-2-nitrobenzyloxy)	5.25	3060	219(29800)	56.45	3.49	5.04	12.66
	diphenyl silane	7.32 - 8.07	2900	270(15300)	(56.22)	(3.65)	(5.04)	(12.77)
			1530					
			1520					
			1340					
			1110					

	Sample	H^1-NMR (ppm)	IR (cm^{-1})	UV$\lambda_{max}^{CH_3CN}$ nm(ε)	Elemental analysis (%) found (calcd.)			
					C	H	N	Cl
Si-V	di(4-chloro-2-nitrobenzyloxy) diphenyl silane	5.21 7.34 - 8.06	3070 1530 1345 1085	217(38400) 257(9800) 305(3400)	55.93 (56.22)	3.59 (3.63)		
Si-VI	di(2-nitrobenzyloxy) diphenyl silane	5.27 7.31	3090 1530 1340	219(23200) 263(11900)	64.06 (64.18)	4.34 (4.56)		
Si-VII	5-methyl-2-nitrobenzyl (triphenyl)silyl ether	2.41 5.28 7.22 - 8.02	3050 2850 1540 1435 1120	218(27000) 253(4400) 258(5500) 264(6500) 270(6700) 278(6200)				
Si-VIII	3-methoxy-2-nitrobenzyl (triphenyl)silyl ether	3.86 4.89 7.23 - 7.67	3040 1590 1530 1285 1120	217(32800) 254(1700) 260(2000) 265(2100) 272(1800)				
Si-IX	5-chloro-2-nitrobenzyl (triphenyl)silyl ether	5.27 7.29 - 8.08	3060 1518 1338					

tetrahydrofurane was added to the reaction mixture. The Grignard reagent was added dropwise to the refluxing solution of Ph_2SiCl_2 (16.6 g) in absolute tetrahydrofurane (100 ml) and refluxed for 5 h. The mixture was cooled, then poured into a mixture of triethylamine(6.7 g), diethylether(250 ml) and water(250 ml) at 0°C. The reaction mixture was extracted with ether. The ether layer was concentrated under reduced pressure. The resultant gum-like material was dissolved in chloroform/hexane (1:2). The soluble matter was separated with Silicagel-60 (Merck). The diphenyl(vinylphenyl)silanol was obtained in the fraction eluted with chloroform. Yield 12 %, m.p. 84 ∿ 86°C, ^{1}H NMR, (δ ppm, in $CDCl_3$) 2.26 (s, OH), 5.29 (dd, J_{13}, 10.7 Hz, J_{12}, 1.0 Hz, H_1), 5.68 (dd, J_{23}, 17.6 Hz, J_{12}, 1.0 Hz, H_2), 6.74 (dd, J_{23}, 17.6 Hz, J_{23}, 10.7 Hz, H_3), 7.36 to 7.68 (m, aromatic proton) IR(KBr disk),

$$H_3\diagdown \quad \diagup H_1$$
$$C=C$$
$$\diagup \quad \diagdown H_2$$

3250, 1622, 1595, 1590 cm^{-1}.

Polymerization of diphenyl(vinylphenyl)silanol: The diphenyl(vinylphenyl)silanol was polymerized in 50 volume % of d_8-tetrahydrofurane. The polymerization was carried out under UV radiation, and AIBN was used as photo-initiator. The concentration of AIBN was 10 mol% to the monomer. The polymerization was carried out in the NMR tube made of quartz. The monomer was photo-polymerized with a merry-go-round type apparatus equipped with a 400W-high-pressure-mercury lamp at 40°C. The monomer was placed

at 10 cm distance from the lamp. After the signal of the vinyl proton disappeared, the product was poured into methanol and the insoluble matter was dried under reduced pressure. Copolymerization of diphenyl(vinylphenyl)silanol with styrene was carried out in the same way. However, when diphenyl(vinylphenyl)silanol was soluble in the styrene monomer, the tetrahydrofurane was not used. The polymer conversion was almost 100 %, and the molecular weights of the polymer are listed in Table 6 in chapter 7. $Ph_3SiCOPh$ was prepared by the method described in the literature.[3]

Other hydroxy group: Ph_3GeOH was prepared by the method described in the literature.[4] Ph_3SnOH was purchased commercially from Alfa Products and used without further purification. Alcohols were purified by distillation before use. PhSH, $Ph(OH)_2$, Ph_3CSH, PhOH, and Ph_3COH were commercially available and used without further purification. Formaldehyde-diethylmalonate-condensation product was synthesized by the method described in the literature.[5] Aluminum complex: Aluminum complexes were prepared from aluminum isopropoxide and corresponding ligand in toluene or from aluminum sulfate and the corresponding ligand in water.[6] These aluminum complexes and silyl compounds were listed in Table 2. $((CH_3)_3SiO)_3Al$ was prepared by the method described in the literature.[7] Other complexes were purchased from Wako Pure Chemicals. BF_3 complexes

Table 2   The aluminum complexes and silyl compounds used in the present study.

Aluminum complex or silyl compound	Abbreviation
tris(acetylacetonato)aluminum	$Al(acac)_3$
tris(ethylacetoacetato)aluminum	$Al(Etaa)_3$
tris(salicylaldehydato)aluminum	$Al(SA)_3$
other aluminum complexes: see chapter 4	
diphenyl(4-vinylphenyl)silanol	DVPS
triphenylsilanol	
diphenylsilanediol	DP
diphenylvinylsilanol	
diphenylmethylsilanol	
phenyldimethylsilanol	
1,1,4,4-tetramethyl-1,4-dihydroxysilethylene	HMSB
SH6018	
$HO(Ph_2SiO)_nH$: n = 1	Monomer
n = 2	Dimer
n = 3	Trimer
n = 4	Tetramer
alkoxysilanes: see chapter 10-2	
ortho-nitrobenzyl ether: see chapter 10-5	
triphenylbenzoylsilane	
silyl ether: see chapter 10-5 and 12	
$Ph_2Si(OCH_2\underset{\underset{CH_2OH}{\mid}}{C}(COOC_2H_5)_2)_2$	FMSi

were purified by distillation or crystallization before use.

Silica: Silica gel was obtained from Wako Pure Chemicals (C-200, 100-200 mesh). Zeolites were obtained from Gas-Chro Kogyo, sold as 3A, 4A, 5A, 9F (300 mesh). Porous silicas were obtained from Waters, Ltd., sold as gas chromatograph packing agent, Porasil A, B, C, D, E, F. [150 mesh; surface area (m^2/g), mean pore size ($\overset{\circ}{A}$): A, 480, 100; B, 200, 100 - 200; C, 50, 200 - 400; D, 25, 400 - 800; E, 4, 800 - 1500; F, 1.5, 1500]. Zeolites and silicas were used after heat treatment (at 150°C for 2 h).

Polymer Preparation

A solution of metal compound in cyclohexene oxide was mixed with a solution of the OH compound in cyclohexene oxide in a polymerization tube at -78°C in a N_2 atmosphere. The polymerization tube was warmed to 40°C and held at that temperature. After polymerization the unreacted monomer was removed from the polymerization system under reduced pressure and the polymer was washed with acetone and dried.

Photolysis

In order to examine the photodecomposition of silyl compound, the silyl compounds were photodecomposed in tetrahydrofurane (THF) or acetonitrile, by use of 400W-high-pressure-mercury-lamp. The lamp was surrounded by a

water-cooled Pyrex photolysis well in case of $Ph_3SiCOPh$ photolysis experiment and by a water-cooled quartz photolysis well in case of other experiment. Samples were placed in "merry-go-round" holder that rotates about the lamp to provide even illumination during photolysis. The entire apparatus was immersed in thermostated water at 40°C. The decomposition of silyl compounds was followed by liquid chromatography with an octa-decyl-silane-treating silica column (Zorbax ODS, Shimadzu). The ratio of Ph_3SiOH in $Ph_3SiCOPh$ decomposition products was determined by ^1H-NMR after complete photodecomposition.

Dependence of photolysis on wavelength of UV-light was examined by use of UV-filter. The UV filter (160 x 53 mm) was placed in a stainless case at 5 positions around UV lamp. The filters used are L39 (over 390 nm) and U36 (365 nm) (Riko Kagaku). Experiment using 254 nm was carried out by use of 26W-low pressure mercury lamp (Riko Kagaku).

In order to obtain quantum yield of decomposition of silyl ether, potassium ferrioxalate as a standard chemical actinometer was used.[8]

Photopolymerization

Normal photopolymerization was carried out by the following method: Catalysts were dissolved in cyclohexene oxide in a N_2 atmosphere in a pyrex tube ($Ph_3SiCOPh$) or in a quartz tube (other silyl compounds) with a glass stopper.

The UV irradiation was carried out in a similar manner to photolysis. After polymerization the unreacted monomer was removed from the polymerization system under reduced pressure and the polymer was washed with acetone and dried.

Properties of silanol

Stability of silanol against self-condensation was estimated with 0.01 mol of Al(acac)$_3$ and 0.01 OH equiv of silanol dissolved in 5 mL of THF. The mixture was held at 40°C and the course of silanol condensation was followed by GPC.

Relative acidity of silanol was examined by NMR spectra at 35°C with 1.5×10^{-4} OH equiv of silanol in 1 mL of CDCl$_3$ or d$_6$-DMSO.

The decrease in the amount of silanol in the polymerization procedure was investigated: 1×10^{-3} mol of silanol and 1×10^{-3} mol of Al(acac)$_3$ were dissolved in 1 mL of cyclohexene oxide and 1 mL of d$_8$-THF. The decrease in the amount of SiOH was measured by ^{1}H-NMR.

Interaction between aluminum complex and triphenyl silanol

A half value width of NMR peak, assigned to the SiOH group of the Ph$_3$SiOH, was measured in the mixture solution of 0.21M aluminum complex and 0.21M triphenylsilanol in CDCl$_3$. The data were corrected by the subtraction of the half value width of a peak due to tetramethylsilane from

the measured half value width of the signal. T_1 value (spin-lattice relaxation time) was calculated from a slope in $\log(M_0-M(t))$-t plot (M_0: longitudinal component at infinite time; $M(t)$: longitudinal component at time t) or null point in a solution having the same concentration.

Properties of cured epoxy resin

Bisphenol A type epoxide (Epikote 828 (Fig. 1), Shell Chemical Co.,) was used as epoxy resin monomer.
Curing: The epoxy resin monomer containing the catalyst was poured into 1 mm width-opening between two glass plates. The epoxy resin monomer was cured at 150°C for 15 hours.

The measurement of thermal depolarization current was performed in the following manner. A sample was polarized under an electric field (E_p) at 150°C for 30 min. and subsequently cooled rapidly to room temperature without removing the field. After short circuiting the electrodes the sample was heated at constant rate 3°C/min. and the current was measured, using an Electret Thermal Analyzer No. 650 (Toyo Seiki Seisakusho, LTD.)

Volume resistivity was measured as follows. Au electrode was evaporated on the cured epoxy resin plate, as shown in Figure 2. The sample was heated at 0.75°C/min. The impressed voltage was 500 V. (Model 4329, Yokokawa-Hewlett Packard)

Dielectric properties were measured by use of Schering Bridge Type 2759 (Yokokawa Electric Works LTD.) at
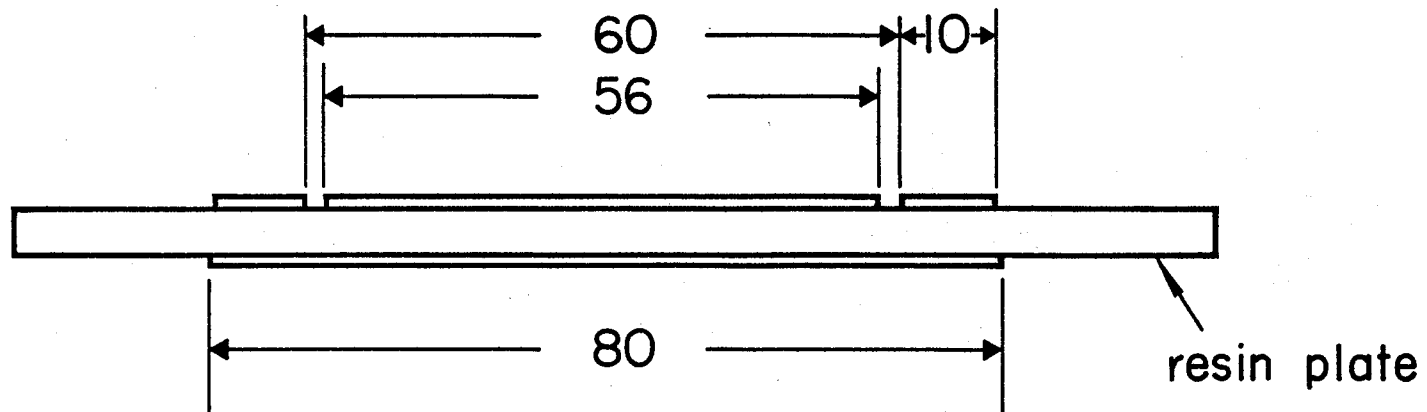
Figure 1   Bisphenol A type epoxy resin.
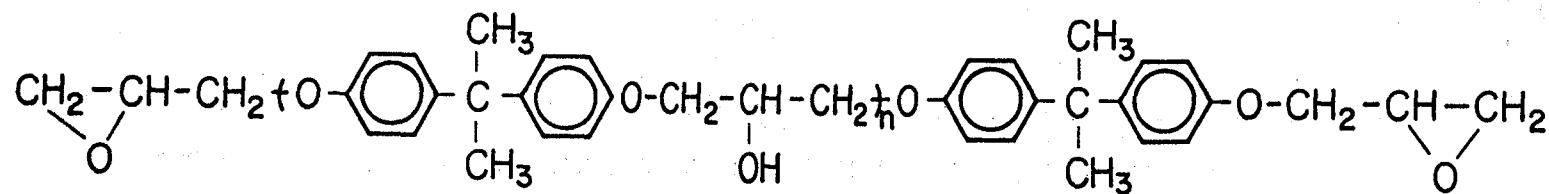
Figure 2   Electrode structure.

50 Hz, 500 V. The dependence of dielectric loss (ε'') on frequency was examined by use of LCR meter Model 4274 A (Yokokawa-Hewlett-Packard) in the frequency range from 50 Hz to 10^5 Hz.

Measurement of breakdown voltage was performed as follows. The sample was placed between stick electrode (6^ϕ)and plate electrode in silicone oil. Applied voltage was increased at 1 kV/sec. at A.C. 50 Hz.

Shear modulus was measured by means of torsional braid analysis (RD 10 type, Resca).

Gelation time was measured by use of curast meter method or test tube method. The curast meter method[9] uses curast meter. Time at which stress on curing was recorded was obtained as the gelation time. The test tube method is as follows. 30 g of epoxy resin monomer was poured into 15 mmϕ test tube. 2 mmϕ glass rod was stood in the epoxy resin and was made up and down. When the glass rod raised with the test tube, gelation was recorded.

Reaction starting temperature was measured by use of heat of reaction. The measurement was carried out by use of the apparatus shown in Figure 3.

Apparatus

The molecular weight distribution of the polymer was determined with a Toyo Soda model 801 gel permeation chromatograph operated at 40°C. The four columns were connected in series, each packed with $G2000H_8$, $G2000H_8$,
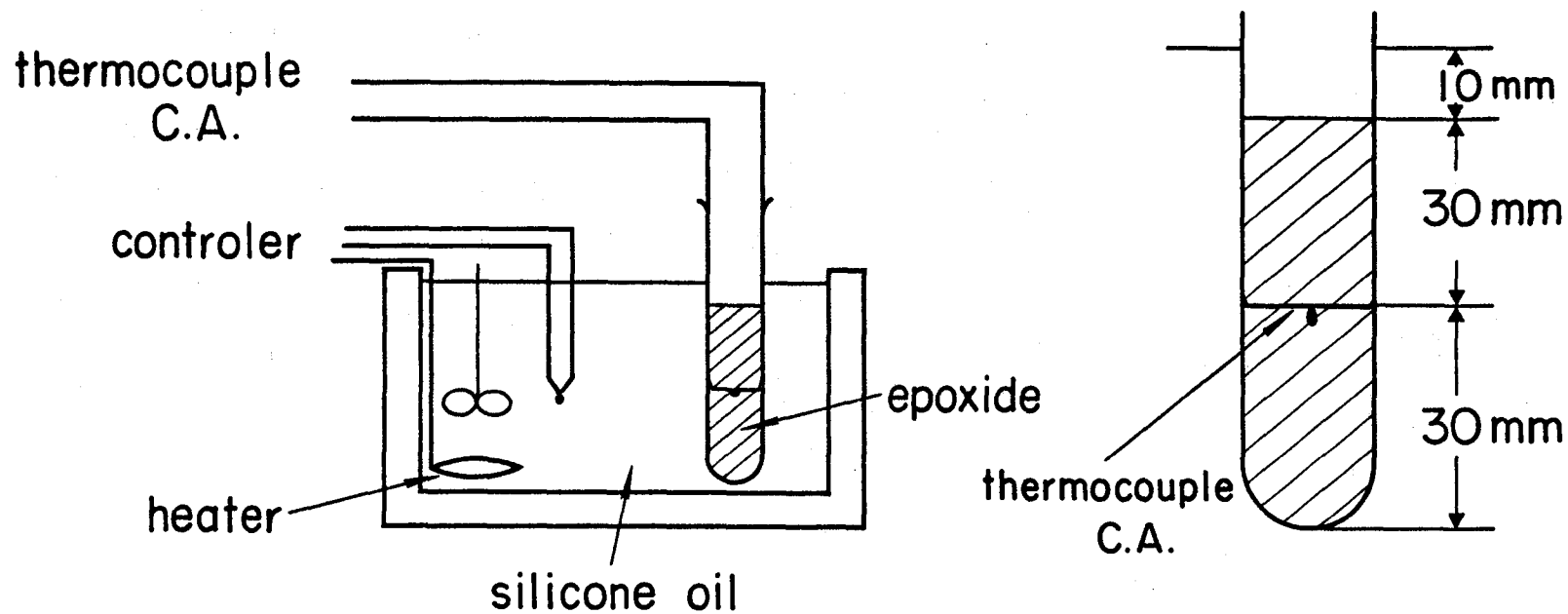
Figure 3   Apparatus for measurement of reaction heat.

G3000H$_8$, and G4000H$_8$ (Toyo Soda polystyrene gel), respectively. THF was used as solvent and the instrument was calibrated to a first approximation with polystyrene of known molecular weights. Nuclear magnetic resonance spectra were determined with FX-100 and FX-90Q (JEOL LTD) instruments. The chemical shifts were referred to TMS. Infrared (IR) spectra were determined with IRA-2 (Japan Spectroscopic Co., Ltd.) equipment. X-ray diffraction of polymers was determined with RU-33L, SG-8R (Rigaku) equipment. Separation of reaction products was carried out with a Toyo Soda model HLC-807 gel permeation chromatograph packed with G-2000H$_8$ (polystyrene gel); chloroform was used as the solvent. A Shimadzu-5A model gas chromatograph with a Apiezon grease L (celite) was used for GC analysis.

Liquid chromatography was performed on a Shimadzu apparatus, model LC-3A, with ODS silica column (Zorbax ODS, Shimadzu), and methanol was used as solvent.

Part II   <u>Selective Synthesis of Structurally Isometric</u>
<u>Poly-β-ester and Poly-δ-ester from β-(2-</u>
<u>Acyloxy-ethyl)-β-propiolactone with Al-H$_2$O and</u>
<u>Zn-H$_2$O catalysts</u>

<u>Syntheses of 2-acetoxyethyl-propionaldehyde, 2-isopropyl-</u>
<u>carboxyethyl-propionaldehyde and 2-(1-chloroethyl)-carboxy</u>

ethyl-propionaldehyde:

These aldehydes were synthesized by the addition of the corresponding carboxylic acid to acrolein in a column containing Amberlite IRA-400 (acetate type, ion-exchange resin).[10] (b.p., yield) 2-acetoxyethyl-propionaldehyde, 55°C/0.9 mmHg, 26.6 %, 2-isopropyl-carboxyethyl-propionaldehyde, 53°C/1 mmHg, 18 %, 2-(1-chloroethyl)carboxyethyl-propionaldehyde, 75°C/0.7 mmHg, 30.5 %.

Syntheses of β-(2-acetoxyethyl)-β-propiolactone (1), β-(isopropylcarboxyethyl)-β-propiolactone (2) and β-(2-(1-chloroethyl)carboxyethyl)-β-propiolactone (3).

β-propiolactones were synthesized by reacting aldehyde with ketene, referring the literature.[11] (b.p., yield, d^{20}, elemental analysis, (calculated)), monomer (1), 104 - 107°C/0.7 mmHg, 18 %, 1.10, C, 53.15 (53.16), H, 6.42 (6.37), monomer (2), 110 - 114°C/0.3 mmHg, 33 %, 1.04, C, 57.87 (58.05), H, 7.64 (7.58), monomer (3), 150 - 155°C/ 0.3 mmHg, 40 %, 1.19, C, 46.22 (46.50), H. 5.43 (5.37), Cl, 16.92 (17.16).

Polymerization of β-substituted-β-propiolactones.

Distillation of solvents, preparation of catalysts and polymerization were carried out under argon atmosphere. Preparation of catalyst: $(EtAlO)_n$ and $Et(ZnO)_2ZnEt$ catalyst were prepared, referring the literature.[11] $SnCl_4$ was used without further purification. BF_4OEt_3 was synthesized, refering the literature.[12]

Polymerization was carried out as follows. Monomer was added to toluene containing a given amount of a catalyst at -70°C under argon atmosphere. After a homogeneous solution was formed by stirring, the polymerization tube was sealed and allowed to stand at a given temperature. Polymerization was terminated by pouring the polymerization mixture into a large excess of diethyl ether or diethyl ether-petroleum ether. Then the polymer precipitated was purified by extraction with diethyl ether. The polymers were tacky except for rubberlike (poly(3)-(Al)). Tg of the polymers are summarized in Table 7. (chapter 11)

Thermal decomposition of polymers:

Thermal decomposition of the polymers was carried out in an all glass apparatus consisting of two cylindrical tubes with a bridging arm (Figure 4). One gram of a polymer sample was heated in vacuo in one of the tubes at a given temperature while the other tube was cooled to -78°C to collect the decomposed products.

Preparation of 5,6-dihydro-2-pyrrone:

5,6-Dihydro-2-pyrrone for identification of the thermal decomposition product of poly-β-ester was synthesized from vinyl acetate and paraformaldehyde by the method described in the literature.[13]
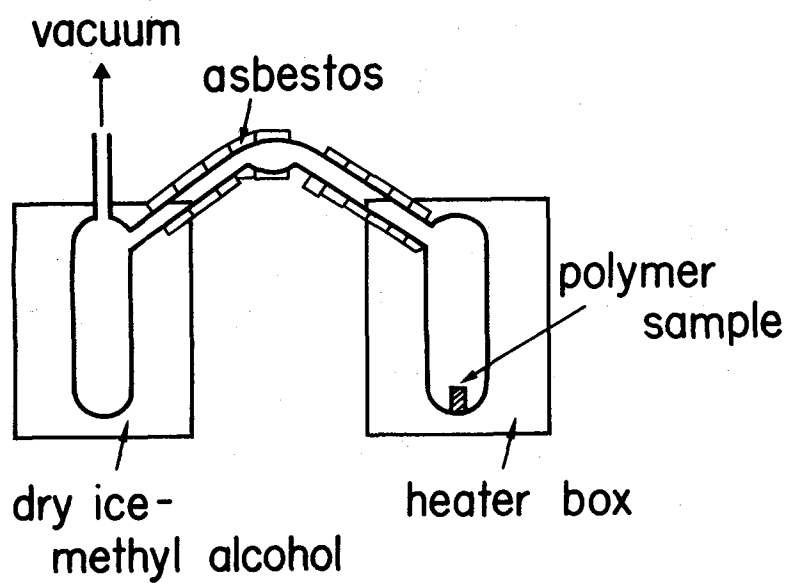
Figure 4   Apparatus for thermal decomposition
    of polymer.

Apparatus:

IR spectra of the polymers were measured with a Hitachi model EPI2 spectrometer with a KBr disc method. NMR spectra were taken at room temperature with Varian T-60, Varian A-60 and Varian XL-100 spectrometers. ^{13}C-NMR spectra were recorded at 38°C with a Varian Model XL-100 spectrometer at 25.16 MHz with a FT accumulator. Number of the data point in the FT accumulation was 8192 data length value. The molecular weight and the molecular weight distribution of the polymers were measured by gel permeation chromatography with a Shimadzu-Du Pont 830 type apparatus (column constitution, HSG-60(50cm)-HSG-40(50cm)-HSG-20(50cm)) by eluting with THF at 45°C. Calibration was carried out with standard polystyrene mixtures. Thermal behavior of polymers was measured by a differential scanning calorimeter (Rigaku Denki). X-ray diffraction experiments were carried out with Cu/K_α source.

Words

OH equivalent: molecular weight/the number of OH in a molecule.

OH equivalent %: (the number of OH equivalent/mole of monomer) × 100.

References

1. T. Takiguchi, J. Am. Chem. Soc. (B), 81, 2359 (1959)

2. G. I. Harris, J. Chem. Soc. (B), 1963, 5973 (1964)

3. A. G. Brook, J. Am. Chem. Soc., 82, 5102 (1960); ibid., 91, 355 (1969)

4. A. G. Brook and H. Gilman, J. Am. Chem. Soc., 76, 77 (1954)

5. U. Michel and S. Tchelitcheff, Bull. Soc. Chim. Fr., 2230 (1964)

6. E. W. Berg and N. M. Herrera, Anal. Chim. Acta., 60, 117 (1972)

7. H. Schmidbaur, Chem. Ber., 96, 2696 (1963)

8. C. G. Hatchard, C. A. Parker, Proc. R. Soc. London, A235, 518 (1956)

9. JSR type curast meter, technical paper (Nichigo Shoji)

10. Reynir Eyjolfsson, Acta. Chem. Scand., 24, 3076 (1970)

11. K. Teranishi, T. Araki and H. Tani, Macromolecules, 5, 660 (1972); H. Tani, S. Yamashita and K. Teranishi, Polym. J., 3, 417 (1972); K. Teranishi, M. Iida, T. Araki, S. Yamashita and H. Tani, Macromolecules, 7, 421 (1974); M. Iida, T. Araki, K. Teranishi and H. Tani, Macromolecules, 10, 275 (1977); M. Iida, S. Hayase and T. Araki, Macromolecules, 11, 490 (1978)

12. Organic Synthesis, <u>46</u>, 113

13. L. J. Polby, C. N. Lieske, D. R. Rosencrantz and
    M. J. Schwarz, J. Am. Chem. Soc., <u>85</u>, 47 (1963)

Acknowledgments

List of publication

1. "Polymerization of cyclohexene oxide with Al(acac)$_3$-silanol catalyst" S. Hayase, T. Ito, S. Suzuki and M. Wada, J. Polymer Sci., Polym. Chem. Ed., 19 (9), 2185 (1981)

2. "Polymerization of cyclohexene oxide with Al(acac)$_3$-silanol catalyst supported by zeolite and porous silica" S. Hayase, T. Ito, S. Suzuki and M. Wada, J. Polymer Sci., Polym. Chem. Ed., 19 (10), 2541 (1981)

3. "Polymerization of cyclohexene oxide with aluminum complex/silanol catalysts. Part III. Dependence of catalytic activity on bulkiness of silanol and its intramolecular hydrogen bond" S. Hayase, T. Ito, S. Suzuki and M. Wada, J. Polymer Sci., Polym. Chem. Ed., 19 (11), 2977 (1981)

4. "Polymerization of cyclohexene oxide with aluminum complex/silanol catalyst. IV. Photopolymerization with Ph$_3$SiCOPh/Al complex/alcohol catalyst system" S. Hayase, T. Ito, S. Suzuki and M. Wada, J. Polymer Sci., Polym. Chem. Ed., 20 (6), 1433 (1982)

5. "Polymerization of cyclohexene oxide with aluminum complex/silanol system. V. Dependence of catalytic activity on the structure of aluminum complex" S. Hayase, T. Ito, S. Suzuki and M. Wada, J. Polymer Sci., Polym. Chem. Ed., in press.

6. "Polymerization of cyclohexene oxide with aluminum complex/silanol catalyst. (VI) Oligomer and polymer effect. S. Hayase, Y. Onishi, S. Suzuki and M. Wada, J. Polymer Chem., Polym. Chem. Ed., in press.

7. "Selective synthesis of structurelly isomeric poly β-ester and poly δ-ester from β-(2-acetoxyethyl)-β-propiolactone. A new difference between $(EtAlO)_n$ and $Et(ZnO)_2ZnEt$ catalysts". T. Araki, S. Hayase and M. Iida, J. Polymer Sci., Polymer Letters Edition, 16 (10), 519 (1978)

8. "Selective synthesis of structurelly isomeric poly β-ester and poly δ-ester from β-(2-acetoxy-ethyl)-β-propiolactone with Al and Zn catalysts". T. Araki, S. Hayase and A. Nakamura, J. Polymer Sci., Polym. Chem. Ed., in press.

9. "Isomerization polymerization of β-propiolactones carrying side-chain ester groups". T. Araki, S. Hayase and A. Nakamura, Submitted in J. Polymer Sci., Polym. Chem. Ed.,

10. "Polymerization of epoxide with aluminum complex/silanol catalyst. Part VII. Thermal and electrical properties of epoxy resin cured with the new catalyst. S. Hayase, S. Suzuki, M. Wada, Y. Inoue and H. Mitsui, Submitted in J. Appl. Polym. Sci.